Encoding of Saccadic Scene Changes in the Mouse Retina

Dissertation

der Fakultät für Biologie
der Ludwig-Maximilians-Universität
München

zur Erlangung des akademischen Grades
Doctor rerum naturalium
(Dr. rer. nat)

Angefertigt am
Max-Planck-Institut für Neurobiologie
München

vorgelegt von

Vidhyasankar Krishnamoorthy
geboren am 10. Oktober 1978 in Cuddalore, Indien

München, im September 2012

Betreuer:	Herr Prof. Dr. Tim Gollisch
Erster Gutachter:	Herr Prof. Dr. Tobias Bonhoeffer
Zweiter Gutachter:	Herr Prof. Dr. Rainer Uhl
Eingereicht am:	17. September 2012
Tag der mündlichen Prüfung:	27. November 2012

Five-fold perception gained, what benefits accrue
To them whose spirits lack perception of the true?

-Thirukkural, circa 1 AD (Verse 354)
(G. U. Pope's translation from Tamil, 1886)

Contents

Acknowledgments

First and foremost, I would like to thank Tim Gollisch for giving me an opportunity to work in his research group. His enthusiasm and dedication to research is contagious. I am grateful for his supervision and mentorship throughout my thesis work, especially during the writing stage of this dissertation.

The Visual Coding Group at the Max Planck Institute of Neurobiology provided an excellent atmosphere to conduct research. I am greatly indebted to my colleagues Daniel Bölinger, Christian Mendl, Mona Garvert and Jing Shao for lively discussions. Daniel and Christian were always there to help me understand the beauty of equations. Christian generously helped me in dealing with the computational issues. If the ganglion cells of my recordings had receptive fields, it was only because of Christian! I thank Mona for inspiring discussions in a wide range of topics. A special thanks to Annegret Cerny for her help to deal with the German bureaucracy during my first days in Germany. I thank my colleagues Michael Weick, Daisuke Takeshita, Jain Liu, Fernando Rozenblit, Norma Kühn and Sebastian Bemme for congenial environment at the University Medical Center Göttingen, where I spent my last stages of PhD. I thank Daniel and Fernando for their help with LaTeX typesetting. I thank Jian and Daisuke for their patient proof reading of this dissertation.

I would like to thank Tobias Bonhoeffer and Günther Zeck - the members of my Thesis Advisory Committee - for useful suggestions, advice and guidance. I also thank Günther and Christian Leibig for sharing the rabbit retina used in this work.

I thank Santhosh Sethuramanujam, a friend from my NBRC days, for his constructive criticism at various stages of this work. I also thank my friends on and off the cricket field who made my stay in Munich a pleasant one.

Finally, I would like to thank my mother and sister for their support, love and care. Their indomitable spirit instilled the courage in me to give wings to my aspirations. To them, I dedicate this thesis.

Overview

We perceive the world around us through our senses. Everything we see, hear, taste, feel, or smell is represented as an electrochemical signal and conveyed to higher brain centres. It is this sensory representation of the world that enables us to interact with our environment and shapes our actions and decisions. In a constantly changing environment, for every successful action the sensory representation has to be fast and precise. For example, when you are strolling down the lane, to make every single step, you need a myriad of sensory information, like the objects and people in the front, how far they are, whether they are approaching or moving away, the sound of an approaching car behind you and so on. For successful navigation, the information about the ever changing sensory surroundings must be constantly updated. The statistics and variability of stimuli in our sensory surroundings provide an enormity of stimulus spectra and pose a significant challenge in understanding sensory coding under natural conditions. Nevertheless, understanding the information processing under natural conditions is critical, not only for sensory coding but neuronal coding in general.

In this thesis, we aim to understand the visual information processing in the retina to a stimulus that mimics a natural condition. Vision begins in the *retina*, a thin sheet of neural tissue at the back of the eye, which converts light signals into neural signals. The signals of retinal ganglion cells present a 'bottleneck' in the visual pathway, as they provide the only source of information about the visual world to the rest of the brain (Barlow 1981, Meister and Berry 1999, Dhingra et al. 2003). Thus the representation of our visual world is reconstructed primarily with the signals originating in the retina. Therefore, the visual system is ideally suited to probe coding strategies during naturalistic stimulus conditions.

Among the senses, the visual system is a dominant part for many animals, and a third of our own cortex is dedicated to processing vision. Our visual world is complex with hundreds of objects, some of them moving altogether randomly. Another challenge is our own body, head and eye movements, which pose a significant challenge in extracting the visual information of our surroundings. Despite our constant eye movements, most

of the time we are able to find our way easily and see a stable world. For example, when you read this text, your eyes jump from phrase to phrase, yet you navigate through the text relatively easily. Nevertheless, these fast eye movements known as *saccades* are an essential feature of visual behaviour. We constantly reposition our gaze to fixate the next interesting part of our visual space. Thus the image acquired by the retina during the *fixations* is interrupted by fast and ballistic *saccades*. What is the response of the retina during such saccades? How does a saccade interfere or interact with information about the fixated visual stimulus that follows? In other words, how does the retina cope with such impending eye movements and update the information about the sensory surroundings?

Here, we will address these questions by a systematic investigation of the retinal response to saccadic scene changes. The retina as a model system offers some unique advantages, as it is a readily accessible and an easily approachable part of the brain (Dowling 1987). Also, the vertebrate retina is a self-contained system with minimal feedback. It is easy to isolate and maintain the intact retina and record its output activity for hours while simultaneously stimulating it with a range of visual stimulus.

In the present study, we performed all the experiments in the isolated mouse retina and recorded the activity of the output cells of the retina - the *retinal ganglion cells*. We monitored and recorded the electrical activity of the retina by using microelectrodes (Meister et al. 1994). The isolated retina was placed on a planar multielectrode array with 60 electrodes and a population of up to 30 ganglion cells were recorded simultaneously. We generated the visual stimulus mimicking saccadic scene changes and projected it onto the retina. This enabled us to study the input-output relationship and elucidate the information processing and encoding in the retina.

Retinal processing to saccadic stimulus has been reported earlier (Noda and Adey 1974b, Roska and Werblin 2003). While these studies reported the modulation of ganglion cell activity *during* saccades, the encoding of ganglion cells for fixations *after* the saccades has not been probed. The encoding of the fixation stimulus is critical to represent our visual environment, and it is not known how saccades themselves modulate the representations during subsequent fixations. In the present study, we precisely asked these questions and probed the retina with appropriate stimuli. We found that the ganglion cells are affected by the history of the stimulus before a saccade. Furthermore, we could distinguish five different parallel channels of information, some of which show rather unexpected response properties, encoded by different groups of cells.

This thesis is organized in six chapters.

In the *first chapter*, we describe the architecture and function of the vertebrate retina. We begin with structure and organization of different cell types in the retina and proceed to describe the functional role of each cell type for visual information processing. We then elaborate on the functional classes of ganglion cells and provide a brief history of attempts to classify ganglion cells. Furthermore, we provide an overview of "feature detection" in the retina and highlight some important progress made in this direction. We also introduce the concept of receptive field and how the properties of the receptive field are affected by stimulation far beyond the receptive field. We further introduce the challenges of information processing in the presence of eye movements. Finally, we define the specific goals of this thesis.

In the *second chapter*, we describe our experimental approaches. We explain the procedure of mouse retina isolation and the methods of our electrophysiology experiments using multielectrode arrays. We then outline our methods of data analysis and general characterization of ganglion cells.

Chapter three is the first set of results of this thesis. Here we describe our stimulus that mimics saccadic scene changes and our approach in analysis. For half of the recorded ganglion cells, we found strong spiking activity during saccades. This supports the idea that retina actively encodes the saccade and may signal abrupt scene changes to downstream centres. Furthermore, we characterized the responses to the newly fixated image. Based on this analysis we classified the ganglion cells into five response types. While there appears to be only little influence of the motion signal itself on the responses, the responses depended strongly on the history of the stimulus before the saccade. This suggests that retinal signals under saccadic vision may provide 'context' and encode image transitions rather than currently fixated image.

In *chapter four*, we investigate the effects of "remote stimulation", i.e., a stimulus beyond the classical receptive field. Each ganglion cell is primarily sensitive to visual signals in a small area of space, the cell's spatial receptive field (Hartline 1938, Kuffler 1953). However, it has been known that the ganglion cell responses are also modulated by stimulation far beyond the receptive field (McIlwain 1964). This is particularly relevant in the context of natural stimuli, where spatially extended stimuli may provide a contextual meaning to a different stimulus within the classical receptive field. A striking example is the discovery of a specialized object-motion-sensitive cell (Ölveczky et al. 2003) that responds to differential object motion as opposed to the motion of the whole scene encountered during eye movements. While it has been agreed that there is an effect from the far-periphery, the nature of the effects have remained controversial. While in salamanders, the remote stimulus is shown to inhibit a ganglion cell's

response; in mammals both excitation and inhibition are reported. In this thesis, we revisit the effects of remote stimulation and systematically investigate their properties. During the recording, we present various light stimuli to the receptive fields of the cells in the presence or absence of remote stimulation. As remote stimuli we apply moving as well as contrast-reversing gratings with different spatial and temporal scales. The response characteristics are then compared to the filtering properties of the neurons as measured with white-noise experiments and reverse-correlation analyses.

In *chapter five*, we present the results of ganglion cell activity after *gene therapy*. This is a collaborative research effort, where missing cone photoreceptor function is restored by gene therapy. We evaluated the ganglion cell activity to confirm the proper processing of visual information. We found that the major ganglion cell types are restored and basic cell type specification such as ON, OFF and ON-OFF classification upheld. The results presented in this chapter together with the results of our collaborators have been published (Michalakis et al., 2010).

In *chapter six*, we summarize the major findings of this thesis and discuss the results in detail. Finally, we conclude the thesis and put forth the new ideas that could further the findings of this thesis in the *outlook* section.

1. The Vertebrate Retina

The retina is a thin sheet of neural tissue that lines the back of the eye (Fig. 1.1). The basic organization of the eye and the retina in particular is amazingly similar in almost all vertebrates (Rodieck 1998). The incoming light is focused by the lens onto the retina which translates the visual scene into a set of neural signals. For decades, the general notion had been that the retina provides a generic filtered (i.e., pixel-to-pixel) information to the rest of the brain, where complex visual processing is known to take place. However, growing evidence shows that much more processing takes place in the retina itself, which acts as 'feature detectors' and provides precise and diverse information already segregated to different higher centres (Gollisch and Meister 2010).

In this chapter, we look into the structure and function of the retina, highlight the complexities of retinal processing, and define the goals of the thesis. First, we elaborate on the organization of different cell types of the retina and their role in information processing. We then highlight the functional classification of the output cells of the retina and provide an overview of feature detection in the retina. Finally, we introduce the challenges of information processing in the presence of eye movements and set forth the goals of this thesis.

1.1 Retinal Architecture and Function

The retina consists of five major types of neurons (photoreceptors, bipolar cells, horizontal cells, amacrine cells and ganglion cells), and three types of glial cells (Müller cells, astrocytes and microglia). The neurons are arranged in a laminar architecture with three nuclear layers: Ganglion Cell Layer (GCL), Inner Nuclear Layer (INL) and Outer Nuclear Layer (ONL); and two plexiform layers: Inner Plexiform Layer (IPL) and Outer Plexiform Layer (OPL) (Fig. 1.2). The retinal tissue is arranged in such a way that the photoreceptors are loosely attached at the back of the eye with the retinal pigment epithelium and the ganglion cell side towards the inside of the eye. The light travels through the nearly transparent retina before it reaches the photoreceptors,

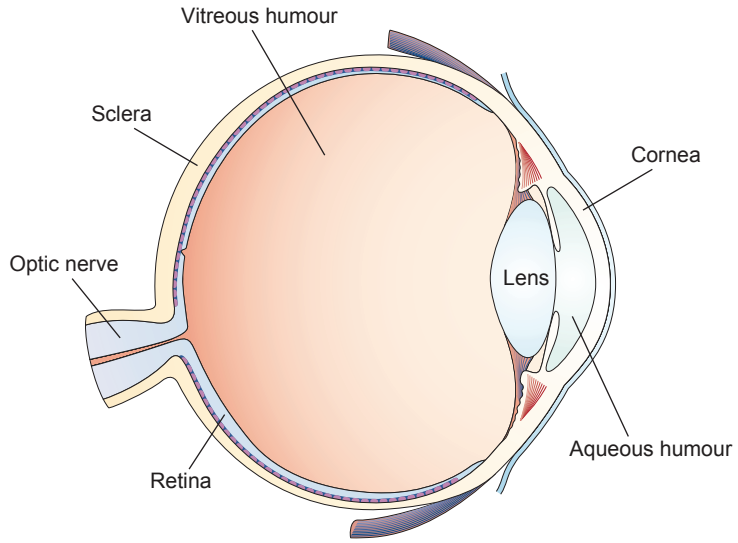

Figure 1.1: Schematic diagram of the human eye. The light enters through the lens which projects the image onto the retina that lines the back of the eye. The information of the image processed by the retina is carried by the optic nerve to the rest of the brain. Image adapted from Martinez-Conde et al. (2004).

where the light signals are transduced to electrical signals. These signals are then processed by the successive layers in the retina, before finally reaching the ganglion cells, the output stage of the retina.

Photoreceptors are the primary light sensitive cells of the retina and are of two types: rods and cones. Our natural environment consists of varied levels of light intensities ranging over 10^{10} (10 log units), and rods and cones divide the job by covering different ranges (Sterling and Demb 2004). Rods are active in dim light conditions such as a starlight evening (scotopic) and cones are active in bright light conditions such as daylight (photopic), while both rods and cones are active at middle intensity range such as dawn and dusk (mesopic). Rods are of single type with rhodopsin photopigments and provide achromatic, low spatial but high temporal resolution vision in dim light conditions. There are two or more cone subtypes, depending on species, with each subtype having different spectral sensitivity. For example, humans are trichromatic with three cone subtypes - the short wavelength sensitive (blue cones), medium wavelength sensitive (green cones) and long wavelength sensitive (red cones). The difference in wavelength sensitivity is because of the presence of different types of photopigment in each subtype. Cones typically provide high spatial resolution vision. Several photoreceptors, typically 10-100, converge onto a single bipolar cell. Foveas of primates and

raptors (e.g., eagles) are a special case, where a single cone connects to a single bipolar cell which in turn connects to a single ganglion cell, thus providing high spatial acuity.

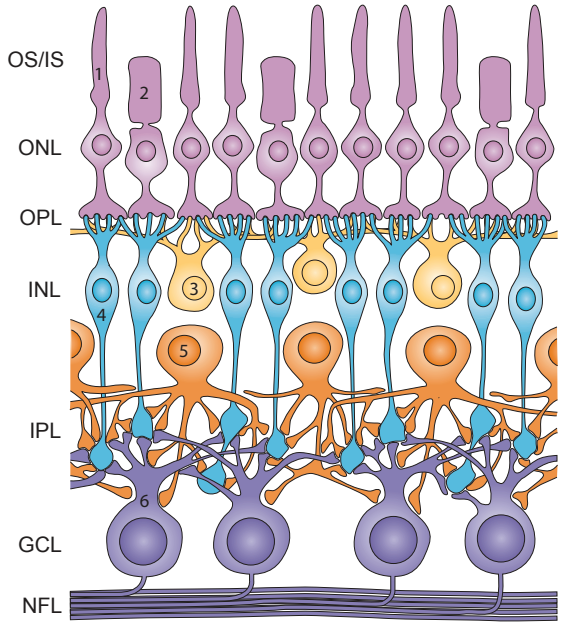

Figure 1.2: Laminar architecture of the retina. The neurons in the retina are arranged in a laminar fashion. Rod (1) and cone (2) photoreceptors are the primary light sensitive cells of the retina. Rods are active in dim light (e.g. night vision), and cones are active in bright light (e.g. day-light vision) conditions. Cones are also responsible for colour vision. The interneurons - horizontal cells (3) and bipolar cells (4) - receive information from photoreceptors and further process them before passing on to amacrine cells (5) and the output cells of the circuit, the retinal ganglion cells (6). The different layers of the retina are : IS/OS - the inner and outer segments of photoreceptors where the photopigments are present; ONL - outer nuclear layer where the cell bodies of photoreceptors are present; OPL - the outer plexiform layer comprises the photoreceptor-bipolar-horizontal cell synapses; INL - the inner nuclear layer where the cell bodies of bipolar, horizontal and amacrine cells are present; IPL - the inner plexiform layer comprises the bipolar-amacrine-ganglion cell synapses; GCL - the ganglion cell layer; and NFL - the nerve fibre layer where the axons of the ganglion cells bundle together and run towards the optic disc. The ganglion cell axons exit the retina at the optic disc and form the optic nerve. Image adapted from Wässle (2004).

Bipolar cells represent the next stage in visual information processing and are broadly divided into two types: rod bipolar cells and cone bipolar cells. Functionally, cone bipolar cells are further divided into ON and OFF bipolar cells based on response polarity. ON bipolar cells are active at light onset and OFF bipolar cells are active at light offset (Kolb 1994). It is at this stage that the light information is detected either as

increments or decrements against the mean background illumination. The difference in response polarity arises due to the presence two different types of glutamate receptors. ON cells have metabotropic glutamate receptors in their dendrites, which invert the photoreceptor signal, whereas OFF bipolar cells have ionotrpoic glutamate receptors and they preserve the photoreceptor signal. Rod bipolar cells are typically of only ON type. ON bipolar and OFF bipolar axons terminate at two different strata (also known as sublaminae) in the IPL. Based on morphology and stratification of bipolar cell axons in the IPL, they are further classified into ten subtypes: nine cone bipolar type and one rod bipolar type (Wässle et al. 2009). Each cone contacts all of the nine cone bipolar type, thus the same information is processed in parallel circuits already at the first synapse in the visual pathway (Wässle et al. 2009). Information from the bipolar cells is then sent to ganglion cells, the output neurons of the retina.

Retinal ganglion cells(RGC) represent the final stage of information processing in the retina, and they are the output cells of the retinal circuit. Ganglion cells are divided broadly into ON type, OFF type and ON-OFF type based on their synaptic contact to bipolar cells(Fig. 1.3). They inherit the response polarity from bipolar cells - ON cells respond to light increments, OFF cells to light decrements, and ON-OFF cells to both (Sterling and Demb 2004, Kolb and Nelson 1993, Nelson et al. 1993). Based on morphology they are further classified into 10-15 subtypes in mouse retina (Badea and Nathans 2004, Wässle 2004, Kong et al. 2005, Coombs et al. 2006, Völgyi et al. 2009). It has been proposed that each subtype has a specific role in information processing and projects to a distinct visual area of the brain (Field and Chichilnisky 2007). The axons of the ganglion cells collect to form the optic nerve, which carries the partially processed image information to the lateral geniculate nucleus (LGN), the superior colliculus (SC), suprachiasmatic nucleus (SCN), olivary pretectal nucleus (OPN) and associated optic system (AOS), and other visual areas depending on animal species.

Apart from the vertical pathways, there are two major *lateral pathways* which act to further process the visual information. The horizontal cells act at the OPL and the amacrine cells act at the IPL. *Horizontal cells* receive inputs from many photoreceptors and have much larger receptive fields. They provide negative feedback at the photoreceptor to bipolar cell synapse. They are also coupled to each other by gap junction, thus extending the spatial interaction of light stimulus. Furthermore, the reciprocal synapse between cones and horizontal cells is implicated in the generation of characteristic antagonistic centre-surround organization of the bipolar cell receptive field (Kolb 1994). Recently, Jackman et al. (2011) reported that horizontal cells also provide local positive feedback to cones that amplify the cone signal. *Amacrine cells* act at the bipolar to

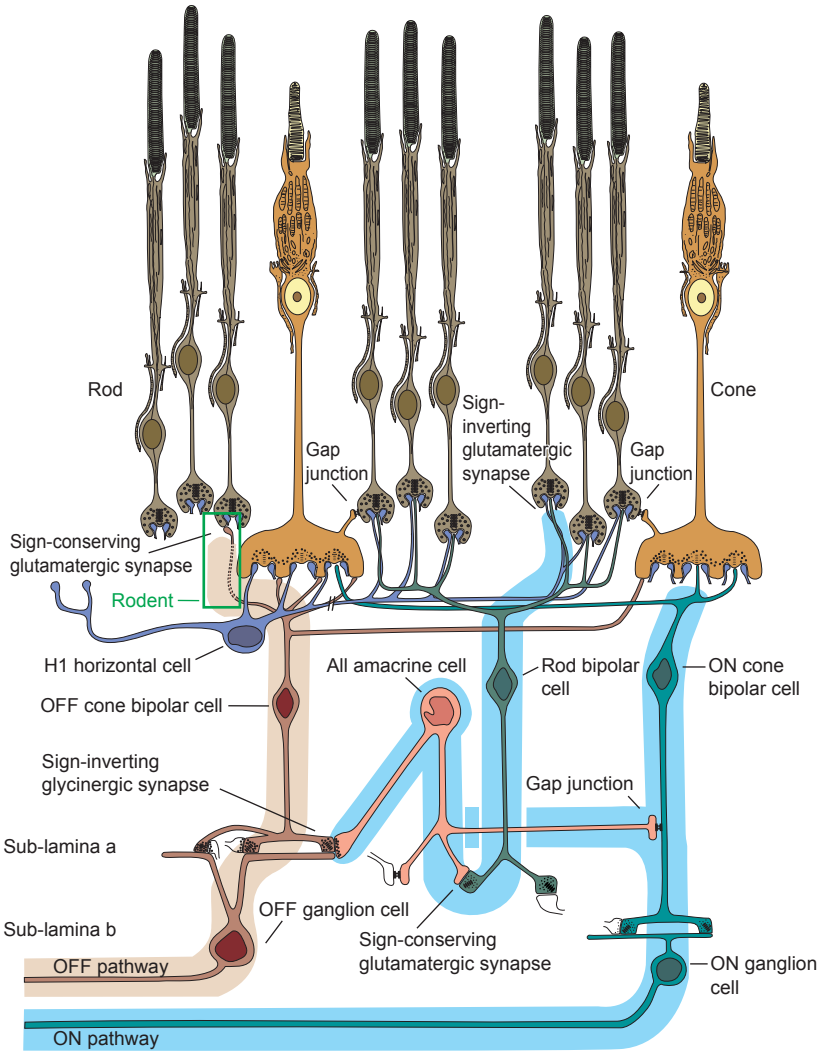

Figure 1.3: ON and OFF pathways in the retina. Cone signals are channelled to the ganglion cells by distinct OFF and ON bipolar cells. Rod signals are channelled by only one type of bipolar cell. Nevertheless, the AII amacrine cells channel the rod signals to ON and OFF pathways. However, there are evidences for direct rod-OFF cone bipolar synapses in the mouse retina (Soucy et al., 1998). The important synapses are indicated. Image adapted from Sharpe and Stockman (1999).

ganglion cell synapses. They come in a variety of morphology and neurotransmitter presence and are further subdivided into nearly 20 subtypes (Masland 2001). They act to modulate the ganglion cell response either by inhibitory or excitatory synapses. It is thought that several complex response properties of ganglion cells are brought about by different amacrine cells. For example direction selectivity is brought about

by a special type of amacrine cell known as starburst amacrine cell. They contain two neurotransmitters - acetylcholine which is excitatory; GABA which is inhibitory. Some amacrine cells also inhibit other amacrine cells, thus bringing more complexity to their modulation. Although morphology of amacrine cells is well studied, the function of many cell types is poorly understood.

1.2 Functional Classes of Ganglion Cells

Ganglion cells are the functional units of information transmission in the retina. They can be classified based on their physiological function and response properties. Such a classification was made as early as 1938 by Hartline and he was the first to record from the individual ganglion cells of the vertebrate retina (Hartline 1938). He found that the ganglion cells responded not only to light increments, some of them also to light decrements, while some responded to both. Thus according to response, three functional classes of ganglion cells emerged. Those that responded to increments of light were called "ON" cells; those that responded to decrements were called "OFF" cells; and cells that responded to both were known as "ON-OFF" cells. This functional classification is based on polarity of response of a ganglion cell and holds good in all vertebrate retinas studied since then (Fig. 1.3). Hartline's study also showed that each ganglion cell primarily responded to a light stimulus restricted in visual space known as its "receptive field". Detailed experiments by Kuffler (1953) revealed that this receptive field is further divided roughly into a concentric centre and an antagonistic surround. Centre-surround organization of the receptive field shows that the integration of stimuli within the receptive field is much more complex than simple summation. Later, Enroth-Cugell and Robson (1966) found that the cat ganglion cells can be classified based on their property of spatial summation of stimuli over their receptive field - X cells with linear summation over their receptive field and Y cells with non-linear summation. When presented with reversing sinusoidal gratings with four different spatial phases, X-cells respond with a preferred phase and null phase, since they summed the stimulus linearly over the receptive field. Y cells, on the other hand, respond to all spatial phases, indicating that these cells show non-linear stimulus integration over their receptive field. Furthermore, each class has ON and OFF subtypes. Anatomical studies by Boycott and Wässle (1974) showed that X and Y cells correspond to two known morphological classes, beta (smaller dendritc field) and alpha (larger dendritc field) types, respectively, thus establishing *morphology-function relationship* in the retinal ganglion cell classes.

Apart from the classification schema described above, there have been attempts to

classify mouse ganglion cells based on additional response parameters such as response latency, response duration (transient and sustained), response nonlinearity, and receptive field size (Carcieri et al. 2003, Farrow and Masland 2011). Carcieri et al. (2003) arrived at five distinct physiological clusters; whereas Farrow and Masland (2011) using different criteria, described 12 distinct physiological clusters.

Although several advances have been made since the first classification by Hartline (1938), the physiological classification is not yet conclusive. Thus, it is possible to find more classes of ganglion cells when probed through different physiological properties and response profiles.

1.3 Feature Detection in the Retina

For decades, the general notion among vision researchers had been that the retina merely filters the visual information, and complex processing is left to the higher brain centres. However, analysis with more complex stimulus patterns revealed the presence of diverse functional classes of ganglion cells which act as "feature detectors". Earliest such finding was the presence of the so-called *bug detectors* (Lettvin et al. 1959) in the frog retina, where a particular type of ganglion cell responded only to motion of small objects, with convex curvature. Motion of larger objects and a straight edge elicited little or no response. Although the authors referred to this cell type as "convexity" detectors, it has become anecdotally referred to as "bug" detectors because small convex moving objects relevant for frogs are usually bugs. Another such finding was the presence of *direction selective* ganglion cells in the rabbit retina (Barlow and Hill 1963), which respond to light spots moving in a particular direction. These cells responded to motion of light spots or rectangular stripes moving in a preferred direction but not in the opposite direction ("null" direction). It is now known that there are different subclasses of direction selective cells, with cells responding to a particular cardinal direction (dorsal, ventral, nasal and temporal) and projecting to different targets in the brain (Kay et al. 2011, Rivlin-Etzion et al. 2011). More findings followed, again in the rabbit retina. Levick (1967) described the presence of three more feature detectors. *Local edge detectors* responded to motion of a contrast edge within the receptive field; *orientation selective* cells responded to either horizontally or vertically oriented bars; and *uniformity detectors* stopped their high maintained rate when the light intensity changed within their receptive field. Experiments in other species revealed the presence of more complex feature detectors. Ölveczky et al. (2003) reported the presence of *object motion sensitive* (OMS) cells, which respond to differential motion of objects

against the background motion. Münch et al. (2009) reported the presence of *approach sensitive* ganglion cells. These cells responded to an expanding spot similar to an approaching object. It is speculated that these cells are useful to detect an approaching threat such as a predator. These cells are similar to *looming detectors* reported in the frog retina (King et al. 1999, Ishikane et al. 2005), but the underlying mechanism is different for frogs and mouse. Another interesting type of response is the *omitted stimulus response* (OSR) described by Schwartz et al. (2007). When the retina is presented with periodic flashes, with one flash in the sequence omitted, some cells respond with strong spiking activity to the missing stimulus. Thus it is evident that these cells report an abrupt change in the stimulus pattern. Bölinger and Gollisch (2012) recently reported that a subset of ganglion cells in the axolotl retina is specialized in detecting spatially homogeneous stimuli. These cells, known as *homogeneity detectors*, are particularly useful in the detection of large objects. More recently, Zhang et al. (2012) showed in the mouse retina a special cell type W3, which is active only to small moving objects on a featureless background. These cells remain silent to most of the other natural stimuli and are specialized in providing alarm signals by responding only to distant predators in the sky.

Feature detection was initially thought to be present only in the lower vertebrates. However, the discovery of more such types in different mammalian species has changed this notion. Thus, the increasing evidence shows that the processing in the retina extracts several interesting features and probably projects to distinct regions of the brain also in primates and humans (Field and Chichilnisky 2007, Schiller 2010).

1.4 Beyond the Receptive Field

The receptive field region of a ganglion cell corresponds to a roughly concentric area of a few hundred micrometers, over which the cell collects its inputs (Kuffler 1953). Kuffler (1953) showed that the receptive field has a concentric centre and an antagonistic surround. For several decades, however, it has been known that the cell's responses to stimuli in its receptive field can be modulated by the visual signals outside the receptive field in the far-surround. A rapid shift or motion of the image in the periphery can modify various response characteristics of a ganglion cell, including contrast sensitivity and response dynamics (McIlwain 1964, Krüger and Fischer 1973, Fischer et al. 1975, Barlow et al. 1977, Enroth-Cugell and Jakiela 1980, Geffen et al. 2007). Hence, the region remote to the cell's classical receptive field has been denoted as 'extra-classical receptive field' (Passaglia et al. 2009).

The effects of remote stimulation have been studied in the retina of several species including, salamander (Werblin 1972, Cook and McReynolds 1998), turtle (Schwartz 1973), cat (McIlwain 1964, 1966, Barlow et al. 1977), rabbit (Watanabe and Tasaki 1980, Taylor 1999), guinea pig (Demb et al. 1999) and monkey (Solomon et al. 2006), and have been called 'shift effect' and 'periphery effect'. In salamander retina, the global motion activates glycinergic amacrine cells which in turn inhibit ganglion cells (Werblin 1972, Werblin and Copenhagen 1974, Thibos and Werblin 1978, Cook and McReynolds 1998). By contrast, in mammals there are contradictory reports that show remote stimulation causing both excitation (McIlwain 1964, 1966, Krüger and Fischer 1973, Noda and Adey 1974b, Fischer et al. 1975, Barlow et al. 1977, Ross et al. 2001) and inhibiton (Enroth-Cugell and Jakiela 1980, Demb et al. 1999, Taylor 1999, Flores-Herr et al. 2001). Although these effects were known for several decades, the cellular mechanism has been elusive. Also their role in active vision is poorly understood. The remote stimulus is relevant in the context of global motion of stimuli, such as saccadic eye movements. In this study, we revisit some of the issues and study them in relation to saccadic eye movements.

1.5 Eye Movements and Image Representation

Eye movements or "saccades" are an essential feature of natural vision in almost all vertebrates, even for lower vertebrates and insects (Land 1999). One hypothesis is that eye movements are made to stabilize gaze against the body movements of the animal and to constantly relocate gaze to scan the visual scene. In a series of elegant experiments, Yarbus (1967) demonstrated the presence of eye movements in humans. One thing that is clear from the human and animal observations is the pattern of eye movements - brief fixations interrupted by fast ballistic saccades (Fig. 1.4). Thus, the image on the retina is acquired as a brief snapshot and abrupt image motion. The information transmission of the retina should accommodate these abrupt changes and periods of fixation.

It has been shown that the saccade-like image shifts strongly modulate the activity of a ganglion cell. Noda and Adey (1974b) showed that saccadic eye movements elicited strong spiking activity in some ganglion cells of the cat retina, whereas Roska and Werblin (2003) showed suppression of activity in some ganglion cells of the rabbit retina. Moreover, the initial period of fixation has been shown to provide the most information about object size in archer fish retina (Segev et al. 2007). In rabbit retina, the sudden changes in mean luminance induced by saccade-like shifts elicits a variety of

responses in different ganglion cells ranging from strong activation to strong suppression (Amthor et al. 2005). In salamander retina, certain OFF ganglion cells change their response polarity transiently to ON-like after a saccade-like image shift (Geffen et al. 2007).

The studies mentioned above have found several interesting responses during a saccade. However, it is not known how the subsequent fixations are represented. It is also not known how the history of the saccade or the previous fixation modulates the response of the current fixation. In the current study, we address these questions by analysing the ganglion cell responses to stimuli mimicking saccadic scene changes.

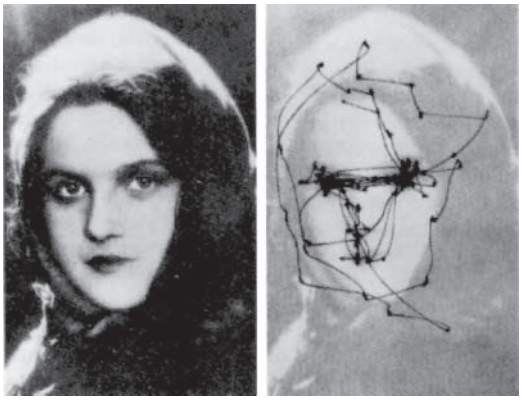

Figure 1.4: Saccadic eye movements. Eye movements for a duration of one minute are recorded (right) from an observer viewing a picture (left). Note that the eyes fixate and make a saccade to a new location of interest on the picture (Yarbus 1967; image adapted from Martinez-Conde et al. 2004).

1.6 Aims of this Study

Natural vision such as a saccadic scene change provides complex spatio-temporal visual input to the retina. However, the information processing in the retina is usually studied with much simpler stimulus conditions, which do not reveal the coding strategies for natural vision. Here we address this problem by studying the retinal coding under saccadic vision. The central goal of this thesis is to understand the retinal information processing in the presence of eye movements. We approach this goal by dividing the study into two parts: 1) to understand the retinal encoding of saccadic scene changes; 2) to understand how the global motion signals induced by saccades interfere with the ganglion cell response to local stimuli.

In the *first part* of the study (Chapter 3), we ask what the responses of ganglion cells are during a fast and ballistic saccade and how the saccades are represented in the retinal output. Furthermore, we aim to understand the encoding of fixations after a saccade and ask if the saccadic motion and the fixation prior to the saccade influence the response to the newly fixated image after a saccade. Finally we test if the saccadic vision reveals any feature detectors in the retina. In the *second part* of the study (Chapter 4), we address how the global motion signals induced by saccades influence the encoding of local stimuli incident on the cell's receptive field. More precisely, we aim to understand the changes in ganglion cell's filtering properties and its sensitivity to visual stimuli.

2. Experimental Methods

In this chapter, we describe the experimental procedures for measuring the ganglion cell activity using multi-electrode arrays. We provide the details of tissue preparation, electrophysiology and our approaches in analysing the data. We also discuss the rationale for using the mouse as a model system in the present study.

2.1 Animals

We investigated the retina of adult mice (*Mus musculus*, C57BL6/J) for this study. Our choice of mouse as a model system is made for the following considerations.
1) The mouse retina lacks a fovea, and thus the entire retina is comparable to the peripheral retina of primates. Another interesting feature is the near homogeneous distribution of ganglion cell types in the mouse retina (Jeon et al. 1998, Sun et al. 2002, Badea and Nathans 2004). This is particularly advantageous as the recordings of retinal ganglion cells are independent of eccentricity or retinal location.
2) Mouse retina has $\approx$ 20 types of RGCs (Völgyi et al. 2009) similar to the primate retina (Field and Chichilnisky 2007).
3) The visual system of the mouse is extensively studied, from the retina up to the extrastriate cortex (Huberman and Niell 2011, Niell 2011, Andermann et al. 2011, Marshel et al. 2011). The present schema of the mouse visual system includes the putative dorsal stream and ventral stream ("where" and "what" pathway; see Wang and Burkhalter 2007, Wang et al. 2011).
4) In an elegant set of behavioural experiments, Naarendorp et al. (2010) showed that the mouse vision is comparable to that of human peripheral vision.

Furthermore, the availability of a variety of genetic tools makes the mouse a key species in vision research. Due to the reasons mentioned above, the mouse as a model system for vision research is gaining importance in the past decade (Huberman and Niell 2011).

Therefore, the results of our study from the mouse retina are readily comparable to the results from other laboratories interested in mouse vision in a larger context.

2.2 Tissue Preparation

All experimental procedures were performed in accordance with institutional guidelines of the Max Planck Institute of Neurobiology, Martinsried, Germany. A mouse was dark adapted for at least 30 min, sacrificed by cervical dislocation, and eyes were enucleated quickly and kept in oxygenated (95% O_2 and 5% CO_2) Ames' medium buffered with 22mM $NaHCO_3$ to maintain pH 7.4 (Sigma-Aldrich, St. Louis, USA; Ames and Nesbett 1981). In some eyes, the superior part was marked before enucleation to know the axes of the tissue. The eyes were then hemisected under a stereo zoom dissection microscope (model SZX7, Olympus, Japan) equipped with infra-red illumination and a pair of night vision goggles (model PS-14, ATN Corporation, San Francisco, USA) attached to the microscope's eye pieces. The posterior eye-cup was stored in oxygenated Ames' medium at room temperature till further use. The retina was isolated from the eye-cup just prior to the electrophysiology experiments. We have observed that it is critical to complete the dissection within 10-15 min to get a healthy retina and stable recordings, as has been noted by others (Wei et al. 2010). All the procedures mentioned above were carried out in a dark room, with minimal dim red light illumination when necessary.

2.3 Electrophysiology

Spike trains of ganglion cells were recorded using planar microelectrode array (MEA; Multi Channel Systems, Reutlingen, Germany) with 60 electrodes, each of 10 µm diameter and a minimum spacing of 100µm between the electrodes(Fig. 2.1; see tom Dieck et al. 2012). One half of the retina with ganglion cell side down was placed on the electrode array and gently held in place by a dialysis membrane attached to a plastic holder. Prior to mounting on the electrode array, the vitreous humour was removed carefully from the retina to improve better contact with the electrodes. The retina was continuously superfused with oxygenated Ames' medium at 8-10 ml/min. The medium was warmed with an in-line heater (model PH01; Multi Channel Systems) just before it entered the MEA recording chamber which was also maintained between 33°C and 35°C. We rested the preparation in this setting for at least 45-60 min before the start of the recording to ensure better contact of electrodes and good signal-to-noise ratio. The temperature and flow rate were continuously monitored; constant temperature and flow

rate of the medium proved critical to achieve stable recordings of at least 3-4 hours. Voltage traces from electrodes were amplified, band-pass filtered between 300 Hz and 5 kHz and stored digitally (25 kHz sampling rate) for offline analysis.

2.4 Visual Stimulation

Visual stimuli were generated by custom written software in C++ with OpenGL libraries. The stimulus display on a cathode ray tube (CRT) monitor was projected onto the photoreceptor layer of the retina using a mirror and projection lens. Each pixel of the monitor impinged on a 6 µm x 6 µm area on the retina. The 100 Hz temporal refresh rate of the monitor was fast enough to be assumed as a continuous image for the retina. A light-tight Faraday's cage around the recording set-up ensured that the retinas were driven only by the visual stimuli presented. All the stimuli used in this study were in photopic light levels. We used two set-ups with monitor intensities 10.19 mW/m^2 and 18.23 mW/m^2, and did not find any difference in the results. We also simultaneously generated a small light pulse in a corner of the stimulus monitor during every change in the stimulus. We recoded this pulse using a photodiode, which served as a marker for stimulus timing.

2.5 Spike Sorting

Recording using microelectrode array poses significant challenges in identifying and isolating spikes from a single cell. There are two main issues to be considered: 1) signals from two or more cells could be picked up by one electrode, 2) signals from one cell could be picked by two or more electrodes. These issues were addressed by spike shape cluster analysis, considering spike shape as a 'signature' of each cell (Pouzat et al. 2002). Spikes of different shapes were assigned to different clusters and thus to different cells. Also, spike events with identical timings in neighbouring channels (i.e., electrodes) were taken together as one cluster and thus as signal from one cell. In this way duplication of the same cell was avoided. Only well separated clusters with a clear refractory period between the spikes were used in this study. Spike sorting incorporating these principles were done using custom-written software (originally developed by Dr. Ofer Mazor, Harvard University, Cambridge, USA) in Igor Pro 6.03A (WaveMetrics, Lake Oswego, USA). We also routinely marked and isolated axonal spikes by their typical triphasic shape.

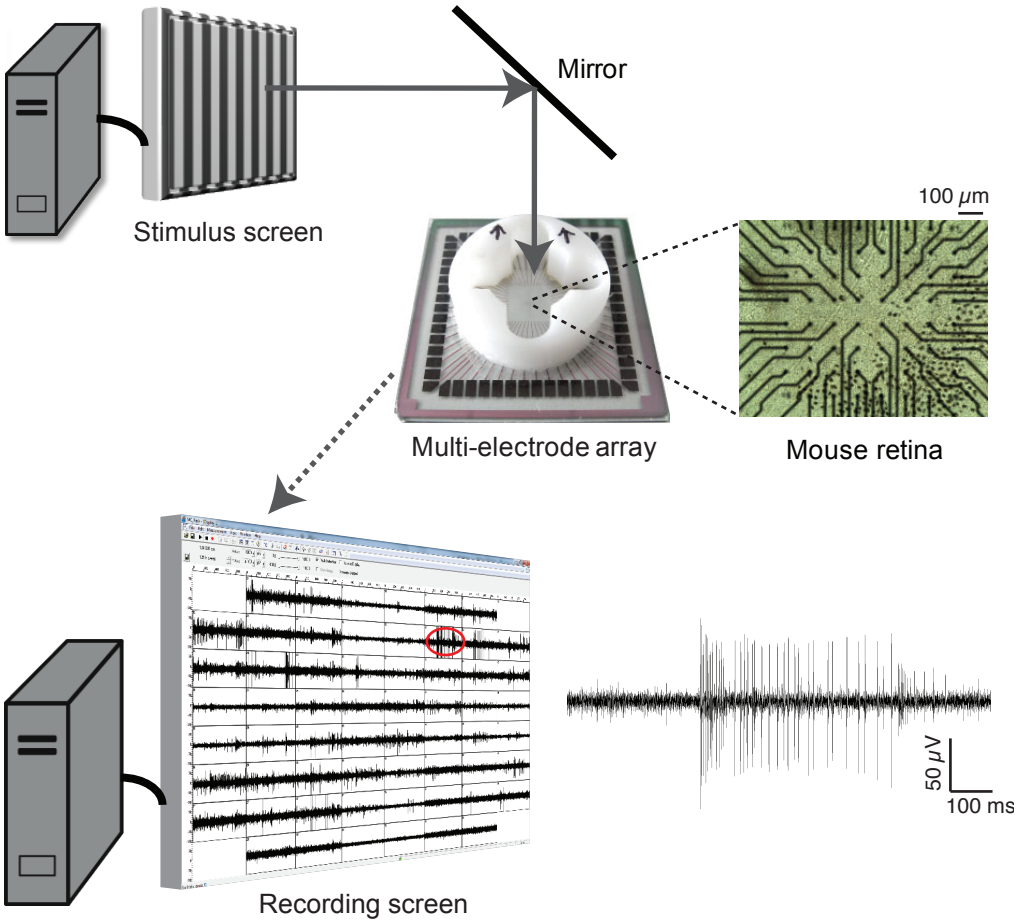

Figure 2.1: Schematic illustration of the electrophysiology set-up. The visual stimulus generated on a computer screen is projected on to the retina mounted on a multi-electrode array. The voltage traces from several channels are amplified and stored in a recording computer for further processing and analysis. A sample voltage trace from one channel (highlighted in red on the recording screen) is shown on the lower right.

2.6 Basic Characterization of Ganglion Cells

Retinal ganglion cells were characterized by a series of stimuli to reveal their basic cellular properties. The characterization included, polarity of response (ON, OFF, ON-OFF), receptive field estimation, X and Y cell analysis, direction selectivity and linear-nonlinear systems analysis. Characterizing the ganglion cells is an important step before analyzing them for a novel stimulus of interest.

2.6.1 Polarity of Response

The fundamental characterization of a ganglion cell is its response polarity. Hartline (1938) found that some cells respond to light increments, some respond to light decrements, while others responded to both. To determine the response polarity, we presented a full field square wave light step stimulus with step duration of 500ms. Thus, the stimulus consisted of a full step increment and a full step decrement of light level. Spike responses were recorded for a duration of 2-3 min. Cells responding to increment steps were classified as ON cells, those responding to decrement steps as OFF cells and those responding to both increments and decrements as ON-OFF cells (Fig. 2.2).

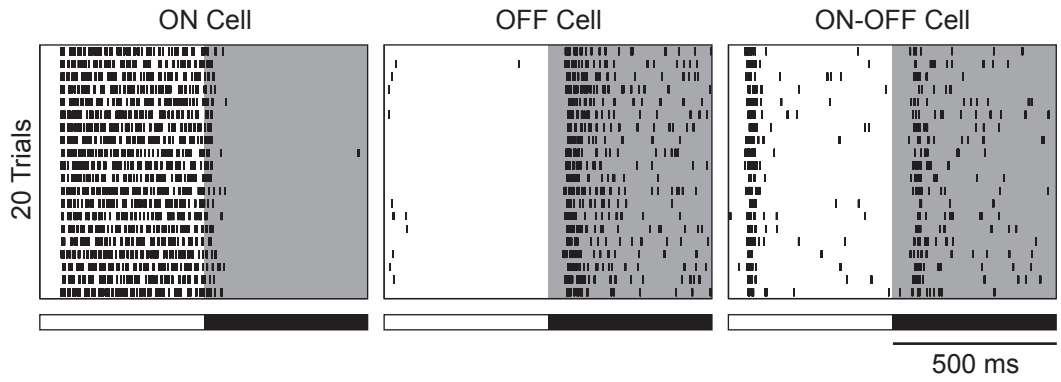

Figure 2.2: ON, OFF, ON-OFF cells. The ganglion cells were classified based on their response to periodic flashes of light. For each representative cell type, responses to 20 successive presentations are shown. Stimulus phase is indicated at the bottom of each panel.

2.6.2 Spike Triggered Average

We analysed the ganglion cell for its filtering properties, which is given by 'spike-triggered analysis'. We stimulated the retina with a pseudorandom Gaussian white

noise stimulus, where the intensity of the full field stimulus was changed every 20ms (Fig. 2.3 A). A short temporal window of stimulus preceding every spike is collected to give an ensemble of stimuli that elicited the response of a cell (Fig. 2.3 B). An average of such a stimulus ensemble is referred to as *spike triggered average* (STA; Fig. 2.3 C), which is given by

$$A = \frac{1}{N} \sum_{i=1}^{N} s_i$$

where, N is the total number of spikes, and s_i is the stimulus vector preceding spike i. The shape of the STA also reveals the response polarity of the cell. A positive peak preceding a spike represents the cell's preference of light increments and thus corresponds to an ON cell (Fig. 2.3 C *left*). Similarly, a negative peak represents an OFF cell(Fig. 2.3 C *right*). However, the classification based on STA does not allow the identification of an ON-OFF cell and all the cells are classified as either ON or OFF.

The STA also represents the linear filter of a cell (Chichilnisky 2001, Schwartz et al. 2006). The biphasic shape of the STA corresponds to the sensitivity of the cell to temporal frequency of the stimulus. For example, an increased biphasicness could be interpreted as a decreased sensitivity to low temporal frequencies.

2.6.3 Receptive Field Estimation

The response of a ganglion cell is influenced best by a light stimulus in a restricted area of visual space. The region on the retina which collects the stimulus of this region is commonly referred to as 'receptive field' (Kuffler 1953). The receptive field of a ganglion cell is estimated by a white noise analysis (Chichilnisky 2001). We stimulated the retina with a pseudorandom binary white-noise flickering checker-board stimulus. Each field of the checker-board was 60µm on a side and was changed randomly to either black or white every 20ms (Fig. 2.4 A). The average 800ms stimulus preceding every spike was computed. This average stimulus has two parts - time course of the stimulus and spatial location. A 2D Gaussian fit of the spatial part is used as a best approximation of the receptive field of the ganglion cell (Fig. 2.4 B). This method identified the receptive field size and position of many simultaneously recorded cells. In a typical recording we obtained a heterogeneous population of about 15 - 30 cells with different receptive field sizes (Fig. 2.4 C).

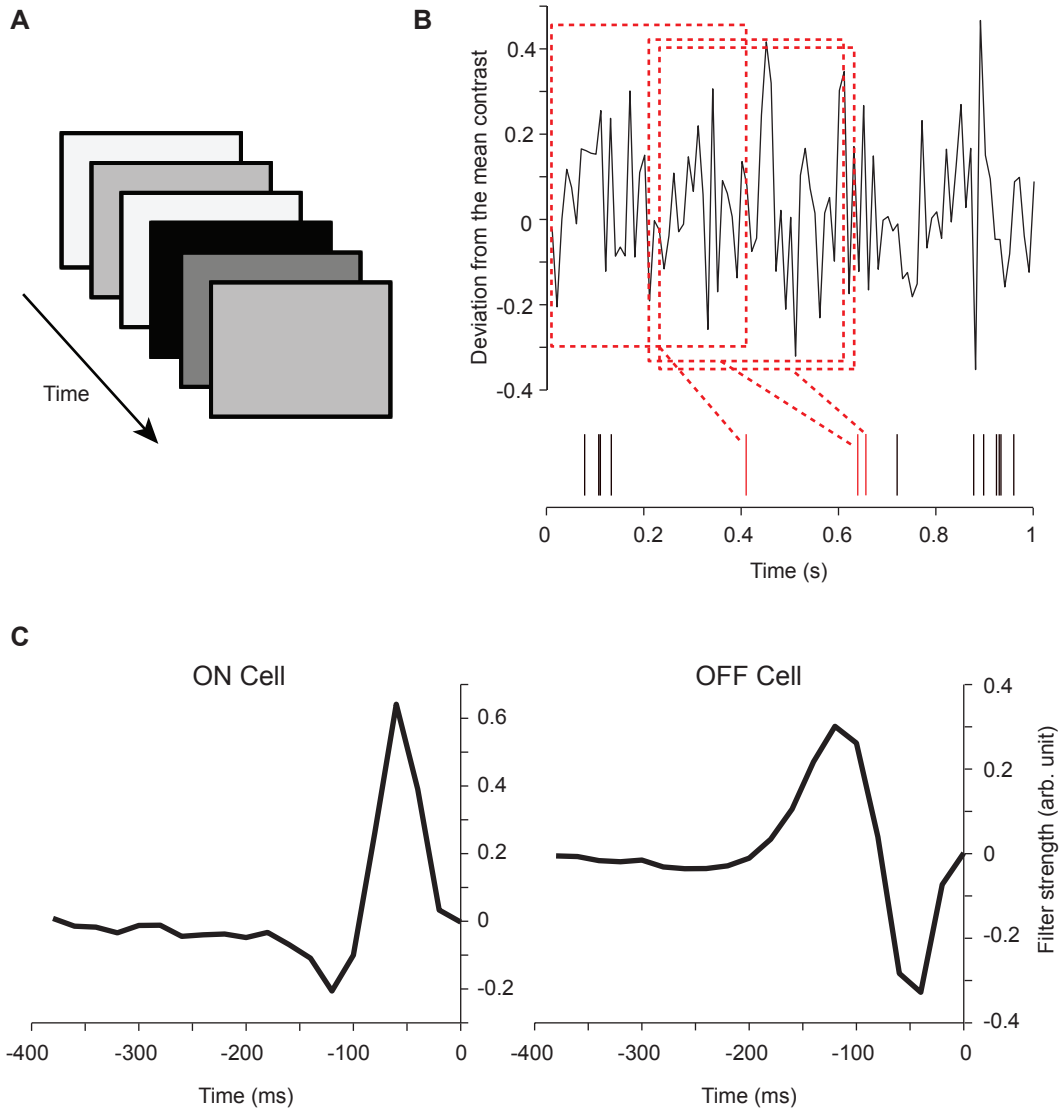

Figure 2.3: Spike triggered average (STA). A) Schematic of a Gaussian white noise stimulus. The intensity of the stimulus screen was changed every 20 ms with values drawn randomly from a Gaussian distribution. B) A sequence of stimulus where the light intensity deviation from mean contrast is plotted as a function of time and the response of a ganglion cell is shown below. The average stimulus segment preceding every spike (illustrated in red box for three sample spikes in red) is computed to produce a "spike triggered average (STA)". C) STAs for an ON cell and an OFF cell. Time zero is the occurrence of a spike. The temporal STA represents the linear filter of a cell. Note the biphasic shape of the filters in the examples shown here. Different cells exhibit varying levels of biphasic shape which represents the sensitivity to temporal frequencies of the stimulus.

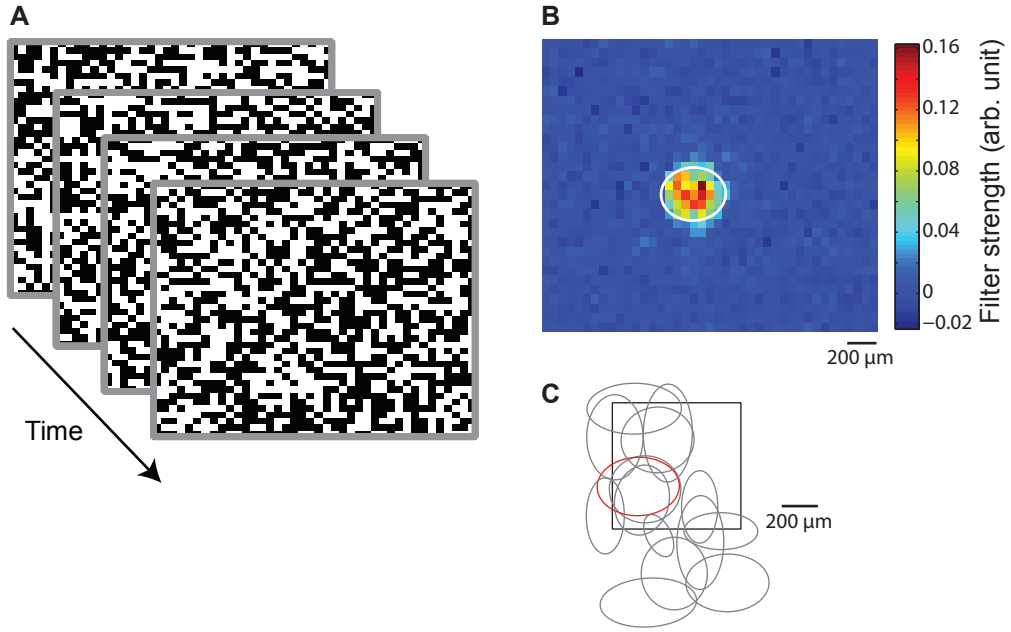

Figure 2.4: Receptive field estimation. A) Spatio-temporal binary white noise stimulus, where each square (or stixel) in the flickering checker-board was changed to either black or white every 20 ms in a pseudorandom fashion. The size of each square on the retina is 60 x 60 µm^2. Shown here are sample screen-shots of stimulus appearing 20 ms apart. B) Spatial component of spike triggered average (STA), resolves the region of stimulus that evoked spikes. A 2D Gaussian fit (white ellipse) is the best approximation of a ganglion cell's receptive field centre. Note that this measurement does not reveal the receptive field surround. C) Receptive fields of 15 cells recorded simultaneously. Red ellipse is the receptive field of the cell shown in B. Note the different sizes of receptive fields. The square indicates the outline of the 60 electrode array (700µm x 700µm). Receptive fields lying outside the electrode array region were measured from the cells' axons passing through the recording region.

2.6.4 X- and Y- Cell Analysis

Ganglion cells can be classified into two functional classes - *X-like* cells with linear summation over their receptive fields and *Y-like* with non-linear summation (Enroth-Cugell and Robson 1966). We identified the cells as X-like and Y-like based on their response profile to reversing sinusoidal grating stimuli. A sinusoidal grating with bar width of 480µm was presented. The intensities of the grating was reversed every 560ms. After 30 repetitions of each reversing grating, the spatial phase of the grating was shifted by 45°. Thus reversing gratings in eight spatial phases were presented. X cells responded with a preferred and null phase, whereas Y cells responded to all the phases

(Enroth-Cugell and Robson 1966). We applied Fourier analysis to deduce the first harmonic (F1) and the second harmonic (F2) components of the response amplitudes. Y cells had a strong second harmonic response component (i.e. F2>F1), whereas X cells did not (Hochstein and Shapley 1976, Freeman et al. 2010). We also calculated a *nonlinearity index*, which is the ratio of the mean of the second harmonic to the maximum of the first harmonic for all spatial phases (Hochstein and Shapley 1976, Carcieri et al. 2003) to objectively classify the cells. Cells with nonlinearity index > 1 were classified as Y-like, < 0.5 as X-like and between 0.5 and 1 as intermediate types (Fig. 2.5).

2.6.5 Direction Selectivity

A subset of ganglion cells in the mouse retina is direction selective (Weng et al. 2005, Sun et al. 2006, Elstrott et al. 2008, Kim et al. 2008). We identified the direction selective ganglion cells by presenting a full-field drifting square wave grating (700µm /period) stimulus in eight different directions. The stimulus lasted for 5 s in one direction, followed by 2 s grey screen, followed by 5 s drifting grating in a different direction and so on. We presented two variations of the stimulus (1s /period; velocity 22.5° /s; or 0.5s /period; velocity 45° /s), with no difference in the results. The average spike rate, $r(\varphi)$ for each direction φ was calculated and represented in a polar plot (Fig. 2.6 A). We calculated the mean preferred direction φ_p as the angle of vector sum in a polar plot of responses,

$$\varphi_p = arg \sum_k r(\varphi_k) e^{i\varphi_k}$$

where, the eight directions are given by $\varphi_k = 0°$, 45°, 90°, 135°, 180°, 225°, 270°and 315°.

We computed a direction selective index which is the length of the vector sum divided by sum of all responses,

$$D = |\sum_k r(\varphi_k) e^{i\varphi_k}| / \sum_k r(\varphi_k)$$

The index ranges from 0 to 1, where 0 represents for a cell with equal responses in all directions and 1 represents a cell responding in only one direction. We classified cells with index ≥ 0.2 as direction selective.

Apart from direction selective cells, we also found *orientation selective* cells (Fig. 2.6 B, C) in the mouse retina. These cells responded to either vertically or horizontally oriented

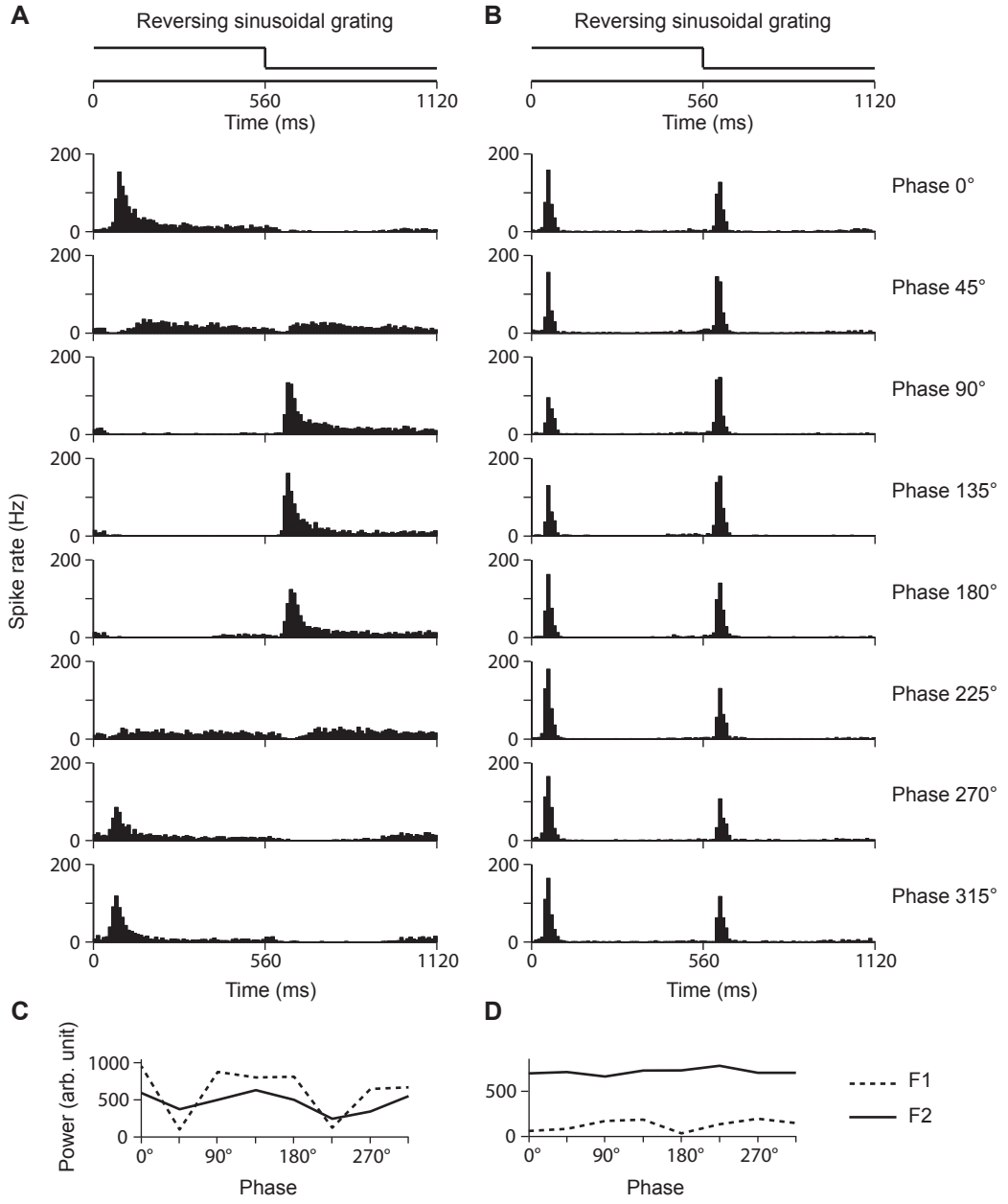

Figure 2.5: X- and Y-cell analysis. Ganglion cells were classified based on their property of stimulus integration over space. A sinusoidal grating stimulus with a stripe width of 480µm was presented. The stripe intensities were reversed every 560 ms as indicated in top panels in A and B. After 30 repetitions of each reversing grating, the spatial phase of the stimulus was shifted by 45°. A) A representative X-like cell, which responded to only one phase of the reversing grating, indicating linear summation of stimulus. Note that the phases 45°and 225°are "null phases" with no response. B) A representative Y-like cell, which responded to both the phases of the reversing grating, indicating nonlinear summation of stimulus. C & D) Fourier analysis of response amplitudes of X-cell and Y-cell illustrated in A and B respectively. Note that typically F1 > F2 for X-cell and F2 > F1 for Y-cell.

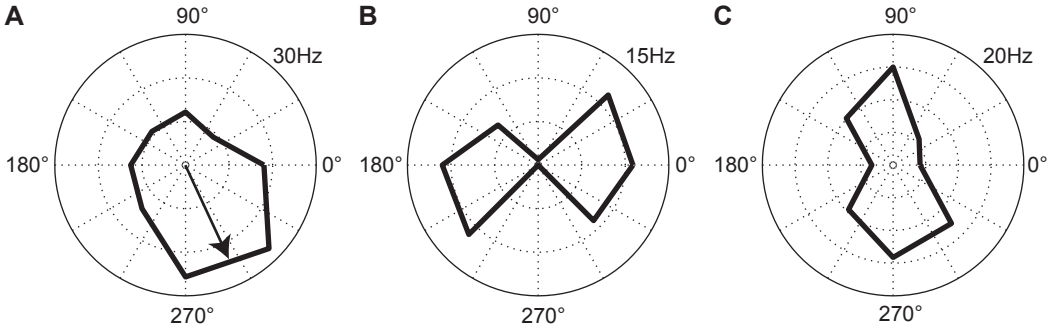

Figure 2.6: Direction and orientation selectivity. Polar plots showing mean spike rate of responses to square-wave grating motion is eight directions. The mean spike rates were computed for 30 repeats of the stimulus each direction. A) An example of direction selective cell. The arrow indicates the mean preferred direction of the cell. B) An example of a vertical orientation selective cell. This cell responded to preferably vertical grating moving in orthogonal axis in both the directions. C) An example of horizontal orientation selective cell. This cell responded to preferably horizontal grating moving in orthogonal axis in both the directions.

stimulus moving in either of the orthogonal directions. Orientation selective cells have been described in the rabbit retina (Levick 1967, He et al. 1998, Venkataramani and Taylor 2010), but there are no reports for mouse retina to date. This study is the first report to identify both vertical and horizontal orientation selective cells in the mouse retina.

3. Encoding of Saccadic Scene Changes

3.1 Eye Movements and Vision

Fast and sudden eye movements known as 'saccades' form an essential feature of visual behaviour (Land 1999). We make saccades to scan our visual scene in everyday life. The scene could be static - like a picture of a face (Yarbus 1967), or dynamic - like a game of cricket (Land and McLeod 2000). The strategy for most animals including humans is to constantly reposition the gaze to different target locations in the scene by making ballistic saccades (Land 1999). Thus the visual information acquired by the retina is a sequence of brief 'snapshots' interrupted by saccadic 'motion blur'. In such a scenario, the information transmitted by the retinal ganglion cells is critical for the downstream brain centres to make sense of the visual world (Barlow 1981, Meister and Berry 1999). How does the retina cope with such impending saccades and encode information reliably about our visual world?

Saccade-like image shifts are known to strongly modulate the activity of a retinal ganglion cell. Noda and Adey (1974b) showed that saccadic eye movements elicited strong spiking activity in some ganglion cells of cat retina, whereas Roska and Werblin (2003) showed suppression of activity in some ganglion cells of rabbit retina.

Little is known, however, about how the responses to saccade-like motion signals interact with the encoding of image content at the subsequent fixations. Earlier investigations about coding strategies of fixations revealed some interesting phenomena. The initial period of fixation has been shown to provide the most information about object size in archer fish retina (Segev et al. 2007). In rabbit retina, sudden changes in mean luminance induced by saccade-like shifts elicits a variety of responses in different ganglion cells ranging from strong activation to strong suppression (Amthor et al. 2005). In salamander retina, certain OFF ganglion cells change their response polarity

to ON-like for a brief period, after a saccade-like image shift (Geffen et al. 2007). These studies taken together underscore that saccades modulate the ganglion cell response to a fixated image. However, these reports did not take into account the history of the fixated stimulus. In other words, it is not known how the stimulus history (i.e., the saccade and an earlier fixation) shapes the response to the current fixation (i.e., the visual 'snapshot' of the world).

In this study, we address this question by analysing ganglion cell responses in isolated mouse retina to simulated saccadic scene changes. For half of the recorded ganglion cells, we found strong spiking activity during saccades. This supports the idea that the retina actively encodes the saccade and may signal abrupt scene changes to the downstream centres. Furthermore, we characterized the responses to the newly fixated image. While there appears to be only little influence of the motion signal itself on the responses, the responses depended strongly on the history of the stimulus before the saccade. This suggests that retinal signals under saccadic vision may encode image transitions rather than the currently fixated image. Based on this analysis we classified the ganglion cells into five response types.

3.2 The Saccade Stimulus

The stimulus in our experiments was designed to mimic a saccade-like scenario with brief image fixations separated by global motion. The saccade duration of 100 ms and amplitude range of 8°to 40°was chosen to be approximately close to that observed in mouse (duration: $\approx$ 60ms and average amplitude: $\approx$ 14°; maximum amplitude: $\approx$ 40°; Sakatani & Isa, 2007). The duration of fixated image was 800ms, chosen to be slightly longer than average fixation of $\approx$ 300ms to $\approx$ 400ms observed in many animals. The slightly longer duration of fixation ensured that each fixation influenced only the next fixation and not the subsequent fixations. This way, for each fixation we minimized the effects of 'history of history'. So the stimulus was a sequence of 800ms fixations separated by 100ms saccade-like transitions.

Fixation Images: The fixation images consisted of square-wave gratings at four different spatial phases(Fig. 3.1 B). These four different images were labelled as image No. 1, No. 2, No. 3 and No. 4. The sequence of these fixation images was chosen in a pseudorandom order. The width of each bar of the grating was either 240µm or 120µm. The bar width was chosen in such a way that it covers the receptive field centre of a small cell (receptive field <150µm).

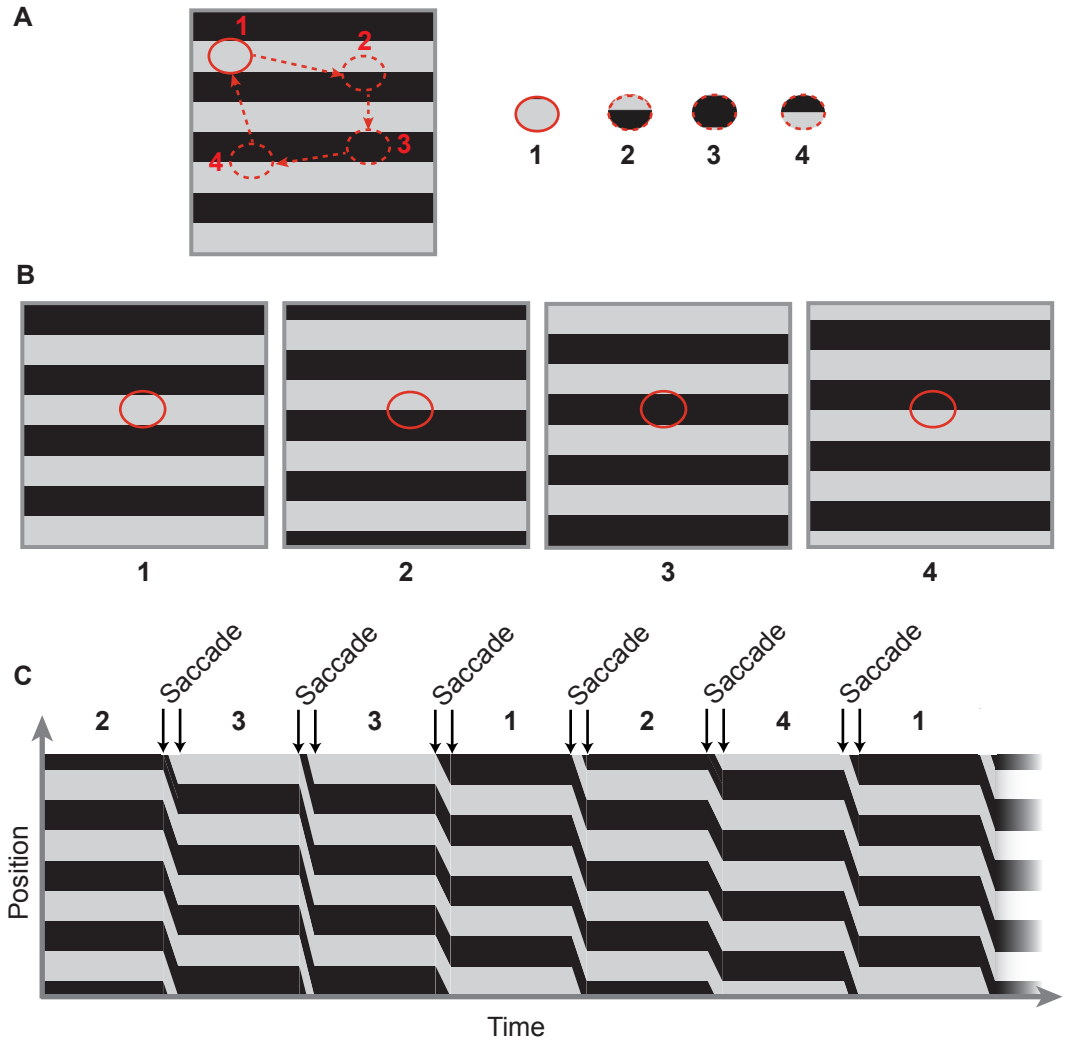

Figure 3.1: The saccade stimulus. A) A schematic illustration of saccadic eye movements, when an observer views a stationary grating. The fixations at four regions of interest are indicated as 1, 2, 3 and 4. The ellipses at each of those fixations indicate the receptive field of a ganglion cell. The image for a ganglion cell is different at each of these fixations as shown in the right. Note that another ganglion cell would experience a completely different image, thus creating several possible images for a cell even when viewing a simple grating shown in this example. The possibilities also increase due to the fact that there are several cell classes with varied receptive field sizes. B) Since the retina is stationary in our recording set-up, we mimicked the fixations by presenting stationary grating at four different spatial phases each labelled 1, 2, 3 and 4. C) The stimulus configuration. A saccadic scene change is mimicked by presenting a sequence of fixation and saccade-like motions by shifting the image. The fixation images are chosen randomly from one of the four images depicted in B. Refer to Table 3.1 for different spatio-temporal parameters of stimulus used in this study.

	Grating period (µm)	Fixation duration (ms)	Motion duration (ms)	Motion period	Saccade amplitude (µm on retina)	Saccade amplitude (degrees)
Stimulus 1	480	800	100	≈ 2	480, 720, 960 or 1200	16°, 24°or 32° or 40°
Stimulus 2	480	800	100	≈ 1	240, 360, 480 or 600	8°, 12°, 16° or 20°
Stimulus 3	240	800	100	≈ 2	240, 360, 480 or 600	8°, 12°, 16° or 20°

Table 3.1: Parameters of different saccade stimulus used in this study

Transition: The transition between fixation images lasted for 100ms. The transition from one fixation to the next fixation in the sequence mimicked a saccade-like motion (Fig. 3.1 C). That is, the fixated image moved for approximately one full period depending on the next image. We also ensured the shifts are at least half a period or more to avoid shorter amplitudes such as one-fourth period. For a stimulus with grating bar width of 240µm, consider a sequence of fixations images 3, 3, 1, 2. The transition from 3 to 3 would be a motion of one period of grating, the transition from 3 to 1 would be half a period and transition from 1 to 2 would be one and one-fourth of a period. For stimulus with grating bar width 120µm the transition was approximately two periods so that the motion distance covered across the visual space is the same for both the stimuli. The distances covered by motion in both the stimuli were 240µm, 360µm, 480µm and 600µm, on the retina. These values correspond to approximately 8°, 12°, 16° and 20° of visual angle for a mouse, as 1° of visual angle corresponds to 31 µm on the retina (Remtulla and Hallett 1985).

3.3 Analysis of Responses to the Saccade Stimulus

We recorded a total of 114 retinal ganglion cells (RGC) from six retinas isolated from five mice. We tested different variants of the saccade stimulus (Table 3.1) initially. We did not find major differences in RGC response to these stimuli and we performed

majority of our experiments with Stimulus 3 (see Table 3.1). So we combined the results from all the three stimuli from different retinas.

We analysed the RGC responses to both the saccade-like motion and the fixation after a saccade. For a sample cell illustrated in Fig. 3.2 A, we analysed the stimulus transition image 1➔ image 2. This cell did not respond to the presentation of image 1 or to the saccade-like motion, but there was an increase in firing rate ≈ 70ms after image 2 appeared. We call the image 1 in this transition as the '*starting image*' and image 2 as the '*target image*', considering this image to be target of the saccadic gaze shift. Thus, the short stimulus sequence illustrated in Fig. 3.2 A is "*starting image - saccade - target image*". From looking at this transition alone, it appears that the cell prefers image 2 over image 1. Since our stimulus consisted of four fixation images (Fig. 3.1 B), 16 possible transition scenarios emerge (1➔1, 1➔2, 1➔3, 1➔4, 2➔1 and so on). We analysed the spike responses to all these 16 transitions, and the results are displayed in one matrix plot, as illustrated in Fig. 3.2 B. Our stimulus presentation was long enough (≈ 15min) to have about 30 repeats of each of these scenarios interleaved and we constructed a peri-stimulus time histogram (PSTH) of the spike responses for each scenario (Fig. 3.2 C). The matrix plot of PSTH revealed the characteristic feature of each cell; its response to each *target image* for different histories of *starting image*. The sample cell illustrated in Fig. 3.2 prefers image 2, almost independent of its stimulus history, and this cell does not respond to saccade-like motion. This response type is the characteristic feature of this cell. Applying the same analysis strategy to all the cells, we found there were different response profiles. We elaborate on each of these response profiles in the next section.

3.4 Five Types of Responses to the Newly Fixated Image

We characterized the response of a ganglion cell to the newly fixated image after a saccade. The analysis of the entire ganglion cell population in our data revealed that different cells had different response patterns, both to target image and saccade-like motion. Based on this analysis we could classify the ganglion cells into different '*response types*'. Of the five types, except *Response Type I*, all types responded to saccade-like motion.

Response Type I - Classical Encoder: Cells that responded to their preferred stimulus irrespective of starting image were classified as '*Classical Encoders*'. The

example cell illustrated here, responded to *target image* 2 preferentially, irrespective of its temporal history (Fig. 3.2 B, C). Although there are some differences in the peak firing rates and response latencies, it is clear that *target image* 2 is the preferred stimulus. In our recordings, we also found cells that had two or rarely three preferred fixated images. The cells of this type were also characterized by their sustained firing pattern (Fig. 3.2 A, B). These characteristics indicate that these cells are most likely analogous to the *pixel detectors* identified in cat (beta cells; Saito 1983) and primates (midget cells; Benardete and Kaplan 1997, Dacey 1993). Furthermore, there was either no response or suppressed spiking activity during the saccade in most scenarios. Roska and Werblin (2003) described similar cells that were strongly suppressed by saccadic shifts in the rabbit retina. However, they did not analyse the fixations after the saccade. It is likely that the *Classical Encoder* type described by us is a mouse analogue of the cells described in rabbit. *Classical Encoders* formed half of all our recorded cells (n=57 out of 114 cells).

Response Type II - Offset Detector: Surprisingly, we found cells that responded only to the saccade-like motion part of the stimulus and not to any of the fixated images (Fig.3.3). Further experiments (detailed later in Section 3.8) where uniform grey illumination presented in place of motion also produced similar results. Thus

Figure 3.2 *(following page)*: Analysis of RGC response to the saccade stimulus.
A) *Top*: The stimulus sequence *fixation image 1* ➔ *motion* ➔ *fixation image 2*.
Middle: Raster plot show response of a ganglion cell to the 20 interleaved repeats of stimulus sequence shown above. The duration of saccade-like motion is indicated in the grey shaded region. The example cell shown here responded reliably to fixation image 2 but not to motion or fixation image 1.
Bottom: Peri-stimulus time histogram averaged over all the trials shown in the raster plot. Spikes were averaged in 10 ms bins and represented in Hz. The image before the saccade-like motion is designated as *starting image* and the image after the motion is designated as a *target image*. Here only one combination of stimulus is shown, namely *fixation image 1* ➔ *motion* ➔ *fixation image 2*.
B) The voltage traces from extracellular recording shows the responses to all *target images* with different *starting images*. Only the response to motion and initial 300ms of *target image* is shown. The duration of saccadic motion is depicted in grey shaded region. The rectangle at 1➔2 indicates the response window highlighted in A.
C) Peri-stimulus time histograms (PSTH) of responses shown in B. This cell did not respond to the motion in most of the stimulus combinations. Also the cell's preferred responses were to *target image* 2 irrespective of the starting image. We classified such cells with one or more preferred *target images* as *Classical Encoder*.The rectangle at 1➔2 indicates the response window highlighted in A.

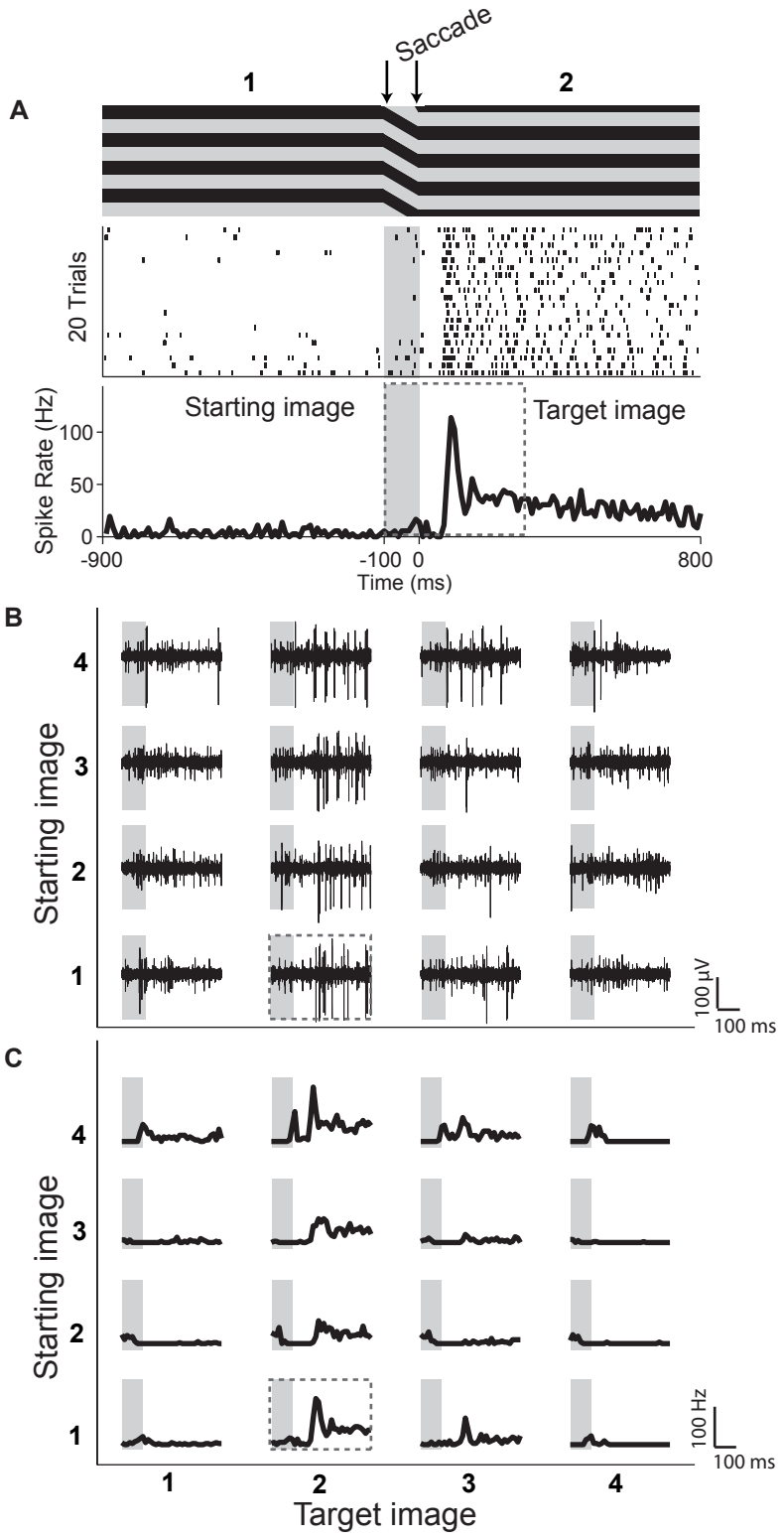
A
Saccade
1
2
20 Trials
Starting image
Target image
Spike Rate (Hz)
100
50
0
-900
-100 0
800
Time (ms)
B
Starting image
4
3
2
1
100 µV
100 ms
C
Starting image
4
3
2
1
100 Hz
100 ms
1
2
3
4
Target image

it was evident that the responses were most likely triggered by the offset of an earlier fixated image (i.e., *starting image*) rather than actual saccade-like motion itself. So they were classified as '*Offset Detector*'. Similar cells that respond to saccade-like motion have been described previously in cats (Noda and Adey 1974b), but the response to the fixation image has not been investigated. It is likely that *Offset Detector* is a specialized feature detector, which preferentially codes for transitions rather than fixations. 12% of the recorded cells were of this type (n=14).

Response Type III - Indifferent Encoder: Another group of cells responded to both saccade-like motion and all the fixation images (Fig. 3.4). Since these cells were indifferent to the stimulus features and responded to all images, we classified them as '*Indifferent Encoder*'. It is possible that these cells are a group of heterogeneous cell types, or the saccadic scene shifts are not the best suited stimulus. These cells may or may not act as feature detectors in saccadic vision. Nevertheless, they report every fixation and every transition. The variation in their peak firing rate and response latencies may be influenced by their immediate temporal history. However, these variations do not affect our present classification, which is based on overall response profile. These cells formed 14% of our recorded cells (n=16).

Response Type IV - Change Detector: This type also responded to saccade-like motion, but it had an interesting pattern in its response to fixation images. The spiking activity to the *target image* was strongly affected by the history of the stimulus before the saccade. It responded to the *target image* only if the starting image was a different one (Fig. 3.5). The responses to fixations after the saccade during the scenarios 1➔1, 2➔2, 3➔3 and 4➔4 were completely abolished (note the diagonal along the matrix plots in Fig. 3.5). Since they responded only to a change in the fixations, we classified them as '*Change Detector*'. This response type is a highly selective feature detector, in that it compares the fixations before and after a saccade and reports if the stimulus is different. In other words, this type encodes the difference across saccades. Although, this type responds to saccadic transition, surprisingly the history even before the saccade strongly influences the responses. Thus, the response to fixations is influenced by a 'temporal context'. This type formed 8% of the cells recorded (n=9). Additionally, the response profile of the cells (8 out of 9 cells) was neither transient nor sustained (Fig. 3.5) with a lower peak firing rate.

Response Type V - Similarity Detector: Saccade-like motion elicited a response in this type also but its response profile to fixations was quite opposite to that of a *Change Detector*. It responded to the target image only if the *starting image* was the same (Fig. 3.6). There was a strong response to fixations after the scenarios only during

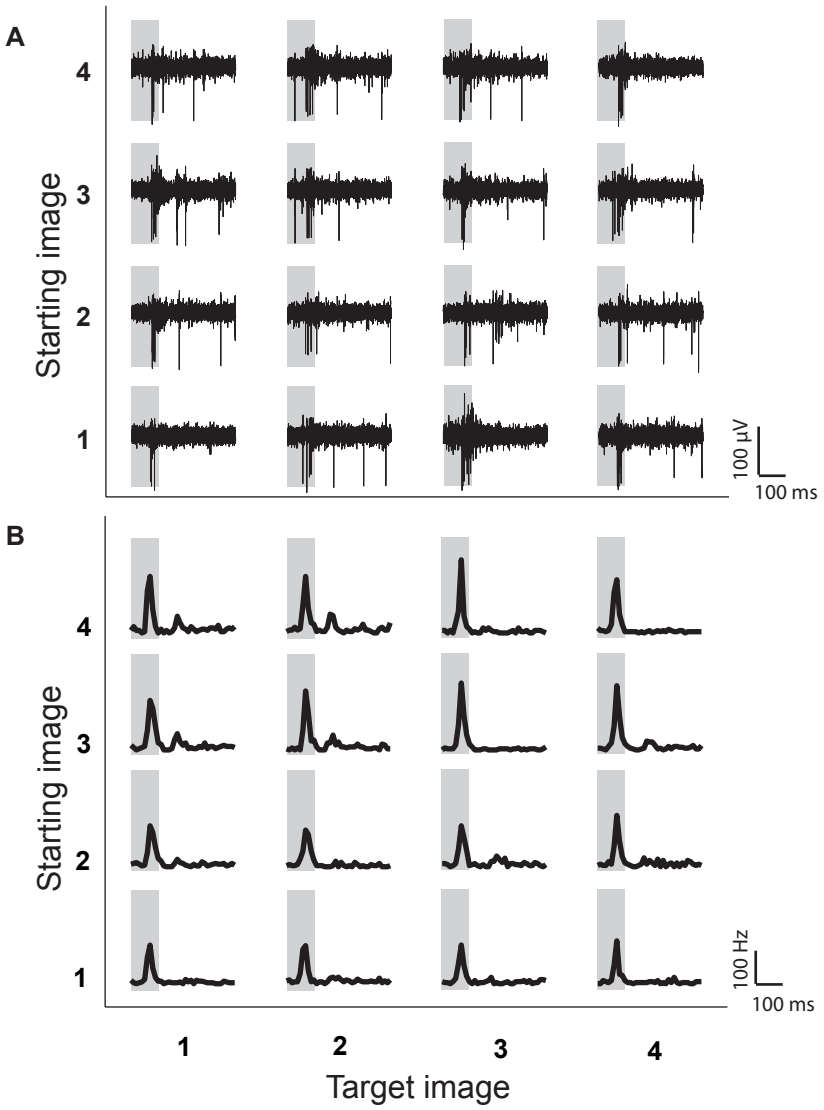

Figure 3.3: Offset Detector. Sample traces (A) and peri-stimulus time histograms (B) show results of a cell that responded preferably to saccadic motion (grey shaded region) rather than for any of the fixated images. The responses are most likely to offset of the *starting image* rather than saccadic motion (see text for details). We classified such cells as *Offset detector*. Conventions are as in Fig. 3.2.

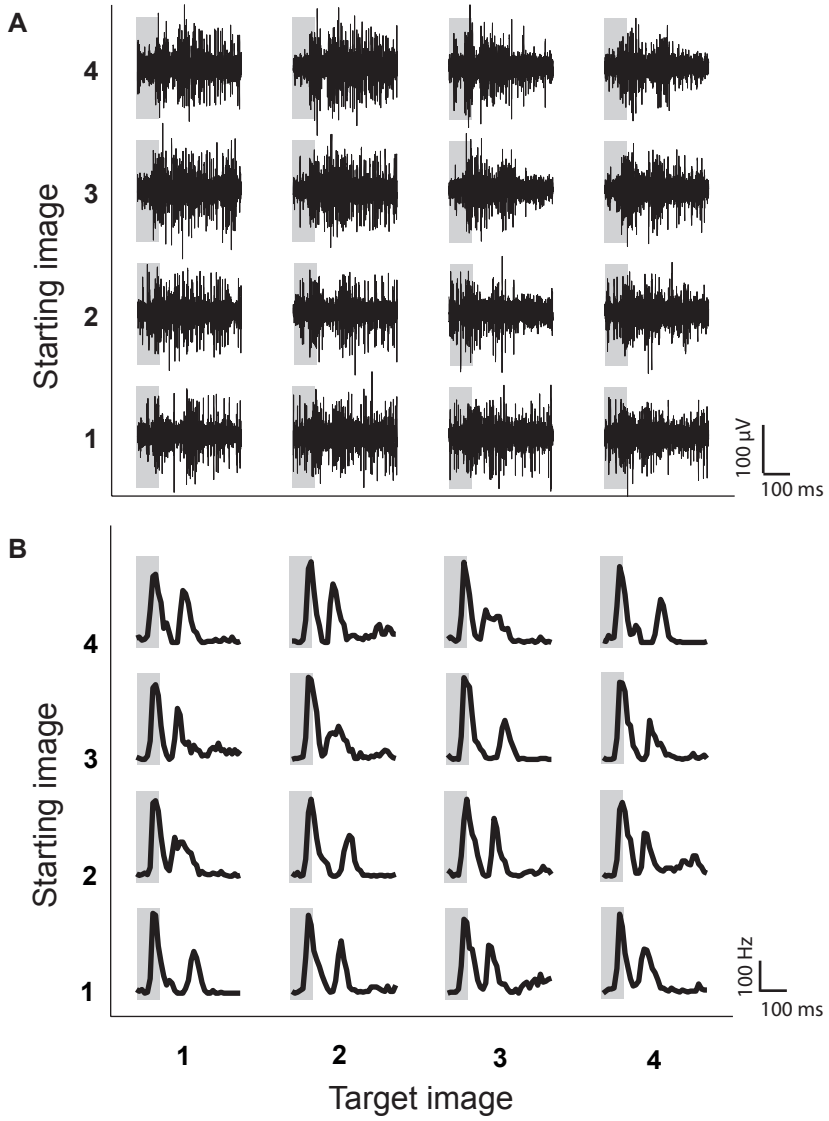

Figure 3.4: Indifferent Encoder. Sample traces (A) and peri-stimulus time histograms (B) show results of a cell that responded to saccadic motion (grey shaded region) and to all fixated images. Since the cells responded to all aspects of the stimulus we classified such cells as *Indifferent encoder*. Conventions are as in Fig. 3.2.

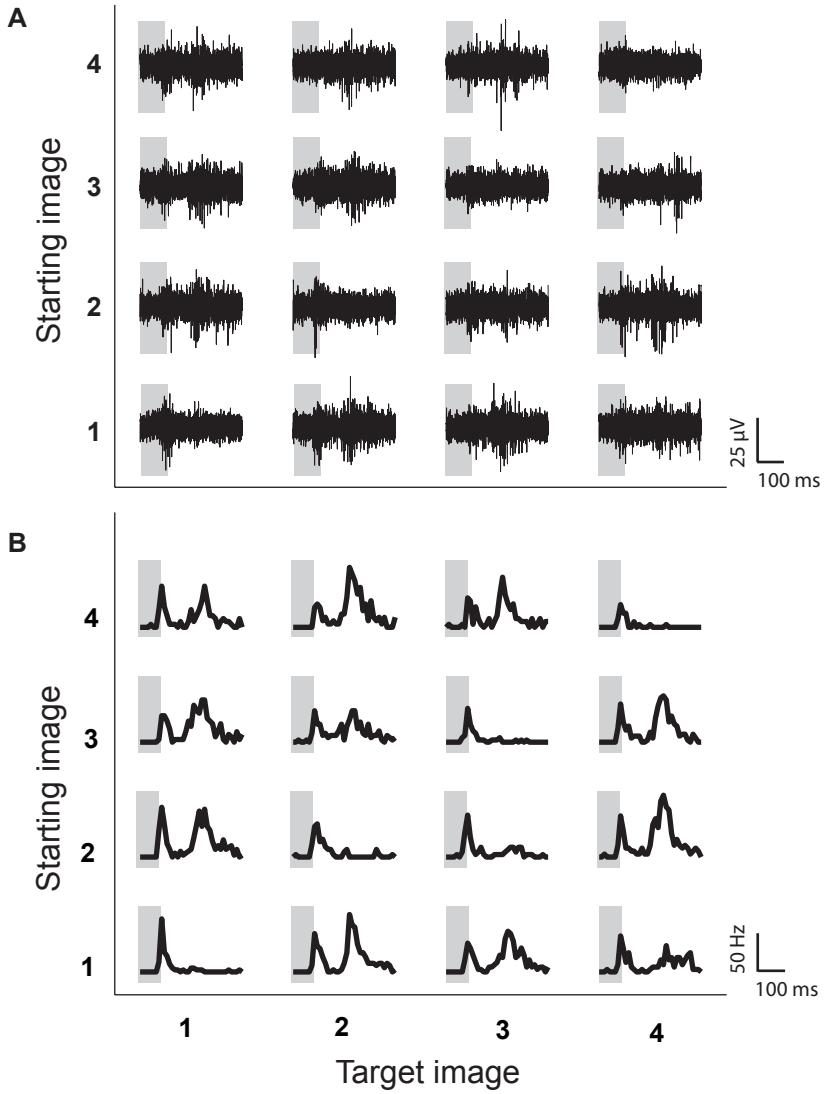

Figure 3.5: Change Detector. Sample traces (A) and peri-stimulus time histograms (B) show results of a cell with complex response profile. The sample cell shown here responded to the saccade-like motion (grey shaded region), but the response to the *target image* was different. This cell did not respond to a *target image* if the preceding *starting image* was also the same image (Note the lack of response to *target image* along the diagonal). In other words, the cell responded primarily to fixations that are different across the saccades. We classified such cells as *Change detector*. Conventions are as in Fig. 3.2.

the scenarios 1➔1, 2➔2, 3➔3 and 4➔4 (note the diagonal along the matrix plots in Fig. 3.6). This response type acts as a specialized feature detector in that it reports the scenarios, where the fixations before and after the saccade have a similar image. In other words, this type encodes the similarity across saccades. Hence we call this type '*Similarity Detector*'. It is an example of invariant coding, that this type responds to all images invariantly, but only under a certain 'temporal context'. 16% of cells in our data set were of this type (n=18). Furthermore, the cells of this type had a transient response profile.

3.5 Automated Classification of Response Types

The classification of response types described in our study is based on complex response patterns of 16 saccadic transitions. Therefore, cell type distinction was initially made by visual inspection based on the features described in the previous section (see Section 3.4). We then tried to find objective criteria based on a few appropriately chosen response parameters that capture the cell types. We considered the peak firing rate, the spike count and the integral over PSTH of *target image* as parameters. The spike count as a parameter was not appropriate as it fails for cells that have high base line firing (i.e., maintained rate). It also fails for cells that respond with a burst of spikes for certain features of stimuli and more sustained firing for other features. The integral over the PSTH also suffers for the same reasons. The peak firing rate does not suffer from the disadvantages mentioned above. Thus, we attempted automated classification, using peak firing rate of the target image as a parameter (Fig. 3.7 A-E). This automated classification is done to address the issue of subjectivity in manual classification.

We easily classified the *Offset Detector* when the peak firing rate of responses to saccade-like motion is 1.5 times (on average) to that of target image (Fig. 3.7 B). We also easily classified *Indifferent Encoder* when there is little or no modulation in the peak firing rates of responses to target image (Fig. 3.7 A). For classifying other cells, we applied Fourier analysis to obtain relative weights contributing to different patterns in peak firing rate. In other words, these relative weights are the strengths of components in each axis in the matrix plot. We also calculated the difference in mean peak firing rates of responses in the diagonal of the matrix plots to off-diagonal rates (Fig. 3.7 C-E). The difference in strength of each axes is plotted against the difference in mean diagonal response and off-diagonal response. For *Change Detector* and *Similarity Detector* the modulation along the diagonal axis of the matrix contributed in their classification. For *Classical Encoder* the difference in relative weights contributed to their clustering

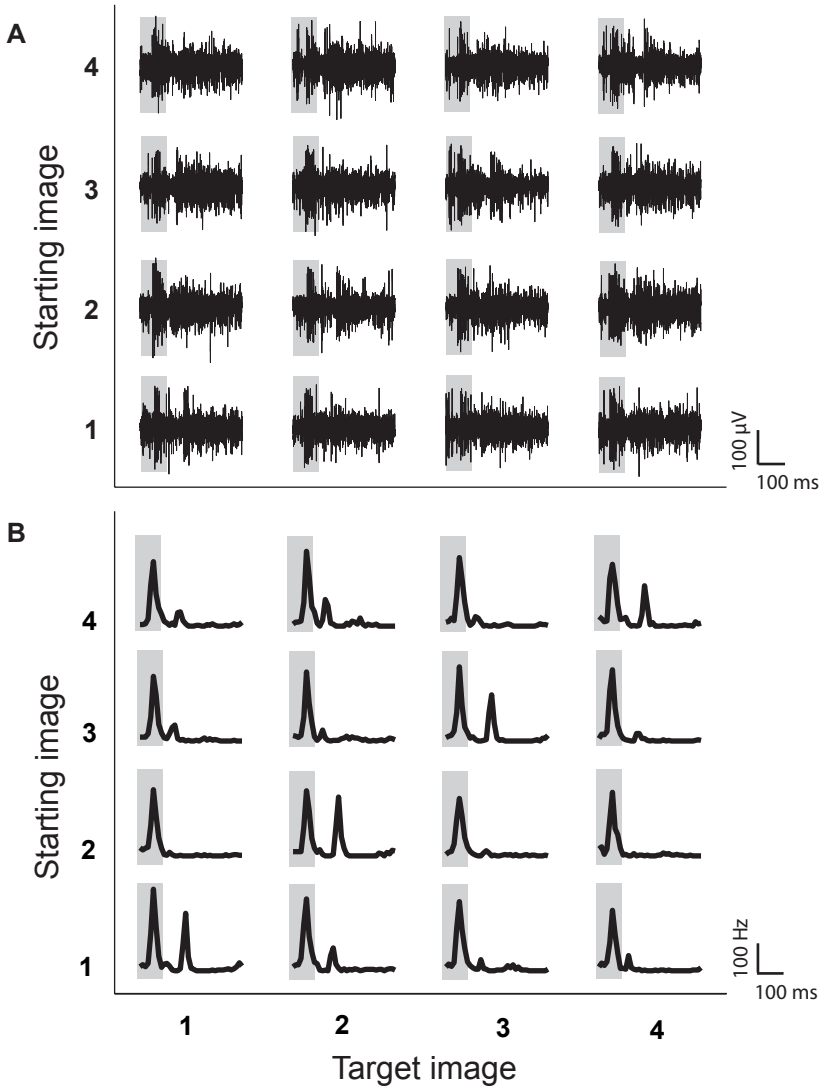

Figure 3.6: Similarity Detector. Sample traces (A) and peri-stimulus time histograms (B) show results of a cell with complex response profile. The sample cell shown here responded to the saccade-like motion (grey shaded region), but the response to the *target image* was different. This cell responds to a *target image* preferably only if the preceding *starting image* is also the same image (Note the strong response to *target image* along the diagonal). Therefore, this cell preferentially responds to fixations that are similar across saccades. We classified such cells as *Similarity Detector*. Conventions are as in Fig. 3.2.

(Fig. 3.7 F).

Our automated clustering of cells based on response to saccade stimulus captured the different *response types* (Fig. 3.7 F). But a closer look revealed that the cells farther from threshold were very distinct examples of *response type*, whereas the ones closer to the threshold showed a slightly different response profile, underscoring variations within each group.

3.6 Distribution of Response Types

The *Classical Encoder* type is the predominant response type in our recording. About half of the recorded cells (57 of 114 cells from 6 retinae; Fig. 3.8) are of this type. These cells showed either no response or suppression of spiking activity during saccades (Fig. 3.2), as shown by Roska and Werblin (2003). The other four *response types* formed the remaining half of the cells. These cells respond to saccade like motion with a short burst of spikes (Fig. 3.3-Fig. 3.6). Similar responses to saccades had been reported earlier in cats (Noda and Adey 1974b, Noda 1975). This supports the idea that the retina actively encodes the saccade and may signal abrupt scene changes to the downstream centres. These four types seemed to be equally distributed except for *Change Detectors* which are least numerous with just 8% (n=9). This could be due to sampling bias in a multi-electrode array (MEA) or *Change Detectors* may actually be a small proportion of total cells. How can one response type, i.e., *Classical Encoder* dominate the recordings? We cannot rule out a bias in sampling ganglion cells in our MEA recordings. However, the basic characterization of ganglion cells described in the next section (see Section 3.7) reveals that they are small cells and are obviously the most numerous type. Nevertheless, the distribution of response types might still closely

Figure 3.7 *(following page)*: Cell type clustering. A-E) Mean peak firing rate of target images of each cell type is shown. We used peak firing rates as a parameter to analyze the ganglion cell response. For indifferent encoder (A) and offset detector (B) there is only a minimal or nil modulation of peak firing rates and were easily clustered. For other cells the modulation is apparent and distinct for each cell type. Classical encoder (C) show modulation in one of the axes whereas, similarity and change detector (D & E) show modulation along the diagonal. F) We applied Fourier analysis to better capture the different components of mean firing rates that contribute to a cell type. The difference in strength of each axes is plotted against the difference in mean diagonal response and off-diagonal response. This captures three *response types - classical encoder, similarity* and *change detector*. The cells in C, D & E are highlighted as thick circles in F.

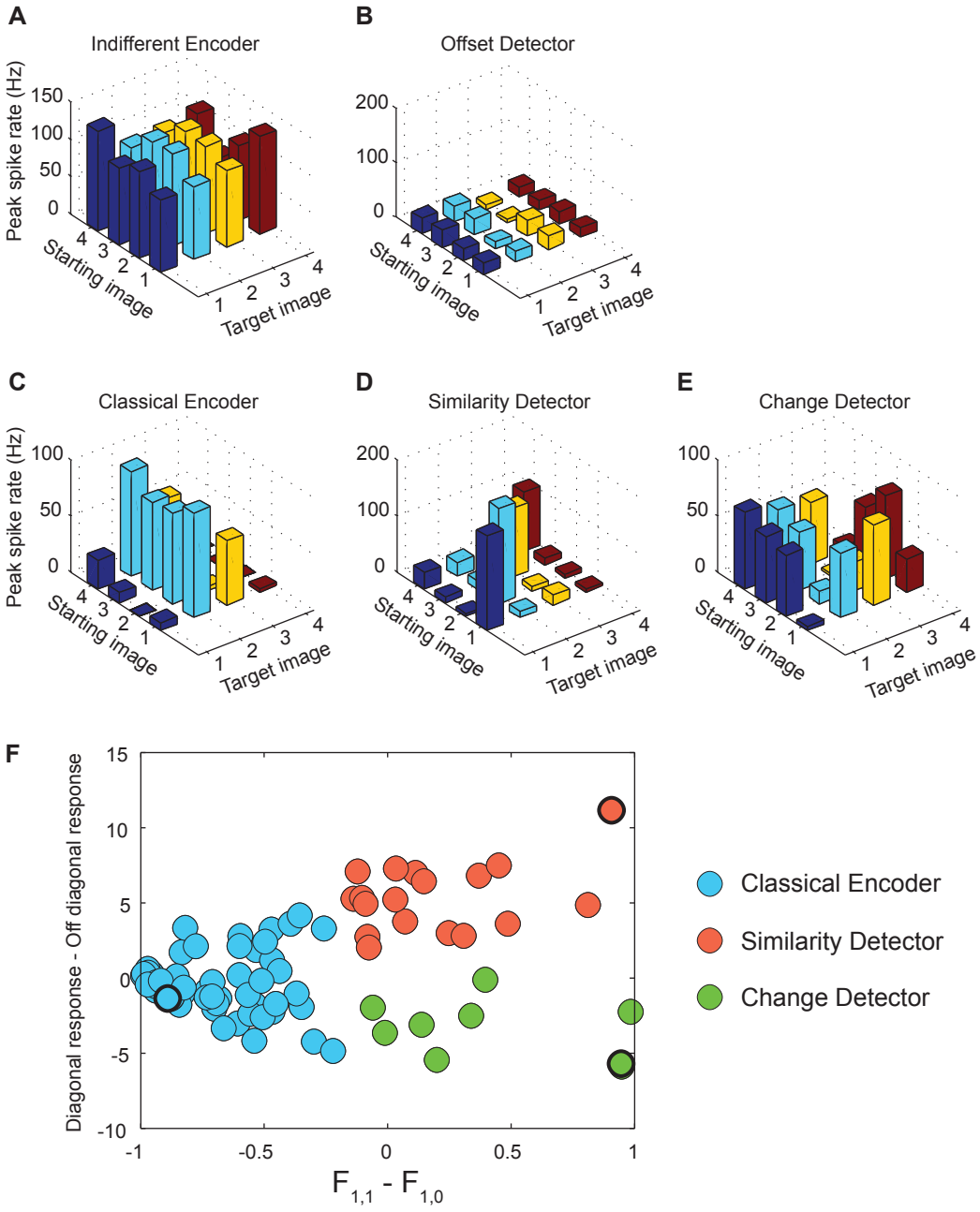
A
Indifferent Encoder
Peak spike rate (Hz)
150
100
50
0
Starting image
Target image
B
Offset Detector
200
100
0
C
Classical Encoder
D
Similarity Detector
E
Change Detector
F
Diagonal response - Off diagonal response
15
10
5
0
-5
-10
-1
-0.5
0
0.5
1
F1,1 - F1,0
Classical Encoder
Similarity Detector
Change Detector

match the actual distribution of cells in the retina.

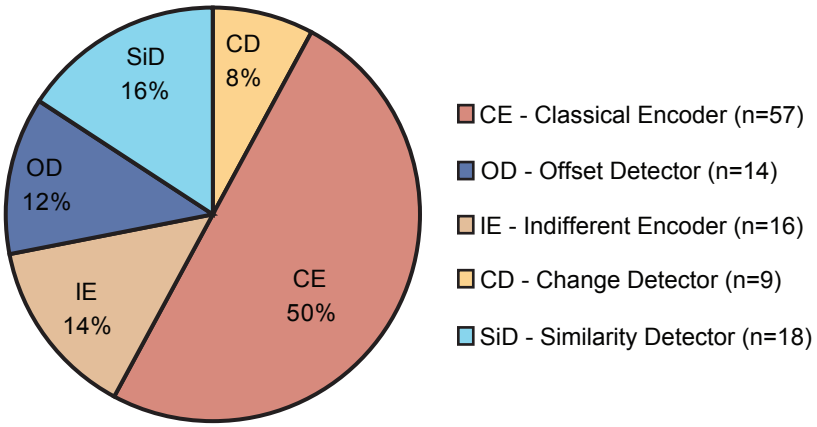

Figure 3.8: Response type distribution. Half of the recoded cells are classical encoders (57 of 114 cells from 6 retinae), which are also the cells with nil or minimal response to saccade-like motion. Indeed, there was suppression in cells that had a high maintained rate. The other half of the cells responded to saccade-like motion. The distribution is nearly equal among the four response types, except for change detector which was only 8%. This could be due to sampling bias in our multi-electrode array recordigs or may actually be a small proportion of total cells.

3.7 General Characterization of Ganglion Cells

Having classified the ganglion cell responses based on our specific saccade-like stimulus, we wanted to know if each *response type* is a specific class of ganglion cell. To this end, we characterized the ganglion cells for their basic response properties like response polarity, filtering property, receptive field size and X-, Y-like response property. Results from each of these characterizations are given in detail below.

Response Polarity - ON, OFF, ON-OFF Cell Types: We classified ganglion cells based on their response to periodic light flashes switching between black and white every 500ms. We found 51 ON, 29 OFF and 34 ON-OFF cells out of 114 cells recorded. Within each saccadic *response type*, the distribution of ON, OFF and ON-OFF cells was different. Only *Classic Encoders* and *Indifferent Encoders* had all three cell types. *Indifferent Encoders* consisted of mostly ON-OFF cells (Fig. 3.9 A). It is not surprising, since these cells responded to motion and all fixated images (Fig. 3.4). Surprisingly, there were no OFF cells in *Change Detector* and no ON cells in *Similarity Detector*. These *response types* encode opposite features under saccadic vision and are apparently of opposite cell types as well. This already indicates that at least some response types

are of specific cell class. Also, we found no OFF cells in *Offset Detector*. These results indicate that at least there are some differences in such a simple classification among different *response types*.

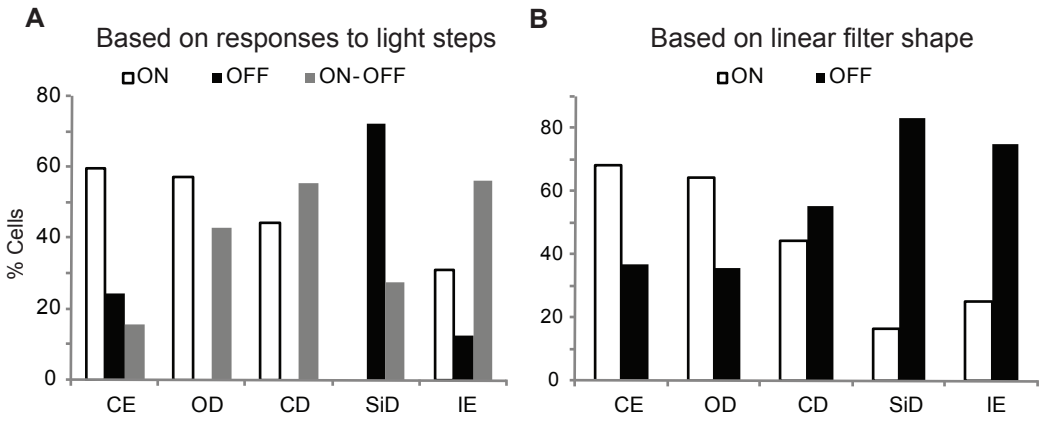

Figure 3.9: ON, OFF, ON-OFF cell type distribution. A) Classical encoders and indifferent encoders are comprised of all three cell types albeit in different proportions. But there were no OFF cells in offset detectors and change detectors, and no ON cells in similarity detectors. B) The classification based on linear filter shape does not have ON-OFF cell class. Note the high proportion of OFF cells in similarity detectors.

Response Polarity - Based on STA Shape: We further classified ganglion cells into ON and OFF based on spike triggered average (STA; see Section 2.6.2; also Fig. 3.10 A). STA is the average stimulus that triggered a spike, when stimulated with a Gaussian white noise stimulus. Since the classification is based on the first peak in the STA, there is no ON-OFF cell type in this classification (Fig. 3.9 B). Again, the results show there are fewer ON cells in *Similarity Detector* type, but *Change Detector* type had many OFF cells due to the fact most ON-OFF cells were classified as OFF cells here. For similar reasons, *Indifferent Encoder* also had many OFF cells.

Biphasic Index: STA also represents the linear filter of a cell (Chichilnisky, 2001; Schwartz, 2006). The biphasic shape of the STA corresponds to sensitivity of the cell to the temporal frequency of the stimulus. For example, an increased biphasicness could be interpreted as a decreased sensitivity to low temporal frequencies (Zaghloul et al. 2007). The biphasic index was calculated as the ratio of the second peak (s2) to the first peak (s1) of the STA (Fig. 3.10 A). The values range between 0 and 1, where 0 is least biphasic and 1 is highly biphasic. About two-thirds of *Classic Encoder* cells are less biphasic (Fig. 3.10 B). More than half of *Similarity Detector* cells are more biphasic(Fig. 3.10 F), indicating that these cells are sensitive to high temporal

frequencies. The other response types did not show a clear pattern in their distribution indicating heterogeneity in their distributions (Fig. 3.10 C-E).

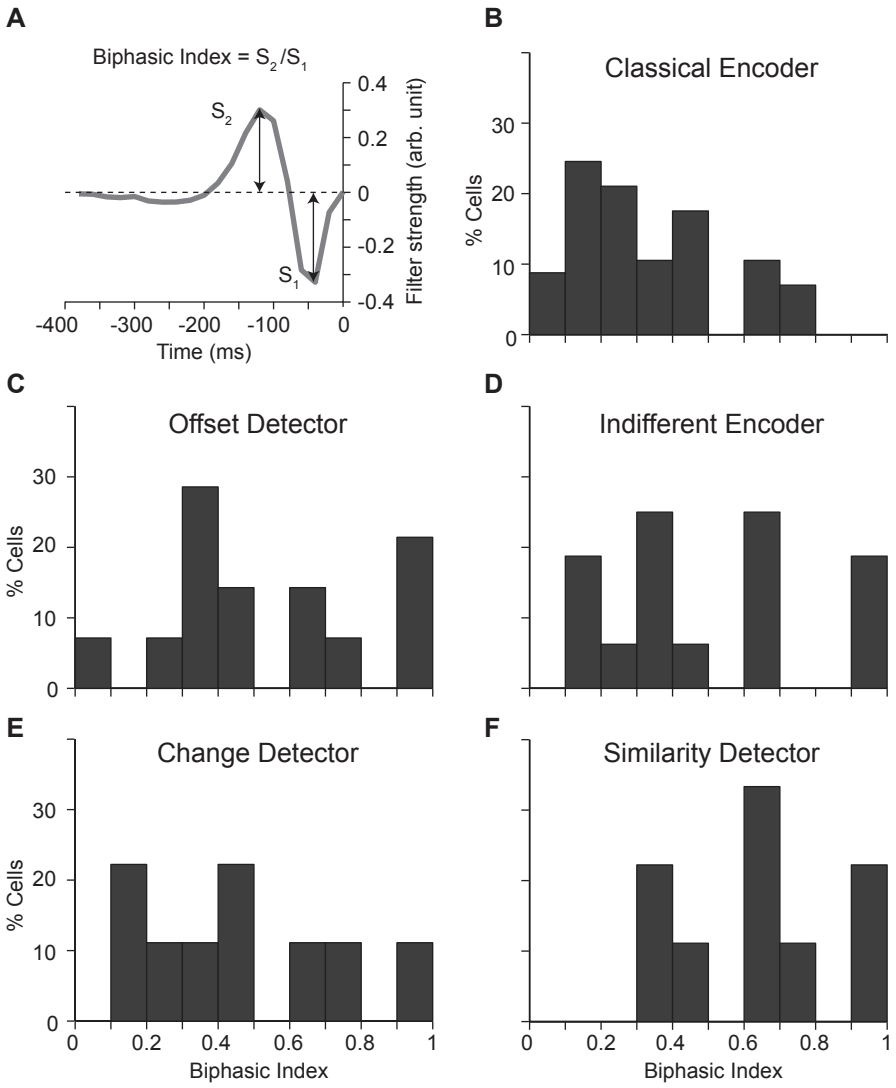

Figure 3.10: Biphasic index distributions. A) Illustration showing the calculation of biphasic index. The biphasic shape of the linear filter (STA) is a characteristic feature of a cell. The values range between 0 and 1, where 0 is least biphasic and 1 is highly biphasic. B-F) Biphasic index distributions for the response types. About two-thirds of classical encoders (B) are less biphasic, whereas about half of similarity detectors are highly biphasic (F). Other response types have mixed distributions and do not show a clear trend.

Receptive Field Size Distribution: We estimated the size of receptive field centre of a ganglion cell by white noise analysis (see Section 2.6.3). We found ganglion cells

ranging from ≈ 150µm in diameter to ≈ 400µm. About 70% of *Classical Encoders* are small cells with receptive field size of ≈ 150µm. The remaining 30% cells consisted of heterogeneous population of cells with receptive field size ranging from 200µm to 400µm. About half of *Similarity Detector* cells were medium sized cells (≈ 250µm) and *Change Detectors* were mostly large cells (≈ 350µm). There was no clear pattern of receptive field size distribution among other *response types* (Fig. 3.11).

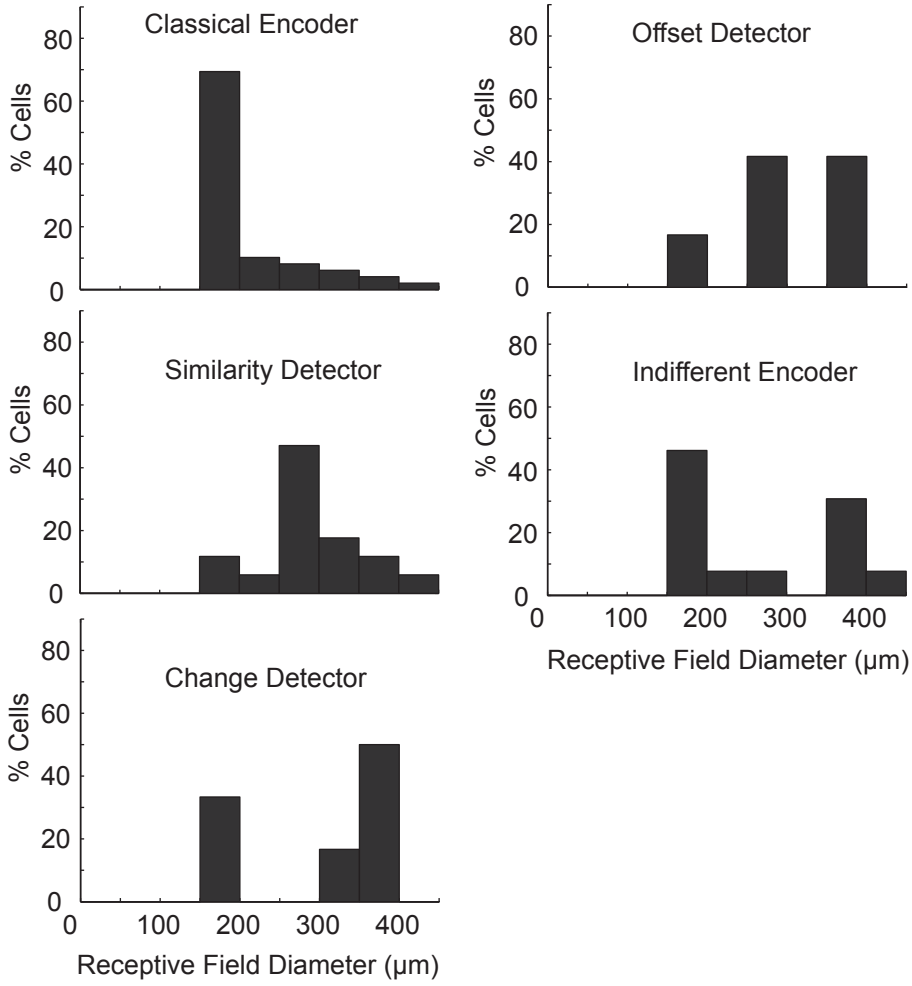

Figure 3.11: Receptive field size distributions. About two-thirds of classical encoders are smaller cells with receptive field diameter of ≈ 150µm. Nearly half of similarity detectors are medium sized with receptive field diameter of ≈ 250µm, and half of change detectors are bigger cells with receptive field size of ≈ 350µm. Cells of offset detectors and indifferent encoders do not show a clear trend.

X, Y cell Analysis: We presented sinusoidal reversing grating at different spatial phases to classify the ganglion cells to X-like and Y-like (see Section 2.6.4 for details;

Fig. 2.5). This analysis indicates the response nonlinearity of a ganglion cell. X-like cells are linear cells whereas Y-like cells are nonlinear (Enroth-Cugell and Robson 1966). The ganglion cell responses were Fourier analysed and a *nonlinearity index* was calculated (ratio of second harmonic to first harmonic F2/F1; see Section 2.6.4; Hochstein and Shapley 1976). Cells with *nonlinearity index* > 1 were classified as Y-like, < 0.5 as X-like and between 0.5 and 1 as intermediate types. We found that most *Classic Encoder* cells were X-like, while most of the other cell types were intermediate type or Y-like (Fig. 3.12, Note that nearly 11% of cells with *nonlinearity index* > 2.5 is not displayed in the histogram).

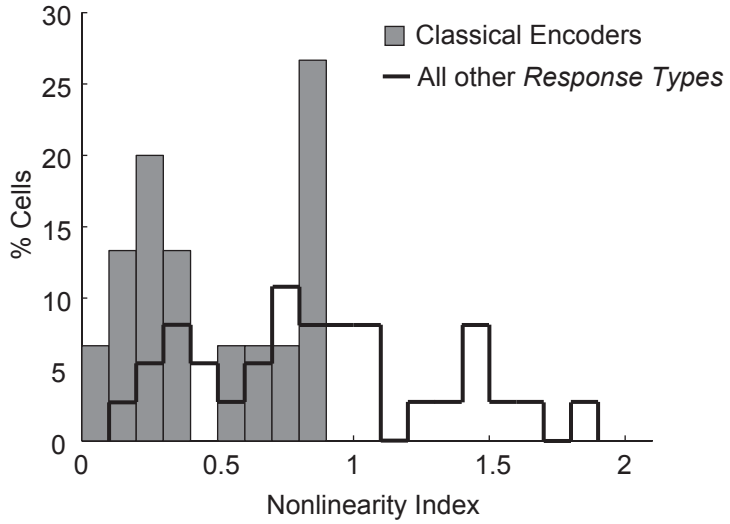

Figure 3.12: Nonlinearity index distribution. Nonlinearity index <0.5 are classified as X-like cells and >1 are classified as Y-like cells. Cells with values between 0.5 and 1 tend be a mixture of non X- and Y- cells. Most of classical encoders are X-like cells, whereas most of all other response types are Y-like. Many cells in both the groups fall under intermediate cell type. Four cells (nearly 11% of other response type) with values > 2.5 are not shown in the histogram.

The general characterization of ganglion cells leads to interesting conclusions about saccadic response types. In general *Classic Encoder* cells were mostly X-like (Fig. 3.12), have small receptive field (Fig. 3.11) and sustained firing pattern (Fig. 3.2 B, C). It is known from several studies that X-like cells have small receptive fields and sustained firing pattern (Enroth-Cugell and Robson 1966, Hochstein and Shapley 1976, Freeman et al. 2010) as found in our recordings. Added to this is their least bihphasicness (Fig. 3.10 B), indicating their linear filter to prefer lower temporal frequencies. All these facts indicate that *Classic Encoder* cells are most likely to be one specific functional

class of cells.

Nearly three-fourths of *Similarity Detector* cells are OFF cell (3.9 A), they are Y-like, have transient firing pattern (Fig. 3.6) and are mostly with medium receptive field centre size ($\approx$ 250µm; Fig. 3.11), indicating they are most likely OFF α-cell or X5 cell type in the classification of Hong et al. (2011). Similarly, *Change Detector* cells are of mostly ON type (Fig. 3.9 A), and with large receptive field centres ($\approx$ 350µm; Fig.3.11), indicating these cells to be most likely ON α-cell or X7 cell type in the classification of Hong et al. (2011). By contrast, other *response types* were characterized as mostly Y-like cells, with intermediate to large receptive field and transient response properties, but did not indicate to any of the anatomical or functional cell classes described in the mouse retina.

3.8 Saccades and Eye-blinks Elicit Similar Responses

To test if different response types were due to saccade-like motion, we characterised the ganglion cells for the stimulus segments where the transition between fixation images was a grey image instead of a saccade (Fig. 3.13). The grey transition between fixations could be considered as an *eye-blink* in a larger sense, although the real eye-blink reduces light falling on the retina by a hundred fold (Burr 2005). The intensity of the grey image used here was the mean of intensities between black and white bars of the grating. The transition between the fixated images was either *saccade* or *eye-blink* chosen randomly (Fig. 3.13). To our surprise we found that the ganglion cell responses were similar to that of a saccade stimulus (Fig. 3.14). Thus the response during transition may not be due to a saccade-like motion but to offset of an earlier image i.e., *starting image*. Also we found all the responses of ganglion cells to *target images* were essentially similar to both the stimuli. The classification of response types did not change at all. These results indicate that these response types do not necessarily arise due to the saccade-like motion stimulus. It is likely that the image falling on the retina during the fast saccade-like motion is blurred resembling a static grey image. Thus a brief transition between fixations - be it a motion stimulus or a static grey image (or an *eye-blink*) - is sufficient to cause a variety of response types described in this study.

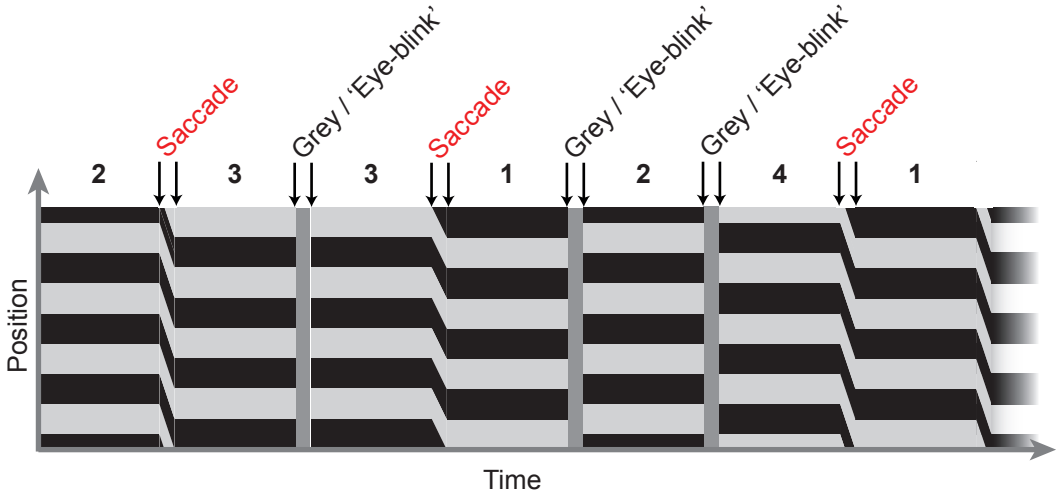

Figure 3.13: Saccadic stimulus with interleaved eye-blinks. The transitions between fixations are either saccade or eye-blinks chosen randomly. The eye-blink stimulus consisted of mean grey intensity.

3.9 Results from Rabbit and Axolotl Retina

Our results from the mouse retina are the first of its kind in characterizing responses to fixations *after* a saccade. Previous reports on saccade-like experiments were performed in retinas from a variety of animals like rabbit (Roska and Werblin 2003, Amthor et al. 2005), cat (Noda and Adey 1974b), salamander (Geffen et al. 2007) and archer fish (Segev et al. 2007). However the goals and conclusions of these studies were different. In order to test if our results are unique to mouse retina or if it is more general phenomenon to vertebrate retina, we performed additional experiments in rabbit (n=1) and axolotl retina (*Ambystoma mexicanum* an amphibian model; n=1).

We found all the response types in rabbit except *Classical Encoders* (Fig. 3.15). Again, as in the mouse retina, the responses were similar to saccades and eye-blinks. In the axolotl retina, we found all the response types except *Classical Encoders* and *Indifferent Encoders* (Fig. 3.16). Note that the ganglion cells of axolotl retina have high response latency to light flashes as high as 180ms (data not shown). Hence, the response to the 100ms transition (saccade or eye-blink) appears after the transition is over. In Fig. 3.16, the first peak is the response to transition and the second peak is the response to the fixations.

Since we performed just one recording each in rabbit and axolotl we cannot say if

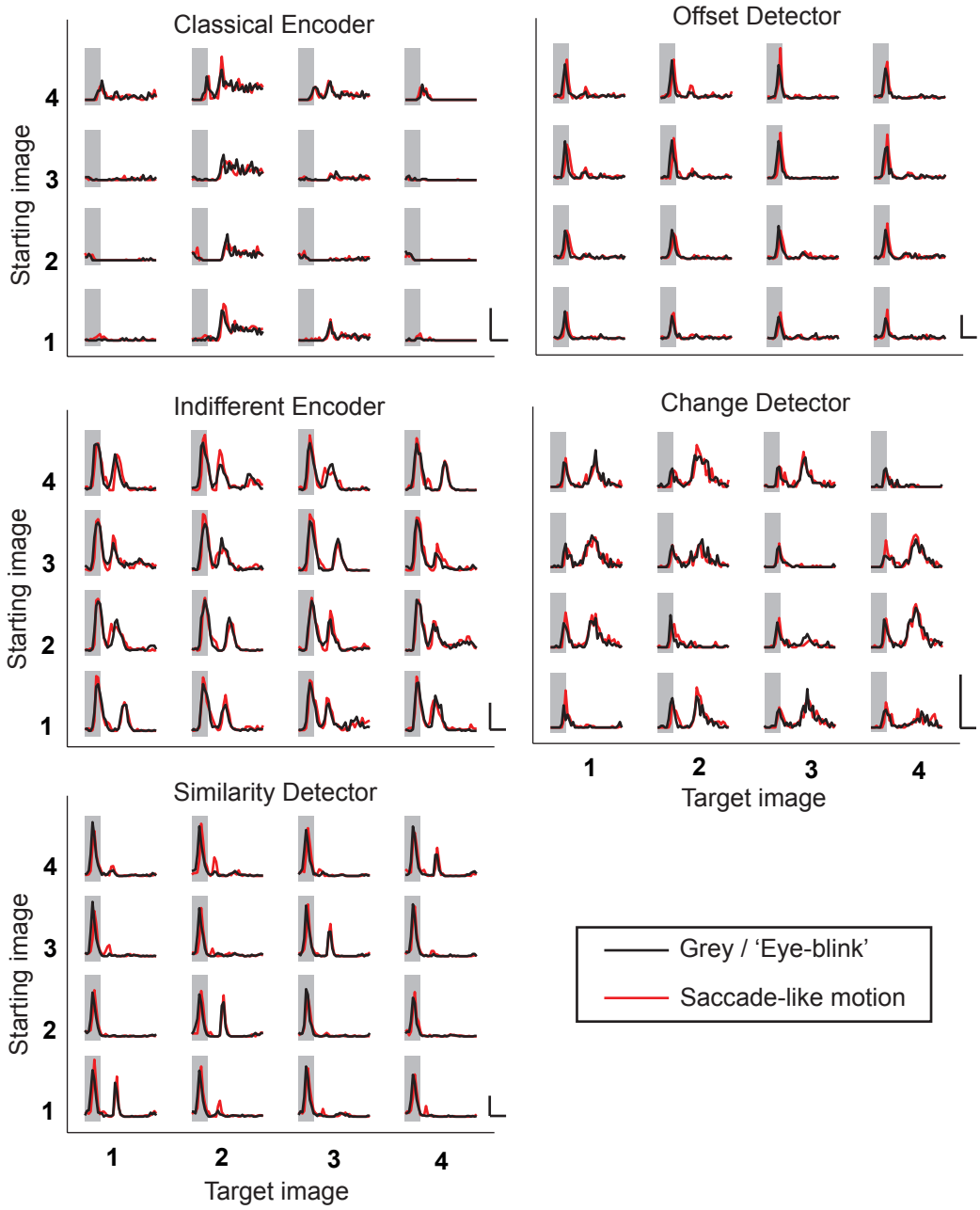

Figure 3.14: Responses arise not necessarily by saccade-like motion but also by brief grey stimulus. The brief grey transitions between fixations that resembled like an eye-blink scenario elicited a similar response to those of saccadic scene changes. All the response types responded in a similar fashion to saccade stimulus when presented with a brief grey stimulus resembling an eye-blink. These results indicate that the saccadic scene change and eye-blinks drive ganglion cells identically. Conventions are as in Fig. 3.2. Scale bar : abscissa-100ms, ordinate-100Hz.

the retina lacks the missing *response types* or it is purely a problem of low sampling. Nevertheless, the presence of other intriguing *response types*, especially *similarity* and *change detector* shows that saccades elicit complex response patterns in rabbit and axolotl similar to mouse retina. Although more thorough experiments are necessary in other species, the results from rabbit and axolotl indicate that our results of the mouse retina could be a more general phenomenon for the vertebrate retina.

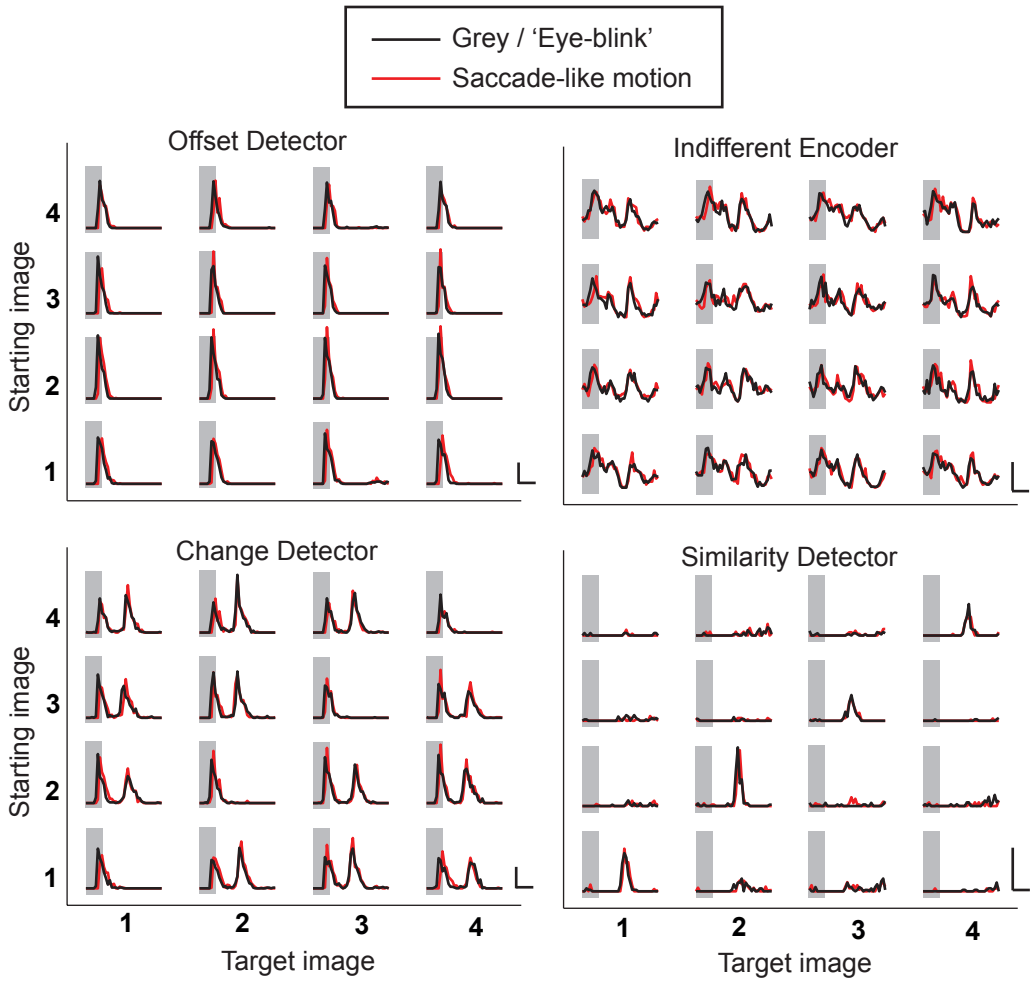

Figure 3.15: Results from rabbit retina. The results from one rabbit retina show similar results to mouse retina, except we did not find classical encoder. Conventions are as in Fig. 3.2. Scale bar : abscissa-100ms, ordinate-100Hz

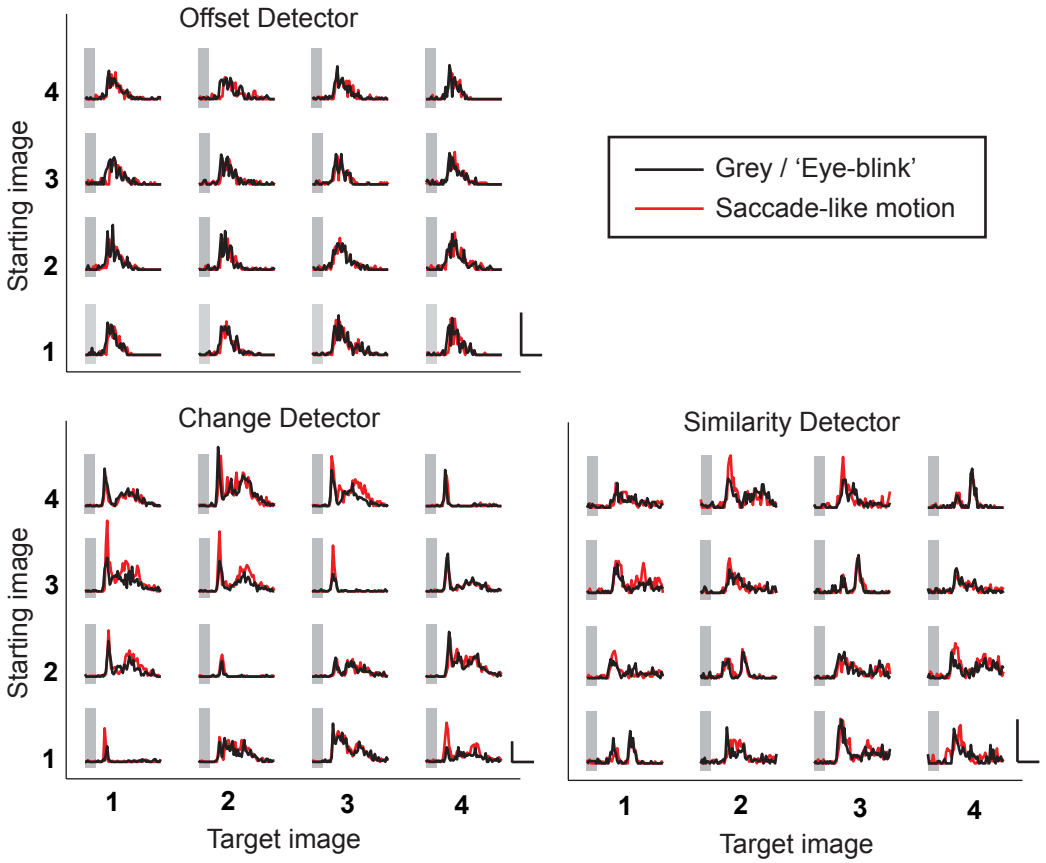

Figure 3.16: Results from axolotl retina. The results from one axolotl retina show similar results to mouse retina, except we did not find classical encoder and indifferent encoder. Note that the axolotl retina has high response latency and due to this fact the response to saccadic transition appears after the end of transition. The second peak is the response to the fixations. Conventions are as in Fig. 3.2. Scale bar : abscissa-200ms, ordinate-50Hz

3.10 Chapter Summary

During saccadic vision, the information acquired by the retina is a sequence of brief 'snapshots' interrupted by saccadic 'motion blur'. We found half of all our recorded cells respond to saccade like motion with a short burst of spikes (Fig. 3.3-Fig. 3.6). This supports the idea that retina actively encodes the saccade and may signal abrupt scene changes to the downstream centres. The rest of the RGCs in our recordings showed either no response or suppression of spiking activity during saccades (Fig. 3.2). Furthermore, we characterized the ganglion cell responses to fixation after a saccade. Our results indicate that the image transitions matter the most, rather than appearance of new image itself. The responses to the new image were influenced by the history of the stimulus before a saccade, suggesting that the saccadic vision may provide 'temporal context' to the retinal coding. Moreover, we could classify ganglion cells into five response types indicating the presence of at least five parallel channels of information for saccadic vision. Similar results for *eye-blink* experiments indicate that the retinal coding strategy for saccades and eye-blinks are similar.

4. Effects of Remote Stimulation

4.1 Extra-Classical Receptive Field

Each ganglion cell is primarily sensitive to visual signals in a small area of space, the cell's spatial receptive field (Hartline 1938).The receptive field region usually comprises a roughly concentric centre and an antagonistic surround (Kuffler 1953). However, it has been known that the motion signals far-beyond the receptive field modulate the cell's response to stimuli in its receptive field. The remote stimulus such as a rapid shift or motion of the image in the periphery can modify various response characteristics of a ganglion cell (McIlwain 1964, Krüger and Fischer 1973, Fischer et al. 1975, Barlow et al. 1977, Enroth-Cugell and Jakiela 1980, Geffen et al. 2007). Hence, the region remote to the cell's classical receptive field has been denoted as 'extra classical receptive field' (Passaglia et al. 2009).

The effects of remote stimulation have been studied in several species including, salamander (Werblin 1972, Cook and McReynolds 1998), turtle (Schwartz 1973), cat (McIlwain 1964, 1966, Barlow et al. 1977), rabbit (Watanabe and Tasaki 1980, Taylor 1999), guinea pig (Demb et al. 1999) and monkey retinas (Solomon et al. 2006), and have been called 'shift effect' and 'periphery effect'. In salamander retina the global motion evoked by a spinning windmill like pattern activates glycinergic amacrine cells which in turn inhibit ganglion cells (Werblin 1972, Werblin and Copenhagen 1974, Thibos and Werblin 1978, Cook and McReynolds 1998). On the other hand, in mammals there are contradictory reports that show remote stimulus causing both excitation (McIlwain 1964, 1966, Krüger and Fischer 1973, Noda and Adey 1974a, Fischer et al. 1975, Barlow et al. 1977, Ross et al. 2001) and inhibiton (Enroth-Cugell and Jakiela 1980, Demb et al. 1999, Taylor 1999, Flores-Herr et al. 2001).

Global motion signals caused by saccades effectively influences the extra-classical receptive field. We have shown in the previous chapter (Chapter 3) that the saccade-like stimulus evokes a variety of responses in the ganglion cells. In this chapter, we re-

visit the effects of remote stimulation with the aim of exploring them in the context of saccade-like scene changes. To this end, we record the spiking activity of ganglion cells in isolated mouse retinas with extracellular multielectrode arrays. During the recording, we present various light stimuli to the receptive fields of the cells in the presence or absence of remote stimulation. As remote stimuli, we apply moving as well as contrast reversing gratings with different spatial and temporal scales. The response characteristics are then compared to the filtering properties of the neurons as measured with white-noise experiments and reverse-correlation analyses.

4.2 The Remote Stimulus Configuration

The remote stimuli in earlier studies have used several patterns ranging from a sectored windmill to sinusoidal gratings. In this study, we designed a simple stimulus configuration with a central region of 1100 µm x 1100 µm (centred on the multielectrode array) and a far-periphery (the 'extra-classical receptive field'). The central region was surrounded by a 100µm thick grey border to separate the stimulus in the central region from the far-periphery. The stimulus in the centre consisted of uniform illumination, light steps or Gaussian white-noise. As a remote stimulus in the far-periphery, we presented drifting or reversing square-wave gratings at different spatial frequencies (Fig. 4.1 A). The remote stimuli used in this study are simple but at the same time cover a range of different interesting features used in the past. For example, the drifting grating is a continuous motion stimulus and similar to the continuous motion of spinning windmill (used by Werblin 1972, Werblin and Copenhagen 1974, Thibos and Werblin 1978, Enroth-Cugell and Jakiela 1980, Cook and McReynolds 1998). The reversing grating represents a stimulus similar to a sudden shift in the far-periphery (used by Fischer et al. 1975, Barlow et al. 1977, Geffen et al. 2007). We recorded ganglion cell responses to centre stimuli with or without remote stimulation. We also estimated the receptive field of a ganglion cell by white-noise analysis (see Section 2.6.3). Only cells with receptive fields within the centre region are included for further analysis (Fig. 4.1 B).

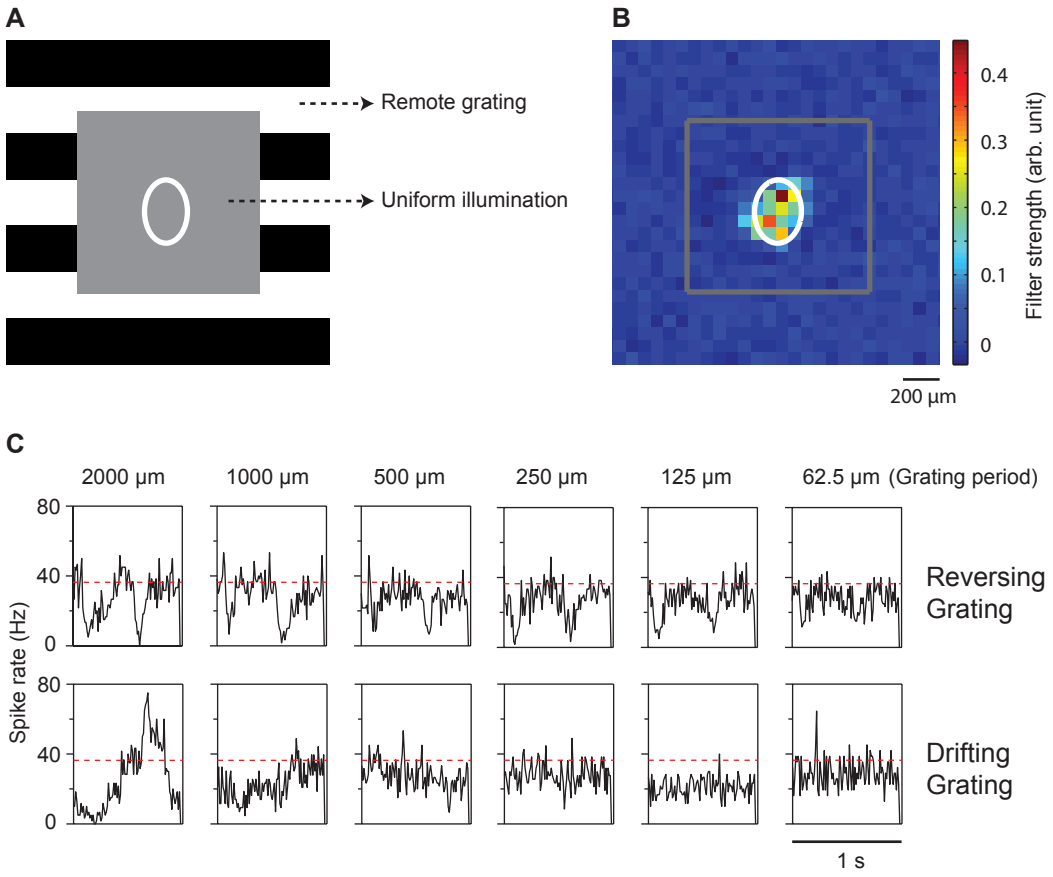

Figure 4.1: Remote stimulation modulates the spontaneous activity. A) Schematic illustration of the remote stimulus. A grey uniform illumination was presented in the central 1100 µm x 1100 µm. The white ellipse represents the receptive field of a ganglion cell. In the far surround, as a remote stimulus, a square-wave grating stimulus at different spatial periods either drifting or reversing at 1Hz was presented. B) Receptive estimation by white noise analysis of an example ganglion cell. The black square represents the central uniform illumination region. Only cells with receptive fields well within the central region were included for further analysis. C) Modulation of spontaneous activity of the cell shown in B, to both reversing gratings (*top*) and drifting gratings (*bottom*) at different grating periods. The red dotted line indicates the maintained rate of the ganglion cell under uniform illumination without any remote gratings. For lower spatial frequencies of gratings, there is both suppression and enhancement of the maintained rate.

4.3 Remote Stimulation Both Enhances and Suppresses the Mean Firing Rate

Stimulation of the extra-classical receptive field is known to modulate the maintained rate of ganglion cells. McIlwain (1964) first reported an increase in mean firing rate due to a high contrast motion stimulus in the far-periphery, which was confirmed by several studies (Krüger and Fischer 1973, Fischer et al. 1975, Barlow et al. 1977). There were other studies that reported suppression of mean firing rate (Enroth-Cugell and Jakiela 1980, Krüger 1980, Rapaport and Stone 1988). These conflicting reports might have arisen because of differences in stimulus parameters. Also the dependence of spatial scale on these effects has remained controversial. Here we revisit these issues and systematically study the effects on maintained rate by using two types of stimuli - *drifting gratings* and *reversing gratings*.

The stimulus consisted of uniform grey illumination of a central region of 1100 µm x 1100 µm and either drifting or reversing grating at 1 Hz in the periphery (Fig. 4.1 A). We presented remote gratings with five different spatial frequencies. The period of the gratings ranged from 2000µm to 62.5µm. Remote gratings modulated only a subset of ganglion cells - ON cells (6 out of 10 cells), OFF cells (4 out of 10 cells) and ON-OFF cells (5 out of 6 cells). To our surprise we found both increase and decrease of mean firing for both drifting and reversing gratings. Also the effects were stronger for gratings of lower spatial frequency (Fig. 4.1 C). The reversing grating elicited sharp decreases and increases, whereas drift gratings elicited slow changes in the firing rate. However, gratings with a spatial period of 125µm had an overall suppression of mean firing rate (Fig. 4.1 C). Gratings with a period of 62.5µm did not affect the maintained rate. Thus our results reconcile earlier conflicting reports about the modulation of mean firing rate and dependence of spatial scale of remote stimulation. But how could one explain both enhancement and suppression of mean firing rate? One possible explanation is that the remote stimulus primarily suppresses the mean firing rate and that the enhancement arises from rebound excitation (Mitra and Miller 2007, Margolis and Detwiler 2007) due to disinhibition (Li et al. 1992, Manu and Baccus 2011).

4.4 Remote Stimulation Suppresses the Evoked Response

After testing the effects of remote stimulation on maintained rate, the next step is to study the effects on light evoked responses of ganglion cells. We presented light steps

(100% contrast steps) for the central 900µm x 900µm region (Fig. 4.2 B). The central region was separated from the background by a 100µm wide grey border. We chose three different remote stimuli - 1) light steps in counter phase (Fig. 4.2 A); 2) reversing gratings in two different spatial frequencies; 3) drifting gratings in two different spatial frequencies (grating period 2000µm and 500µm; Fig. 4.2 C, D respectively).

Remote stimulation (both reversing and drifting gratings) suppressed the ganglion cell responses. Again, we found the effects only in a subset of ganglion cells, where the remote stimulus also modulated the mean firing rate. The example ganglion cell shown here is an ON sustained cell. To our surprise, we found that the remote stimulus in counter phase enhanced the initial response to the light steps (Fig. 4.2 A). The reversing grating suppressed both transient and sustained components of the response, but not completely. The drifting grating suppressed the transient component and completely abolished the sustained component. Although the remote gratings enhanced maintained rate (Fig. 4.2 C), no enhancement of evoked response were found in our recordings.

4.5 Remote Stimulation Decreases the Contrast Sensitivity

Retinal ganglion cells are sensitive to small changes in contrasts, as low as 3-4% (Dhingra et al. 2003). Since the remote stimulus suppressed the response to 100% contrast steps, we hypothesised that responses to weaker stimuli may be affected. Therefore, we wanted to know if a remote stimulus affected the contrast sensitivity of a cell. To this end, we tested the cell's response to different contrast steps with and without gratings in the extra-classical receptive field. We used 5%, 10% and 20% contrast steps in the centre region. As expected, increasing the strength of the stimulus elicited a stronger response (Fig. 4.3 A, B). The remote stimulus - both drifting and reversing gratings; both low and high spatial frequencies - suppressed the responses of 10% and 20% contrast steps and completely abolished the response to 5% contrast steps (Fig. 4.3 D).

4.6 Remote Stimulus Modifies the Response Gain

The suppression of evoked responses by reducing the contrast sensitivity (Fig. 4.3 C, D) could arise from a change in the response gain, or more specifically by the 'contrast gain control' mechanism (Shapley and Victor 1978). To test this hypothesis, we applied Linear-Nonlinear (LN) system analysis. The LN model has been shown to capture the

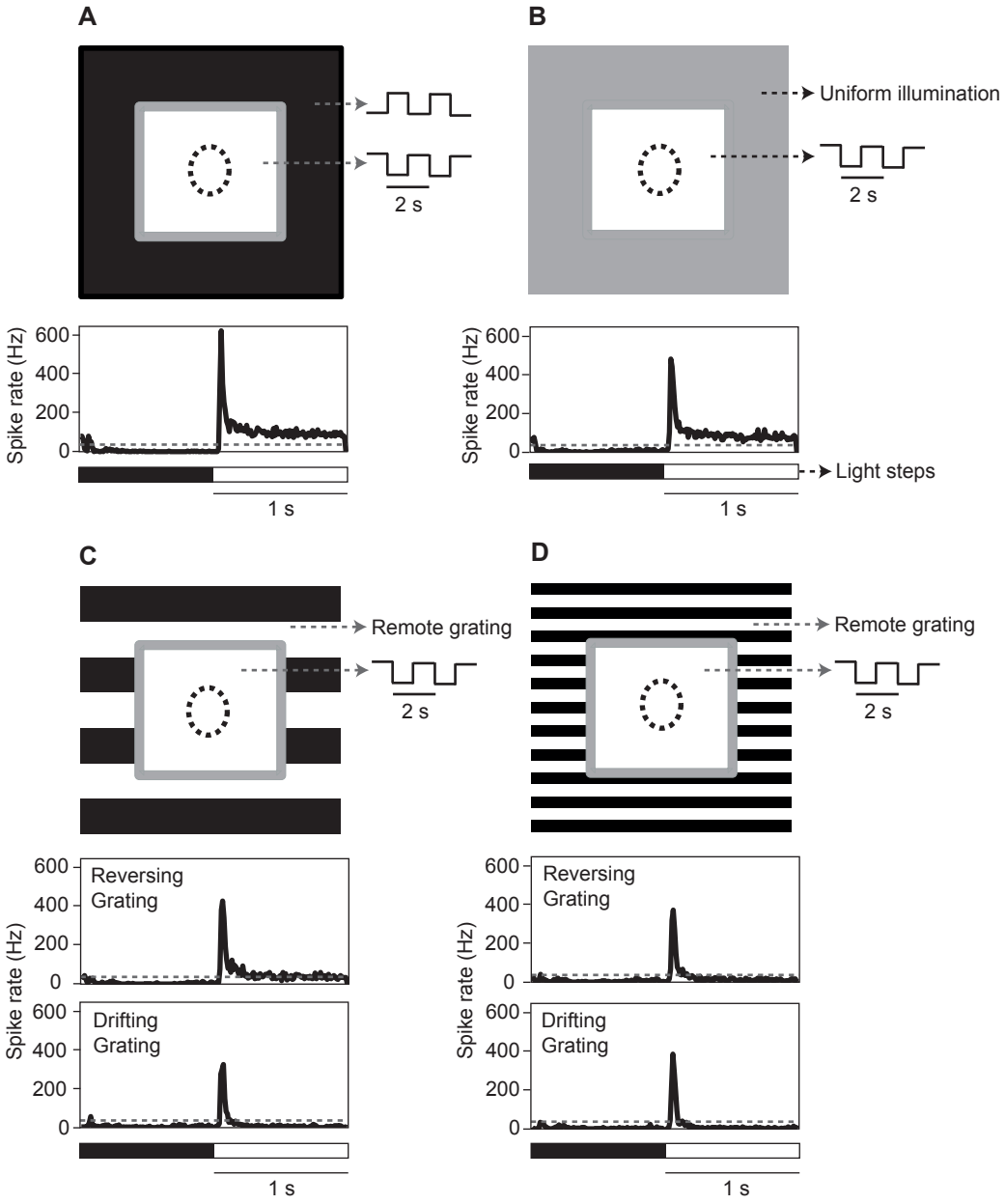

Figure 4.2: Remote stimulation suppresses the evoked activity. A) The stimulus comprised of light flashes in the central 900 µm x 900 µm region. The far surround comprised of light flashes in the opposite polarity. The dotted ellipse represents the receptive field of a ganglion cell. A 100µm thick grey border separated the central region and the far surround. The response of a ganglion cell is in the lower panel. The dotted line indicates the maintained rate of the ganglion cell under uniform illumination without any remote gratings. The stimulus phase of the central region is indicated at the bottom. B) The stimulus was similar as in A, but with far surround only with uniform grey illumination. C) Here the far surround comprised of low spatial frequency grating, either reversing or drifting. D) Here the far surround comprised of high spatial frequency grating, either reversing or drifting. Note the response of central stimulation is suppressed by varying degrees for different stimulus conditions.

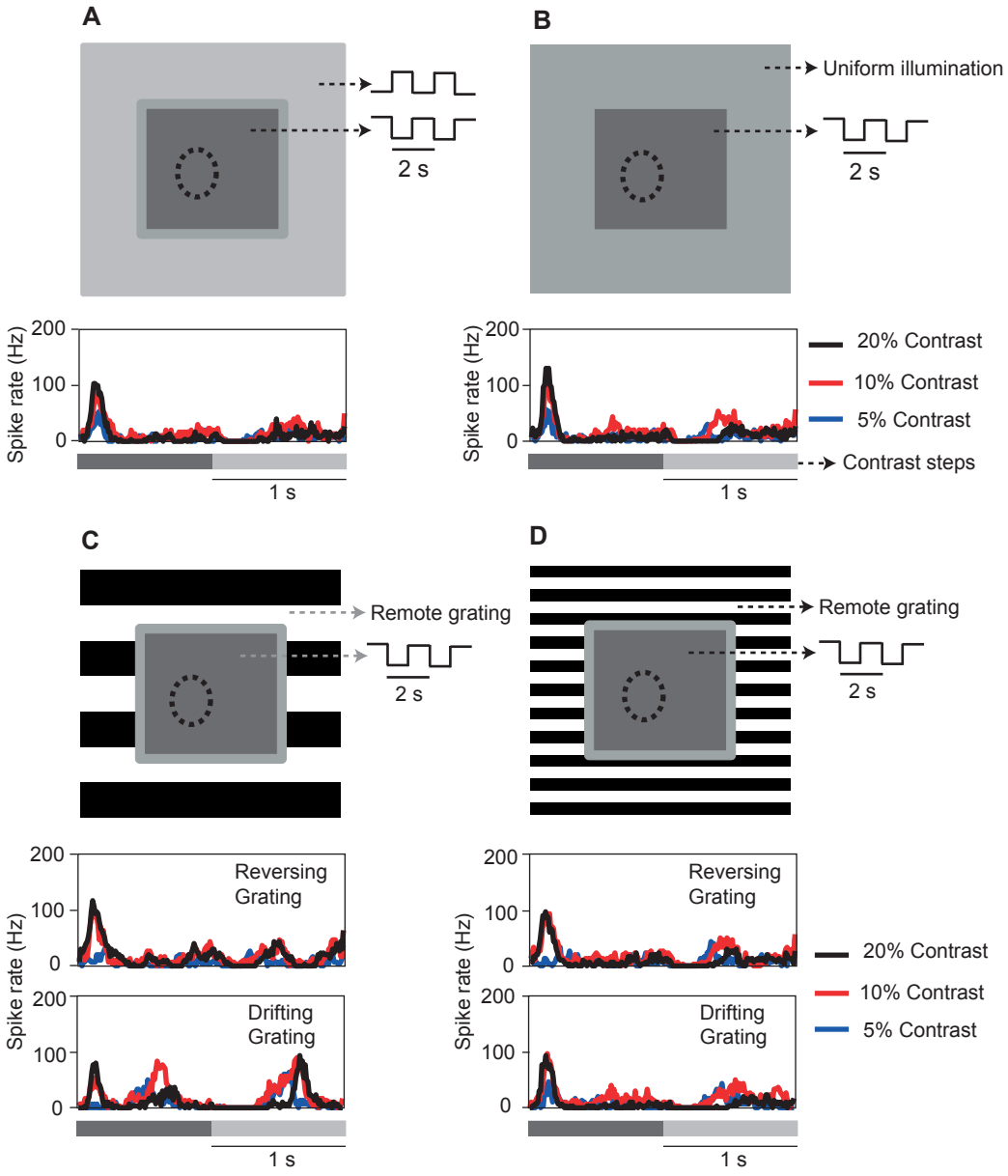

Figure 4.3: Remote stimulation decreases the contrast sensitivity. A) The stimulus comprised of light flashes in the central 900 µm x 900 µm region. The light flashes were presented in three different contrast levels. The dotted ellipse represents the receptive field of a ganglion cell. The far surround comprised of light flashes in the opposite polarity. A 100 µm thick grey border separated the central region and the far surround. The response of a ganglion cell is in the lower panel. The responses are stronger for stronger contrast steps. The stimulus phase of the central region is indicated at the bottom. B) The stimulus was similar as in A, but with far surround only with uniform grey illumination. C) Here the far surround comprised of low spatial frequency grating, either reversing or drifting. D) Here the far surround comprised of high spatial frequency grating, either reversing or drifting. Note the strong suppression of response to 5% contrast steps in the presence of remote gratings.

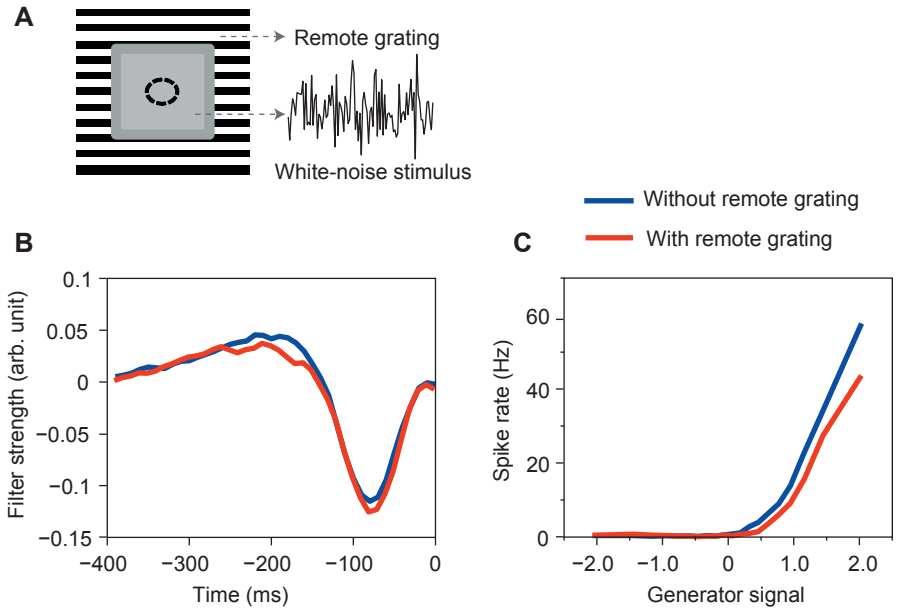

Figure 4.4: Remote stimulation modifies the response gain. A) The central 900 µm x 900 µm region was presented with a Gaussian white noise stimulus, where the stimulus intensities were drawn randomly every 20 ms from a Gaussian distribution. The dotted ellipse represents the receptive field of a ganglion cell. The far surround was presented with either a uniform grey illumination or reversing gratings. B) The spike triggered average (STA) which represents the linear filter of a ganglion cell, did not change in the presence of remote gratings. C) The nonlinearity which represents the response gain of a ganglion cell was shifted to the right in the presence of remote gratings, indicating the increased threshold and lowered sensitivity of the cell.

response of a ganglion cell to its visual stimulus, and has been used to study the response gain (Chichilnisky 2001, Chander and Chichilnisky 2001). We presented a Gaussian white noise flicker stimulus in the central region (900µm x 900µm), with or without reversing remote gratings in the extra classical receptive field (Fig. 4.4 A). The central region was separated from the background remote stimulus by a 100µm wide grey border. The linear filter computed as the spike triggered average (STA) did not change when remote gratings were presented (Fig. 4.4 B). But the nonlinearity which represents the response gain (i.e., input - output relationship) shifted to the right and the slope reduced in the presence of reversing remote gratings. The rightward shift implies an increase in threshold to spike and the reduced slope on the other hand indicated a reduced responsiveness (i.e., gain) of the ganglion cell in the presence of remote gratings. This is consistent with abolishing responses to low contrast in the presence of remote gratings (Fig. 4.3 C, D). Taken together, the suppressive far-surround contributes to

the retinal contrast gain control mechanism.

4.7 Chapter Summary

A saccadic scene change introduces global motion signals in the retina. Motion signals at a remote region in space affect the response properties of a ganglion cell to local stimulation in its receptive field. However, several studies show contradictory results, and the role of remote stimulus in modulating the cell's response remains inconclusive. In this study, we revisited these effects in the mouse retina and found that the remote stimulus 1) primarily suppresses the ganglion cell activity, but also enhances the mean firing rate, 2) suppresses the centre response of a ganglion cell, 3) reduces the contrast sensitivity of a ganglion cell, 4) increases the spike threshold, and 5) modulates the response gain. We propose that the contrast gain control mechanism may provide 'spatial context' to the ganglion cell responses in the presence of remote gratings.

5. Evaluation of Ganglion Cell Activity after Gene Therapy

Inherited retinal degenerative diseases are characterized by selective and progressive loss of specific cell types of the retina, such as photoreceptors and retinal pigment epithelium (Hartong et al. 2006, Sundaram et al. 2012) usually due to a defective gene. These diseases are of a broad spectrum with several genes implicated. Currently there are no effective treatment strategies to restore vision in retinal degenerative diseases in humans. Gene therapy offers a promising approach to restore vision and there are several studies that successfully replaced the missing gene and restored the partial function of the retina in different animal models (Ali et al. 2000, Acland et al. 2001, Alexander et al. 2007, Mancuso et al. 2009, Komaromy et al. 2010, Beltran et al. 2012). However, there is only indirect evidence of restoration of ganglion cell activity after gene therapy such as visual behaviour. A direct evaluation would be to measure the ganglion cell activity. In the present study, we took advantage of the multi-electrode array recordings and evaluated the ganglion cell activity after gene therapy in a mouse model of achromatopsia.

5.1 CNGA3$^{-/-}$ Mouse Model of Achromatopsia

Phototransduction is a process by which light signals are converted to electrical signals in the photoreceptors. The cyclic nucleotide-gated (CNG) channels stand at the end of the phototransduction process and translate the light-dependent changes of cyclic guanosine monophosphate (cGMP) levels into electrical activity, which in turn controls the release of neurotransmitters (Kaupp et al. 1989, Hirano et al. 2000). CNG channels comprise two structurally related subunit types, the A and B subunits. The A subunits form the ion-conducting unit and the B subunits function as modulators (Zagotta and Siegelbaum 1996, Gerstner et al. 2000). The CNG channel is a heterotetramer composed of two CNGA and CNGB subunits: CNGA1/B1 in rods and CNGA3/B3 in cones (Peng

et al. 2004). Nearly one-third of all cases of complete achromatopsia - which severely impairs cone-mediated vision - in humans are caused by gene mutation in either A3 or B3 subunit of cyclic nucleotide gated (CNG) channels (Kohl et al. 2005). The complete lack of cone function in achromatopsia results in daytime blindness, lack of colour discrimination, poor visual acuity, pendular nystagmus and photophobia (Kohl et al. 1998, Michaelides et al. 2004, Thiadens et al. 2009).

Similar to human phenotype, genetic inactivation of CNGA3 in mice leads to selective loss of cone-mediated light responses accompanied by morphological, structural and molecular changes and finally results in cone death (Biel et al. 1999, Michalakis et al. 2005). These changes occur before completion of photoreceptor development, and include a disorganization of cone outer segments, downregulation and mislocalization of cone opsins, and downregulation of other outer segment proteins (Michalakis et al. 2005). Cone degeneration is evident from the second postnatal week and proceeds faster in ventral and nasal parts of the retina, and ventral cones are almost completely missing after the third postnatal week, while the number and morphology of rods were unaffected (Michalakis et al. 2005). Thus, the CNGA3$^{-/-}$ mouse provides an ideal model for exploring approaches that have a goal to restore cone vision in achromatopsia.

Currently, there are no effective treatment strategies available to restore vision in humans with retinal degeneration. In the recent years, there has been considerable progress in developing gene therapy for retinal degeneration using recombinant adeno-associated viral (rAAV) vectors in a variety of animal models including rodents, canines and primates (Ali et al. 2000, Acland et al. 2001, Alexander et al. 2007, Mancuso et al. 2009, Komaromy et al. 2010). The success in animal models has led to human clinical trials (Bainbridge et al. 2008, Cideciyan et al. 2008, Hauswirth et al. 2008, Maguire et al. 2008), with one study to replace RPE65 gene in Leber congenital amaurosis (Bennett et al. 2012) proving successful in rescuing partial vision.

In the present study, our collaborators Dr. S. Michalakis, Dr. M. Biel (Ludwig Maximilians University, Munich), Dr. R. Mülfriedel and Dr. M. Seeliger (Eberhard Karls University, Tübingen) successfully devised a rAAV mediated gene therapy strategy in CNGA3$^{-/-}$ mouse model. Analyis of cone morphology, expression of CNGA3 and other proteins, electroretinogram and behaviour of treated mice showed the rescue of functional defects resulting from congenital absence of CNGA3 channel. Thus, the question arises whether the network of the retina functions in a normal way and whether the ganglion cells respond to visual stimulation in photopic light levels.

As our part of the study, we show that the rescue of restoration of cone function and morphology results in proper transmission of light-evoked signals by measuring ganglion

cell activity with a multielectrode array. The results presented in this chapter together with the results of our collaborators have been published (Michalakis et al. 2010).

5.2 Subretinal Injection of rAAV Vectors

Among different gene delivery systems including non-viral and viral vectors, recombinant adeno-associated viral (rAAV) vectors are found to be particularly effective (Conley et al. 2008, Sundaram et al. 2012). Our collaborators designed rAAV vectors that drive expression of the mouse CNGA3 complementary DNA under control of a 0.5.kb fragment of the mouse blue opsin (S-opsin) promoter (Akimoto et al. 2004). The viral vector particles were packaged with an Y719F-modified AAV5 capsid (AAV5-mBP-CNGA3) that results in higher resistance to proteosomal degradation (Petrs-Silva et al. 2009). They delivered 6-9 x 109 rAAV genomic particles into the subretinal space within the central to ventral part of the retina of 12 to 14-day-old CNGA3$^{-/-}$ mice (Fig. 5.1). The success of the procedure was monitored using scanning laser ophthalmoscopy and optical coherence tomography. It turned out that a single subretinal injection (1-1.5µl volume) covered $\approx$ 30% of the total retina.

5.3 Visual Stimulation

In recordings from treated retinas, placement of the retina on the multi-electrode array roughly aimed at covering the electrode array with the treated region of the retina. To visually stimulate the retina, the screen of a CRT monitor was focused with standard optics onto the photoreceptor layer, covering the recorded piece of retina. Periodic flashes were produced by switching the monitor display every 1 second between black and white, with a contrast (white-black)/(white+black) = 0.97. Overall light level was controlled with neutral density filters in the light path. Recordings for different light levels were always performed in the order of increasing intensities. For each light level, a 10-15 min adaptation period at constant illumination preceded the recordings.

5.4 Results

Ten weeks post-treatment, clear signs of functional recovery were found in electroretinogram (ERG). At dim light levels, there was no difference between treated and untreated groups, thus signifying that the procedure did not interfere with the existing

rod-mediated visual pathway. The rescue of cone function was demonstrated by ERG measurements at photopic light levels (Michalakis et al. 2010). Immunocytochemistry revealed the expression of CNGA3 proteins in the injected region but not the untreated part of the retina. CNGA3 was produced as a result of the gene therapy and was able to restore expression of CNGB3. Furthermore, these proteins were localized in the cone outer segments along with S-opsin (Short wavelength) and M-opsin (medium wavelength), which was not the case in untreated retina. Also the gene therapy resulted in the establishment of a functional visual cascade and delay of degeneration in treated CNGA3$^{-/-}$ mouse (Michalakis et al. 2010). The animals were tested for vision-guided behaviour that highly depends on cone-mediated vision under photopic light conditions. The test was a modified version of Morris water maze (two-choice cued water maze task). Wild-type mice were able to discriminate between two platforms and were matched by treated animals, but not by untreated animals (Michalakis et al. 2010).

Having shown the efficacy of gene therapy by above mentioned tests, it is important to test if the cones in the treated retinas reliably transferred their signals and if the signals were sufficient to drive the ganglion cell. To this end, we performed multielectrode array recordings to measure the spiking activity of ganglion cells from isolated retinas of treated and untreated eyes of CNGA3$^{-/-}$ mice (Fig. 5.1). As expected for a retina limited to rod function only, ganglion cells from untreated CNGA3$^{-/-}$ mice responded well at low-light levels, but did not show any light-evoked activity under photopic conditions (Fig. 5.1 B, D). Much in contrast, many neurons in treated regions displayed strong light-evoked activity for both low- and high-light levels Fig. 5.1 A, C). Specifically, 33 out of a total of 46 recorded ganglion cells from three retinas displayed clear light-evoked spiking activity at photopic light levels, indicating that transmission of cone signals to the inner retina was re-established in the treated retinas.

Among these 33 ganglion cells with photopic responses, the response characteristics revealed ON-type cells, as well as OFF-type and ON-OFF-type cells. Most cells had the same response type at all light levels (12 ON cells, 11 OFF cells, 6 ON-OFF cells); four cells had ON-OFF characteristics at low light intensity, but were classified as either ON-type or OFF-type at high light level (Table 5.1). This may be due to the fact that only a subset of cones are transduced by the rAAV vector and express CNGA3 within the ON-OFF ganglion cell's receptive field. These results indicate that all major response types of ganglion cells are restored by the treatment and that the basic cell-type specification is upheld.

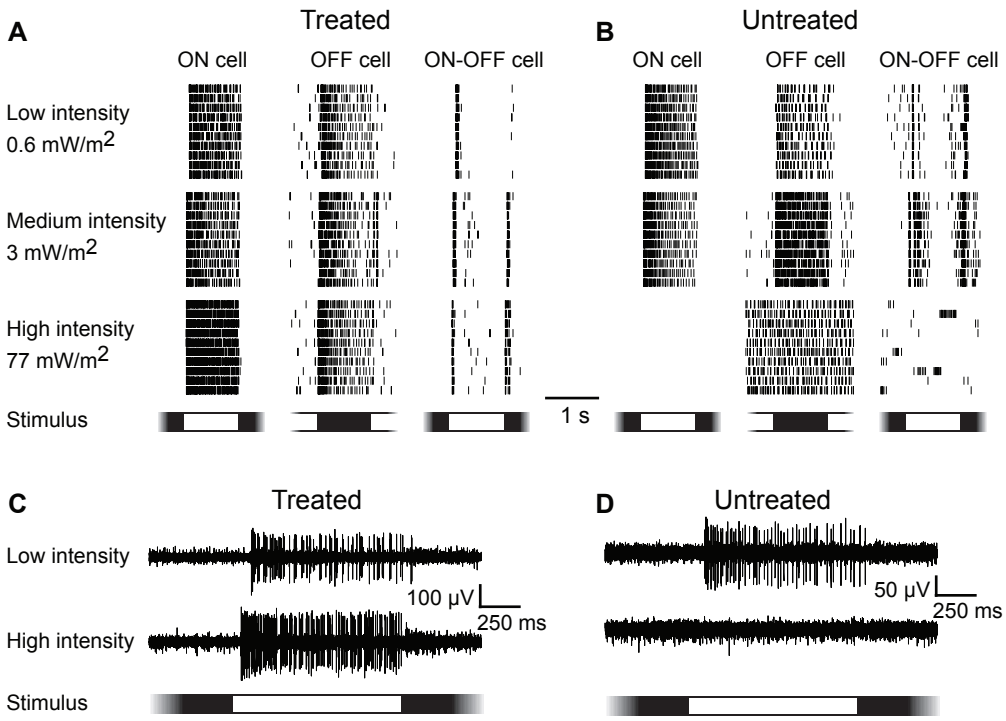

Figure 5.1: Gene replacement therapy restores responsiveness of ganglion cells to photopic stimuli in CNGA3$^{-/-}$ mice. (A, B) Spike trains of different types of ganglion cells from (A) treated and (B) untreated CNGA3$^{-/-}$ mice. Spikes were measured in response to periodic flashes of light at three different intensity levels (left). For each condition, responses to 10 successive presentations are shown. Stimulus phase is indicated at the bottom. The spike trains obtained from the treated mice show reliable response patterns for all applied light intensities. By contrast, ganglion cells from untreated retinas do not respond to light flashes at the highest light level, which corresponds to photopic conditions. Instead, some cells at this light level display spontaneous activity, which is not locked to the stimulus presentation. (C, D) Sample voltage traces recorded from the ON cells shown in A and B, respectively. The image is adapted from Michalakis et al. (2010).

Cell type	Scotopic	Photopic	
ON	12	ON	12
		OFF	0
		ON-OFF	0
OFF	11	ON	0
		OFF	11
		ON-OFF	0
ON-OFF	10	ON	2
		OFF	2
		ON-OFF	6

Table 5.1: Distribution of cell types in treated retinas under different light levels

5.5 Chapter Summary

Gene therapy offers a promising approach in treating inherited retinal degenerative disorders. Success in gene therapy for retinal dystrophies depends on the reliable rescue of ganglion cell activity. Here, we evaluated the ganglion cell activity with a multi-electrode array. We show that the rAAV mediated gene therapy successfully rescued ganglion cell activity in a CNGA3$^{-/-}$ mouse model of achromatopsia. Also, the basic response types in ganglion cells were restored.

6. Summary & Discussion

The task of the visual system is to extract behaviourally relevant information from the visual scene. A common strategy for most animals ranging from insects to humans is to constantly reposition gaze by making saccades within the scene (Land 1999). This 'fixate and saccade' strategy seems to pose a challenge, as it introduces a highly blurred image on the retina during a saccade, but at the same time acquires a 'snapshot' of the world during every fixation (Tatler 2001). The visual signals on the retina are thus segmented into brief image fixations separated by global motion. What is the response of a ganglion cell to 'motion blur' caused by a saccade, and how does it influence the response to subsequent fixations? Also, how does the global motion signal influence the response dynamics of a ganglion cell? In this thesis, we addressed these questions by two complementary approaches.

First, we analysed the retinal ganglion cell responses to simulated saccades (Chapter 3). We analysed two important aspects of the response - 1) response during a saccade-like motion, 2) response to fixation images. For about half of the recorded cells, we found strong spiking activity during the saccade. This supports the idea that the retina actively encodes the saccade and may signal the abrupt scene change to downstream brain areas. Furthermore, we characterized the responses to the newly fixated image. While there appears to be only little influence of the preceding motion signal itself on these responses, the responses depended strongly on the image content during the fixation period prior to the saccade. Thus, saccadic vision may provide 'temporal context' to each fixation, and ganglion cells encode image transitions rather than currently fixated images. Based on this perspective, we classified retinal ganglion cells into five response types, suggesting that the retina encodes at least five parallel channels of information under saccadic visual stimulation. The five response types identified in this study are as follows:

1) *Classical Encoders* - Response only to preferred stimuli
2) *Offset Detectors* - Response only to the saccade

3) *Indifferent Encoders* - Response to all fixated images
4) *Change Detectors* - Response only when the new image after the saccade differs from the previous image
5) *Similarity Detectors* - Response only when the new image after the saccade is similar to the previous image

Second, we analysed the influence of global motion signals on the response of a retinal ganglion cell to the stimulus in its receptive field (Chapter 4).The stimulus beyond the receptive field is designated as remote stimulus. We chose simple stimulus (Fig. 4.1 A) that represent various configurations used in earlier studies, thus allowing us to compare our results. We show that the remote stimulus both enhances and suppresses the mean firing rate, but only suppresses the evoked activity. Furthermore, we show that the remote stimulus decreases the contrast sensitivity (Fig.4.3) and modifies the response gain (Fig. 4.4). Thus, the ganglion cells encode the stimulus in relation to the whole scene, rather than purely respond to the stimulus in the receptive field. Our results suggest that the global motion signals provide 'spatial context' to the response of the stimulus within the receptive field.

6.1 Stimulus History and Context-Dependent Responses to Fixation

In this study, we showed that the responses depended strongly on the history of the stimulus before the saccade. We also showed that the cells could be classified into five response types in such a scenario. Thus, the ganglion cells do not merely convey the information of a fixated image, they convey the information with a 'context', i.e., taking history into consideration. We have shown that the response to a particular fixated image is not the same, when the preceding stimulus history is different. Except *Offset Detectors*, all other response types showed a marked difference in their response to a fixated image, when the preceding stimulus history is different. For *Classical Encoders* and *Indifferent Encoders*, the responses varied by a change in latency and firing rate. For *Change Detectors* and *Similarity Detectors*, the responses varied dramatically.

Our results are particularly interesting, given the fact that the periods of fixations are the most informative about our visual environment. Also, if the gaze is stabilized, the visual perception fades away as fast as $\approx$ 100ms (Martinez-Conde et al. 2004), underscoring the importance of the initial period of fixation. This initial period of fixation

after a saccade has been shown to provide the most information in archer fish retina (Segev et al. 2007). Earlier reports have shown that the firing rate of many ganglion cells increases just after a saccade (rabbit: Roska and Werblin 2003; archer fish: Segev et al. 2007), suggesting that the release of suppression from saccades actually drive the ganglion cells much stronger and make them more informative. Another study showed that the sudden mean luminance changes caused by saccade-like shifts modulated the ganglion cell response ranging from strong suppression to strong activation (Amthor et al. 2005). Saccades are also shown to cause dramatic effects on certain OFF cells to transiently produce ON responses, just after a saccade (Geffen et al. 2007). These studies show that saccades modulate the response to a fixated image, by eliciting a variety of different responses. Nevertheless, the earlier studies mentioned above have not taken into account the history of the stimulus before the saccade.

Stimulus history dependence and providing context to the present stimulus have been shown in motoneurones (Powers et al. 2005) and in different brain regions including retina (Chiao and Masland 2003, Wark et al. 2009), LGN (Fellous et al. 2004), MT (Fellous et al. 2004, Schlack et al. 2007) and in auditory cortex (DeWeese and Zador 1998, Watkins and Barbour 2008, Asari and Zador 2009). Our study reaffirms that neurons have the capacity to encode the information about the stimulus and additionally add 'context' taking recent history into consideration (see DeWeese and Zador 1998, Kording et al. 2007). Thus, saccades may provide context to each fixation, and ganglion cells encode image transitions rather than the currently fixated image.

6.2 What Causes a Particular Response Type?

Classical Encoders are the predominant response type, and are mostly X-like cells (Fig. 3.12). X cells are characterized by sustained response and also responded with a preferred and null phase to reversing gratings (Enroth-Cugell and Robson 1966, Stein et al. 1983). Thus, the response profile of *Classical Encoders*, which are also spatial phase dependent and have sustained firing (Fig. 3.2 A, B), is easily explained by their basic physiological property.

Response types other than *Classical Encoders* are mostly Y-like cells, which respond with 'bursty' firing to fast moving gratings (Stein et al. 1983). This property explains the transient firing during saccade-like scene shifts. But Y cell properties alone could not explain the response to fixated images. For *Change Detectors*, long-lasting adaptation might cause the response attenuation if the same stimulus appears after a saccade. Synaptic facilitation may cause enhanced response in *Similarity Detectors* if the same

stimulus appears after a saccade. Alternatively, there may be a common circuitry that differentially modulates these two types simultaneously, producing opposite response patterns. More than half of *Indifferent Encoders* are ON-OFF cells, thus explaining their response to all of the fixated images. *Offset Detectors* may have a similar mechanism to local edge detectors (LED) which respond only to moving edges and not to fixated images.

6.3 Comparison with Other Classification

Retinal ganglion cells of mouse have been classified extensively by several research groups based on morphology, physiology, dendritic arborisation, dendritic thickness, molecular and genetic markers, projection to different brain regions etc (Doi et al. 1995, Sun et al. 2002, Carcieri et al. 2003, Badea and Nathans 2004, Kong et al. 2005, Völgyi et al. 2005, 2009, Coombs et al. 2006, Hattar et al. 2006, Loopuijt et al. 2007, Huberman et al. 2008, 2009, Kim et al. 2008, Siegert et al. 2009, Yonehara et al. 2008, 2009, 2011, Farrow and Masland 2011, Hong et al. 2011, Kay et al. 2011, Rivlin-Etzion et al. 2011). The five response types described in our study arise when ganglion cells were tested with a specific type of stimulus namely the saccade stimulus. We sought to look into some of the earlier classifications and see how well our classification fits or deviates from the existing schema.

Comparison with anatomical/morphological classification: There are at least 12 types of ganglion cells based on anatomical classification alone (Badea and Nathans 2004, Kong et al. 2005, Coombs et al. 2006, Völgyi et al. 2009).We wanted to know if each response type belongs to a specific anatomical or morphological cell class. In our experiments we do not have access to the morphology of a ganglion cell. Nevertheless, the receptive field size of a ganglion cell estimated by reverse correlation (see Section 2.6.3; Fig. 2.4) offers some clue about a cell's dendritic field size. Our results show that each response type comprises cells with different receptive field sizes (Fig. 3.11). *Classical Encoders* were mostly small cells ($\approx$ 150µm) though some large cells were also found. The other response types are even more heterogeneous, comprising cells with different receptive field sizes . Thus it is clear that a response type may contain more than one anatomical cell class.

Comparison with functional classification: We used a nonlinearity index to classify cells into X-like and Y-like. Although we found X-like and Y-like cells, they did not form separate group of cells, rather formed a continuum as reported by Carcieri et al. (2003). *Classical Encoders* were mostly X-like, although some Y-like cells were found. The rest

of the cells, on the other hand, were mostly Y-like, although some X-like cells were present. Y-like cells in mouse are known to have three anatomical subtypes based on their electrical coupling patterns (Völgyi et al. 2005). It is not clear if each of these subtypes corresponds to different response types described in our study.

Furthermore we also identified direction selective and orientation selective cells in our recordings, but they do not cluster into a single response type.

While it is difficult to assign different cell classes to different response types, one cell class stands out - X-like cells which have small receptive field ($\approx$ 150µm), brisk sustained response pattern, also known as beta cell (based on soma size). This cell type form $\approx$ 70% of *Classical Encoders*. Y-like cells are characterized by medium to large receptive fields and brisk transient response. They are known as alpha cells (based on soma size) and form majority of rest of response types *Offset Detector*, *Indifferent Encoder* and *Similarity Detector*. The cells of *Change Detector* have slightly different response pattern indicating a non-X and non-Y cell type. The response profile of the cells (8 out of 9 cells) was neither transient nor sustained (Fig.3.5) with a lower peak firing rate. Thus we could identify at least three physiological cell classes with each forming predominantly but not exclusively three groups of response types. These three broad physiological cell classes may correspond to S-units (mostly X cells), T-units (mostly Y cells) and M-units described in cat retina during a saccade, described by (Noda 1975).

While there are no OFF cells in *Change Detector*, there are no ON cells in *Similarity Detector*. These are two opposite response types and most likely opposite cell types. In guinea pig retina, it is common to find an ON cell - OFF cell pair (unpublished observation). It is likely that they may exist in mouse retina as well and function as *Change Detector - Similarity Detector* cell pair.

6.4 Does the Retina Contribute to Saccadic Suppression?

During saccadic eye movements, the image on the retina is highly blurred, but our visual perception to this motion blur is suppressed. This process is known as 'saccadic suppression' and it is an important phenomenon, so that we can perceive a stable visual world (Volkmann 1962, Beeler 1967, Noda and Adey 1974a, Burr et al. 1994, Ross et al. 2001). Saccadic suppression has been observed in several species including rodents (Lee et al. 2007, Phongphanphanee et al. 2011), cat (Noda and Adey 1974a), monkey (Ross et al. 2001) and human (Beeler 1967). It is also observed at different stages in

visual processing including lateral geniculate nucleus (LGN; Noda and Adey 1974a), primary visual cortex (V1; Wurtz 2008) and extra striate cortex MT and MST (Wurtz 2008). It has been suggested that elevation of visual threshold in LGN during an eye movement could cause saccadic suppression (Adey and Noda 1973). The elevation of visual threshold in LGN was also observed when the eye is stable but the image across the retina is moved, suggesting a significant retinal component to saccadic suppression (Adey and Noda 1973, Noda and Adey 1974a). Later Noda and Adey (1974b) showed that some ganglion cells strongly responded to saccadic eye movements. They suggested that the active response of retinal ganglion cell might contribute to the observed threshold elevation in LGN and thus to saccadic suppression. Another study, showed that some ganglion cells are inhibited by saccades and suggested this could contribute to saccadic suppression (Roska and Werblin 2003). Our results consolidated these two contradicting reports. We found that half our cells responded actively to saccade. The other half of the cells did not respond (some cells were suppressed) to saccades. But to what extent does the retina contribute to saccadic suppression? Which of these two response types - actively spiking or suppressed - contribute? It is not only tough to predict which of these types contribute, but if there is any evidence to retinal contribution at all, since saccadic suppression is observed even before an eye movement (Ross et al. 2001). Thus the role of the retina for saccadic suppression is inconclusive. So, what may these responses be useful for? Perhaps, the actively spiking ganglion cells report "yes, there was a saccade" to different downstream centres that receive corollary discharge from higher brain centres about the impending saccade initiation and thus suppression. In our recordings the cells that actively spike during a saccade are classified further into four types, it may be conceivable that each one of these projects to different downstream centres conveying the information.

6.5 Retinal Signals during Eye-blinks

Our vision is often interrupted by both spontaneous and intentional eye blinks, to protect our eye from dust and other tiny objects and to moisten and oxygenate our corneas. We blink 10-15 times a minute, with each blink lasting 100-150 ms (similar to saccade duration) and reducing incoming light levels by 100 fold (Burr 2005). Although each blink causes a mini 'black-out', it goes almost unnoticed. The visual perception during an eye blink is suppressed and the process is thought to be by the same mechanism as saccadic suppression (Volkmann 1986, Ridder and Tomlinson 1995, 1997, Burr 2005). Similar to saccadic suppression, blink suppression occurs even when there is a retinal stimulation (Volkmann et al. 1982, Bristow et al. 2005). So, what signals does the

retina send during and after an eye blink?

Eye blinks are also a common feature in rodents, although the blink rate is slightly lower at 5-6 blinks per minute (Kaminer et al. 2011). Our experiments where the transition between fixations is just a grey image instead of saccade-like motion can be considered to mimic eye blink. Our results suggest that the retinal signals during such a 'grey-out' are similar to signals during a saccade (Fig. 3.14) and may provide signals to downstream centres that received a corollary discharge about the impending eye blink. Also the responses to fixation after such a grey image are similar to signals after a saccade. We found the same five response types as for saccade-like scene shifts. Thus fixation after an eye blink may provide segregated information to different downstream visual centres. Furthermore, our results suggest that the retinal signals during saccade-like scene changes and eye blinks are similar, just like saccadic suppression and blink suppression are similar.

6.6 Parallel Processing during Saccadic Scene Changes

The retina of several species consists of at least ten types of ganglion cells (mouse: Sun et al. 2002, Kong et al. 2005, Coombs et al. 2006, Farrow and Masland 2011; rat: Huxlin and Goodchild 1997; rabbit: Rockhill et al. 2002; cat: O'Brien et al. 2002; monkey: Dacey et al. 2003; human: Kolb et al. 1992). Each one of these types encodes different features of the same visual scene, thus providing parallel channels of information to downstream centres (Lennie 1980, Roska and Werblin 2001, Masland 2001, 2011, Wässle 2004, Nassi and Callaway 2009). The five response types for fixation images described in our study reinforce the concept of parallel processing in the context of saccadic scene changes. The visual channels described in our study range from simple pixel detectors to cells that encode either difference or similarity across saccades. There may be more than one cell type that represents a response type; nevertheless there are at least five channels of information.

Each one of these types may project to different regions of the brain, like superior colliculus (SC) and LGN. X cells project to LGN and rarely to SC, whereas a single Y cell projects to both SC and LGN (Nelson and Kolb 2004). A recent study by Kay et al. (2011) shows that subsets of ON-OFF directionally selective ganglion cells project to distinct brain targets. In our recordings, most *Classical Encoders* are X-like (Fig. 3.12) and thus their information is probably projected to LGN. Since this type forms half of the cells, it is likely that there is more than one anatomical cell type within this response type. And each of these cell types could project to different targets within

LGN, thus providing segregated information to different targets.

On the other hand, a single Y cell projects to both SC and LGN, thus possibly conveying the same information to different targets. Our results show that most cells other than *Classical Encoder* are Y-like. Also they respond to saccade-like image shifts. They are again sub-classified into four response types. Saccadic suppression is strongest in SC (Wurtz, 2008). Saccade initiation takes place in inferior layers of SC (Lee et al. 2007, Wurtz 2008, Phongphanphanee et al. 2011). These cells are connected to superficial cells that receive inputs from retina and corollary discharge from cortex. It makes sense that SC receives Y cell inputs that respond to saccades. The sub types of Y cells may project to different layers of LGN as well as conveying 'context' dependent visual information about the fixation.

6.7 Mechanism Underlying the Effects of Remote Stimulation

We found that the remote stimulus both enhances and suppresses mean firing rate (Fig. 4.1), but only suppresses the evoked activity. How are these effects brought about? In salamander and mammalian retinas, inhibition of ganglion cell responses to centre stimuli is amacrine cell mediated. In the salamander retina, it has been shown that wide-field glycinergic amacrine cells in the far-surround inhibit the ganglion cells (Werblin 1972, Werblin and Copenhagen 1974, Thibos and Werblin 1978, Cook and McReynolds 1998). In the cat and guinea pig retina the remote gratings inhibit through GABAergic wide-field amacrine cell (Frishman and Linsenmeier 1982, Zaghloul et al. 2007). It is likely that the same inhibitory mechanism causes suppression of mean firing rate in the presence of remote stimulation. But, how does one explain the enhancement of mean firing rate by remote stimulation (Fig. 4.1)? There are two possible mechanisms 1) rebound excitation and 2) disinhibition. Inhibition of a retinal ganglion cell causes hyperpolarization, and the termination of hyperpolarization results in 'rebound excitation' (Mitra and Miller 2007, Margolis and Detwiler 2007). Disinhibition is the timely release from inhibition of a ganglion cell. Enhancement of ganglion cell firing through 'disinhibition' from the far-periphery was first shown by Ikeda and Wright (1972) and later by Li et al. (1992). Our results show that the enhancement of mean firing rate follows suppression, and is in phases closely matching the reversing gratings. Whereas in drifting motion the enhancement and suppressin are tonic, indicating the effects of remote stimulus following the stimulus phase. It has been shown that the inhibitory effects were stronger in the OFF ganglion cells

in guinea pig retina (Zaghloul et al. 2007). Hence, it is likely that the disinhibitory effects were stronger in OFF cells. Our results show the enhancement of mean firing rate in both ON and OFF cells. However, the enhancement was stronger in OFF cells, thus complementing earlier reports. We found further evidence for 'rebound excitation' or 'disinhibition' in OFF cells. Both ON cells and OFF cells showed suppression of responses in the presence of remote gratings, but only in OFF cells we found burst of spikes 500ms after the onset of a non-preferred light step (Fig. 4.2 and Fig. 4.3). This response is unlikely a response to the light step but a rebound firing to the remote gratings which change their phase every 500ms.

6.8 Remote Stimulation and Contrast Gain Control

The retina adapts to the stimulus statistics and accordingly adjusts its response. Increase in visual contrast reduces the sensitivity of the ganglion cell, a phenomenon known as 'contrast gain control' (Shapley and Victor 1978). This phenomenon is well studied in the retina (Chander and Chichilnisky 2001, Kim and Rieke 2001, Baccus and Meister 2002, Demb 2002, Zaghloul et al. 2005). We show that the remote stimulus suppressed the visually evoked responses (Fig. 4.2) and completely abolished the responses to the weaker stimulus (Fig. 4.3). This suppression is achieved by increased threshold for response and reduced gain (Fig. 4.4). Our results provide a direct evidence for the presence of a 'contrast gain control' mechanism in the presence of remote stimulation. A similar gain control mechanism by remote stimulation has been shown in the guinea pig (Zaghloul et al. 2007) and monkey retinas (Solomon et al. 2006). Thus the retina adapts not only to local stimulus statistics, but to a stimulus over a wider region in space.

6.9 Remote Stimulation in Other Visual Areas

The effects of remote stimulation have been found not only in the retina but throughout the visual system (Allman et al. 1985, Albright and Stoner 2002). It has been observed in LGN (Valberg et al. 1985, Derrington and Felisberti 1998, Bonin et al. 2005, Alitto and Usrey 2008), visual cortex (Rizzolatti and Camarda 1977) and specialized areas of extra striate cortex (Albright and Stoner 2002). The surround suppression and contrast gain control in the retina seems to be the major contributor to the effects seen in LGN (Felisberti and Derrington 1999, 2001, Bonin et al. 2005, Alitto and Usrey 2008). In an elegant set of experiments, Alitto and Usrey (2008) found out that the

effects observed in the LGN originate from the retina and ruled out the possibility of cortical feedback. Solomon et al. (2002) suggested that the suppressive effects of remote stimulation observed in visual cortical neurons could originate from feedforward inputs from LGN. However, the effects of remote stimulus are stronger in the LGN (Kaplan et al. 1987, Cheng et al. 1995), indicating further fine tuning of the effects may take place at each successive stages. Nevertheless, it is clear that the primary site of origin of these effects is the retina.

6.10 Implications for Visual Information Processing

The remote stimulus described in this study mimics a sudden shift of scene (reversing gratings) or an eye movement similar to smooth pursuit eye movement (drifting gratings), both of which are types of saccade. We wanted to know how the global stimulus interacts with the encoding properties of local stimulus. In Chapter 3, we studied the responses of ganglion cells to global saccade-like motion stimuli and found five channels of information encoding in the retina. We found that the effects of remote stimulus in all cell types described in the Chapter 3. Thus these effects might act as an extra layer of information processing over and above the five channels of encoding. In such a scenario, what are the implications of such an effect of extra-classical receptive field? A natural visual scene is rich in features. When making an eye movement, each ganglion cell responds to the stimulus in its receptive field, taking into account the stimulus history and also spatial structure in the far surround. The stimulus in the far surround provides a spatial 'context' to the present stimulus. Thus the retina effectively integrates stimuli over wide regions of visual space. While we found both suppression and enhancement of mean firing rate in the retina, similar effects of both suppression and facilitation have been reported in LGN (Felisberti and Derrington 1999). The fact that these effects of remote stimulation are found all through the pathway provides a natural way of local-global stimulus comparisons (Allman et al. 1985) and may provide important context to encode objects in space.

Outlook

The central finding of this study is that the natural vision involving eye movements and eye-blinks provides context to the retinal coding. Furthermore, we have identified the presence of at least five parallel channels of information in the retinal output. These results offer new insights into the sensory processing in the retina under active vision.

At the systems level, it would be interesting to know the precise neural circuits that generate the different response types. Further experiments would be needed to identify the different circuit elements that contribute to a particular response type. The first set of experiments would be to record the ganglion cells under whole-cell patch clamp mode to measure the excitatory and inhibitory currents. Moreover, the availability of pharmacological agents to block specific channels or to silence different interneurons in the retina would help in teasing apart the circuits involved.

Exploring the quantitative circuit models that explain the input-output relationship of the observed responses would be of great interest. The well-known Linear-Nonlinear (LN) model, which has been used to describe the ganglion cell responses, is not sufficient to explain certain features especially complex response pattern during saccadic vision. For example, the modulation of ganglion cell spiking activity by remote stimulation is one such scenario. Extending the LN model to include the parameters of the remote stimulus would be the next logical step. For this, one needs to identify the specific features of the remote stimulus that contribute to the observed results. Examples include, considering the spatio-temporal features such as grating bar width, motion velocity and direction. Moreover, one should test if such an extension of LN model also explains the responses of individual response types. Such an improved model would be useful in testing the sensitivity of a ganglion cell under different conditions including saccades and eye-blinks.

Understanding the population coding strategies would be the next step. Retinal ganglion cells are known to fire correlated, anti-correlated and synchronous spikes. It has been suggested that such interactions of cells in the network carry substantial information to downstream centres (Meister and Berry 1999). How do the five response

types interact at the network level? To test the network interaction, one should proceed at two levels; 1) the interaction among the cells of the same response types and, 2) interaction among different response types. At present, we could record ≈ 25 cells simultaneously with 60 electrode arrays. However, this does not yield sufficient number of cells of a single response type to quantitatively model the network. To achieve the goal, we could turn to newer arrays with 252 electrodes, where one could record 100 to 150 cells simultaneously. Such a recording would give us sufficient levels of cells of each type to measure synchrony, correlation and redundancy present in the population code.

Does each response type present a genuine cell type and sample the visual scene in a "mosaic" arrangement? It is important to know the morphological identity and the distribution of each type in the retina. The availability of transgenic mouse models with fluorescent markers to specific subsets of ganglion cells have helped in identifying a few functional cell types (Kim et al. 2008, 2010, Zhang et al. 2012). Also, a set of ≈ 100 transgenic mouse lines with different labelled cell types has been described by Siegert at al (2009). Systematic analysis of a select set of mouse lines from this database would be the next step in identifying the cell types. Such an approach would help us in establishing morphology-function relationship. Also, it would resolve if there are any subtypes in each of the response types.

Our results could be useful in improving the existing strategies of restoring vision in retinal degenerative diseases. We have identified the generic pixel detectors (*Classical Encoder*) and other functional types. Present strategies of retinal prosthesis that involve the stimulation of ganglion cells do not involve selective activation of specific population of ganglion cells (Javaheri et al. 2006). We suggest that the development of a prosthesis that takes care of selective activation of different cell types would greatly improve the existing ones.

It would be interesting to know how our results add to the present understanding of signal processing at successive stages of the visual system. Naturally, the following questions arise. What is the specific target site for each of the visual channels identified here? How is this segregated information utilized by the downstream centres? Does the feature detection in the retina actually contribute to the decision making and thus behaviour of the animal? The answers to these questions rely on careful design of experiments using a variety of techniques, ranging from anatomy, electrophysiology, functional imaging and behavioural studies. One promising approach is two-photon calcium imaging of several cells of visual cortex in freely behaving animals. Recent studies have demonstrated the potential of such an approach by resolving long standing

questions in vision research (Dombeck et al. 2007, Kerr and Nimmerjahn 2012, Keller et al. 2012).

Closure

At the beginning of this thesis, we pointed out the challenges of sensory coding under naturalistic stimulus conditions. We approached this problem by studying retinal coding in the presence of saccades. We found that there are five response types including generic pixel detectors and cells that encode either similarity or difference across saccades. This suggests that saccadic vision provides temporal context to retinal coding. Also, there are at least five parallel channels of information already segregated at the level of the retina. Moreover, we showed that retinal coding in the presence of eye-blinks is amazingly similar to the coding under saccadic vision. We further showed that the global motion signals during saccades that modulate ganglion cell activity may provide spatial context to ganglion cell coding. Our results strengthen the notion that the retina does not just provide generic filtered information, but provides highly processed information about different features of the visual world. Our identification of new response types seems to add complexity to retinal coding, but offers new insights to sensory coding. We hope that the results presented in this thesis will lead to interesting directions in vision research.

Bibliography

Acland GM, Aguirre GD, Ray J, Zhang Q, Aleman TS, Cideciyan AV, Pearce-Kelling SE, Anand V, Zeng Y, Maguire AM, Jacobson SG, Hauswirth WW, and Bennett J (2001) Gene therapy restores vision in a canine model of childhood blindness, *Nat Genet* **28**:92–5.

Adey WR and Noda H (1973) Influence of eye movements on geniculo-striate excitability in the cat, *J Physiol* **235**:805–21.

Akimoto M, Filippova E, Gage PJ, Zhu X, Craft CM, and Swaroop A (2004) Transgenic mice expressing cre-recombinase specifically in m- or s-cone photoreceptors, *Invest Ophthalmol Vis Sci* **45**(1):42–7.

Albright TD and Stoner GR (2002) Contextual influences on visual processing, *Annu Rev Neurosci* **25**:339–79.

Alexander JJ, Umino Y, Everhart D, Chang B, Min SH, Li Q, Timmers AM, Hawes NL, Pang JJ, Barlow RB, and Hauswirth WW (2007) Restoration of cone vision in a mouse model of achromatopsia, *Nat Med* **13**(6):685–7.

Ali RR, Sarra GM, Stephens C, Alwis MD, Bainbridge JW, Munro PM, Fauser S, Reichel MB, Kinnon C, Hunt DM, Bhattacharya SS, and Thrasher AJ (2000) Restoration of photoreceptor ultrastructure and function in retinal degeneration slow mice by gene therapy, *Nat Genet* **25**(3):306–10.

Alitto HJ and Usrey WM (2008) Origin and dynamics of extraclassical suppression in the lateral geniculate nucleus of the macaque monkey, *Neuron* **57**(1):135–46.

Allman J, Miezin F, and McGuinness E (1985) Stimulus specific responses from beyond the classical receptive field: neurophysiological mechanisms for local-global comparisons in visual neurons, *Annu Rev Neurosci* **8**:407–30.

Ames A and Nesbett FB (1981) In vitro retina as an experimental model of the central nervous system, *J Neurochem* **37**(4):867–77.

Amthor FR, Tootle JS, and Gawne TJ (2005) Retinal ganglion cell coding in simulated active vision, *Vis Neurosci* **22**(6):789–806.

Andermann ML, Kerlin AM, Roumis DK, Glickfeld LL, and Reid RC (2011) Functional specialization of mouse higher visual cortical areas, *Neuron* **72**(6):1025–39.

Asari H and Zador AM (2009) Long-lasting context dependence constrains neural encoding models in rodent auditory cortex, *J Neurophysiol* **102**(5):2638–56.

Baccus SA and Meister M (2002) Fast and slow contrast adaptation in retinal circuitry, *Neuron* **36**(5):909–19.

Badea TC and Nathans J (2004) Quantitative analysis of neuronal morphologies in the mouse retina visualized by using a genetically directed reporter, *J Comp Neurol* **480**(4):331–51.

Bainbridge JW, Smith AJ, Barker SS, Robbie S, Henderson R, Balaggan K, Viswanathan A, Holder GE, Stockman A, Tyler N, Petersen-Jones S, Bhattacharya SS, Thrasher AJ, Fitzke FW, Carter BJ, Rubin GS, Moore AT, and Ali RR (2008) Effect of gene therapy on visual function in leber's congenital amaurosis, *N Engl J Med* **358**(21):2231–9.

Barlow HB (1981) The ferrier lecture, 1980. critical limiting factors in the design of the eye and visual cortex, *Proc R Soc Lond B Biol Sci* **212**(1186):1–34.

Barlow HB, Derrington AM, Harris LR, and Lennie P (1977) The effects of remote retinal stimulation on the responses of cat retinal ganglion cells, *J Physiol* **269**(1):177–94.

Barlow HB and Hill RM (1963) Selective sensitivity to direction of movement in ganglion cells of the rabbit retina, *Science* **139**(3553):412–4.

Beeler GW (1967) Visual threshold changes resulting from spontaneous saccadic eye movements, *Vision Res* **7**(9):769–75.

Beltran WA, Cideciyan AV, Lewin AS, Iwabe S, Khanna H, Sumaroka A, Chiodo VA, Fajardo DS, Roman AJ, Deng WT, Swider M, Aleman TS, Boye SL, Genini S, Swaroop A, Hauswirth WW, Jacobson SG, and Aguirre GD (2012) Gene therapy rescues photoreceptor blindness in dogs and paves the way for treating human x-linked retinitis pigmentosa, *Proc Natl Acad Sci U S A* **109**(6):2132–7.

Benardete EA and Kaplan E (1997) The receptive field of the primate p retinal ganglion cell, i: Linear dynamics, *Vis Neurosci* **14**(1):169–85.

Bennett J, Ashtari M, Wellman J, Marshall KA, Cyckowski LL, Chung DC, McCague S, Pierce EA, Chen Y, Bennicelli JL, Zhu X, Ying GS, Sun J, Wright JF, Auricchio A, Simonelli F, Shindler KS, Mingozzi F, High KA, and Maguire AM (2012) Aav2 gene therapy readministration in three adults with congenital blindness, *Sci Transl Med* **4**(120):120ra15.

Biel M, Seeliger M, Pfeifer A, Kohler K, Gerstner A, Ludwig A, Jaissle G, Fauser S, Zrenner E, and Hofmann F (1999) Selective loss of cone function in mice lacking the cyclic nucleotide-gated channel cng3, *Proc Natl Acad Sci U S A* **96**(13):7553–7.

Bölinger D and Gollisch T (2012) Closed-loop measurements of iso-response stimuli reveal dynamic nonlinear stimulus integration in the retina, *Neuron* **73**(2):333–46.

Bonin V, Mante V, and Carandini M (2005) The suppressive field of neurons in lateral geniculate nucleus, *J Neurosci* **25**(47):10844–56.

Boycott BB and Wässle H (1974) The morphological types of ganglion cells of the domestic cat's retina, *J Physiol* **240**(2):397–419.

Bristow D, Haynes JD, Sylvester R, Frith CD, and Rees G (2005) Blinking suppresses the neural response to unchanging retinal stimulation, *Curr Biol* **15**(14):1296–300.

Burr D (2005) Vision: in the blink of an eye, *Curr Biol* **15**(14):R554–6.

Burr DC, Morrone MC, and Ross J (1994) Selective suppression of the magnocellular visual pathway during saccadic eye movements, *Nature* **371**(6497):511–3.

Carcieri SM, Jacobs AL, and Nirenberg S (2003) Classification of retinal ganglion cells: a statistical approach, *J Neurophysiol* **90**(3):1704–13.

Chander D and Chichilnisky EJ (2001) Adaptation to temporal contrast in primate and salamander retina, *J Neurosci* **21**(24):9904–16.

Cheng H, Chino YM, Smith r E L, Hamamoto J, and Yoshida K (1995) Transfer characteristics of lateral geniculate nucleus x neurons in the cat: effects of spatial frequency and contrast, *J Neurophysiol* **74**(6):2548–57.

Chiao CC and Masland RH (2003) Contextual tuning of direction-selective retinal ganglion cells, *Nat Neurosci* **6**(12):1251–2.

Chichilnisky EJ (2001) A simple white noise analysis of neuronal light responses, *Network* **12**(2):199–213.

Cideciyan AV, Aleman TS, Boye SL, Schwartz SB, Kaushal S, Roman AJ, Pang JJ, Sumaroka A, Windsor EA, Wilson JM, Flotte TR, Fishman GA, Heon E, Stone EM, Byrne BJ, Jacobson SG, and Hauswirth WW (2008) Human gene therapy for rpe65 isomerase deficiency activates the retinoid cycle of vision but with slow rod kinetics, *Proc Natl Acad Sci U S A* **105**(39):15112–7.

Conley SM, Cai X, and Naash MI (2008) Nonviral ocular gene therapy: assessment and future directions, *Curr Opin Mol Ther* **10**(5):456–63.

Cook PB and McReynolds JS (1998) Modulation of sustained and transient lateral inhibitory mechanisms in the mudpuppy retina during light adaptation, *J Neurophysiol* **79**(1):197–204.

Coombs J, van der List D, Wang GY, and Chalupa LM (2006) Morphological properties of mouse retinal ganglion cells, *Neuroscience* **140**(1):123–36.

Dacey DM (1993) The mosaic of midget ganglion cells in the human retina, *J Neurosci* **13**(12):5334–55.

Dacey DM, Peterson BB, Robinson FR, and Gamlin PD (2003) Fireworks in the primate retina: in vitro photodynamics reveals diverse lgn-projecting ganglion cell types, *Neuron* **37**(1):15–27.

Demb JB (2002) Multiple mechanisms for contrast adaptation in the retina, *Neuron* **36**(5):781–3.

Demb JB, Haarsma L, Freed MA, and Sterling P (1999) Functional circuitry of the retinal ganglion cell's nonlinear receptive field, *J Neurosci* **19**(22):9756–67.

Derrington AM and Felisberti F (1998) Peripheral shift reduces visual sensitivity in cat geniculate neurones, *Vis Neurosci* **15**(5):875–80.

DeWeese M and Zador A (1998) Asymmetric dynamics in optimal variance adaptation, *Neural Computation* **10**(5):1179–1202.

Dhingra NK, Kao YH, Sterling P, and Smith RG (2003) Contrast threshold of a brisk-transient ganglion cell in vitro, *J Neurophysiol* **89**(5):2360–9.

Doi M, Uji Y, and Yamamura H (1995) Morphological classification of retinal ganglion cells in mice, *J Comp Neurol* **356**(3):368–86.

Dombeck DA, Khabbaz AN, Collman F, Adelman TL, and Tank DW (2007) Imaging large-scale neural activity with cellular resolution in awake, mobile mice, *Neuron* **56**(1):43–57.

Dowling J (1987) *The Retina: An Approachable Part of the Brain*, Belknap Press, Cambridge, MA, USA.

Elstrott J, Anishchenko A, Greschner M, Sher A, Litke AM, Chichilnisky EJ, and Feller MB (2008) Direction selectivity in the retina is established independent of visual experience and cholinergic retinal waves, *Neuron* **58**(4):499–506.

Enroth-Cugell C and Jakiela HG (1980) Suppression of cat retinal ganglion cell responses by moving patterns, *J Physiol* **302**:49–72.

Enroth-Cugell C and Robson JG (1966) The contrast sensitivity of retinal ganglion cells of the cat, *J Physiol* **187**(3):517–52.

Farrow K and Masland RH (2011) Physiological clustering of visual channels in the mouse retina, *J Neurophysiol* **105**(4):1516–30.

Felisberti F and Derrington AM (1999) Long-range interactions modulate the contrast gain in the lateral geniculate nucleus of cats, *Vis Neurosci* **16**(5):943–56.

Felisberti F and Derrington AM (2001) Long-range interactions in the lateral geniculate nucleus of the new-world monkey, callithrix jacchus, *Vis Neurosci* **18**(2):209–18.

Fellous JM, Tiesinga PH, Thomas PJ, and Sejnowski TJ (2004) Discovering spike patterns in neuronal responses, *J Neurosci* **24**(12):2989–3001.

Field GD and Chichilnisky EJ (2007) Information processing in the primate retina: circuitry and coding, *Annu Rev Neurosci* **30**:1–30.

Fischer B, Krüger J, and Droll W (1975) Quantitative aspects of the shift-effect in cat retinal ganglion cells, *Brain Res* **83**(3):391–403.

Flores-Herr N, Protti DA, and Wässle H (2001) Synaptic currents generating the inhibitory surround of ganglion cells in the mammalian retina, *J Neurosci* **21**(13):4852–63.

Freeman DK, Grana G, and Passaglia CL (2010) Retinal ganglion cell adaptation to small luminance fluctuations, *J Neurophysiol* **104**(2):704–12.

Frishman LJ and Linsenmeier RA (1982) Effects of picrotoxin and strychnine on nonlinear responses of y-type cat retinal ganglion cells, *J Physiol* **324**:347–63.

Geffen MN, de Vries SE, and Meister M (2007) Retinal ganglion cells can rapidly change polarity from off to on, *PLoS Biol* **5**(3):e65.

Gerstner A, Zong X, Hofmann F, and Biel M (2000) Molecular cloning and functional characterization of a new modulatory cyclic nucleotide-gated channel subunit from mouse retina, *J Neurosci* **20**(4):1324–32.

Gollisch T and Meister M (2010) Eye smarter than scientists believed: neural computations in circuits of the retina, *Neuron* **65**(2):150–64.

Hartline H (1938) The response of single optic nerve fibers of the vertebrate eye to illumination of the retina, *The American Journal of Physiology* **121**(2):400–415.

Hartong DT, Berson EL, and Dryja TP (2006) Retinitis pigmentosa, *Lancet* **368**(9549):1795–809.

Hattar S, Kumar M, Park A, Tong P, Tung J, Yau KW, and Berson DM (2006) Central projections of melanopsin-expressing retinal ganglion cells in the mouse, *J Comp Neurol* **497**(3):326–49.

Hauswirth WW, Aleman TS, Kaushal S, Cideciyan AV, Schwartz SB, Wang L, Conlon TJ, Boye SL, Flotte TR, Byrne BJ, and Jacobson SG (2008) Treatment of leber congenital amaurosis due to rpe65 mutations by ocular subretinal injection of adeno-associated virus gene vector: short-term results of a phase i trial, *Hum Gene Ther* **19**(10):979–90.

He S, Levick WR, and Vaney DI (1998) Distinguishing direction selectivity from orientation selectivity in the rabbit retina, *Vis Neurosci* **15**(3):439–47.

Hirano AA, Hack I, Wässle H, and Duvoisin RM (2000) Cloning and immunocytochemical localization of a cyclic nucleotide-gated channel alpha-subunit to all cone photoreceptors in the mouse retina, *J Comp Neurol* **421**(1):80–94.

Hochstein S and Shapley RM (1976) Quantitative analysis of retinal ganglion cell classifications, *J Physiol* **262**(2):237–64.

Hong YK, Kim IJ, and Sanes JR (2011) Stereotyped axonal arbors of retinal ganglion cell subsets in the mouse superior colliculus, *J Comp Neurol* **519**(9):1691–711.

Huberman AD, Manu M, Koch SM, Susman MW, Lutz AB, Ullian EM, Baccus SA, and Barres BA (2008) Architecture and activity-mediated refinement of axonal projections from a mosaic of genetically identified retinal ganglion cells, *Neuron* **59**:425–38.

Huberman AD and Niell CM (2011) What can mice tell us about how vision works?, *Trends Neurosci* **34**(9):464–73.

Huberman AD, Wei W, Elstrott J, Stafford BK, Feller MB, and Barres BA (2009) Genetic identification of an on-off direction-selective retinal ganglion cell subtype reveals a layer-specific subcortical map of posterior motion, *Neuron* **62**:327–34.

Huxlin KR and Goodchild AK (1997) Retinal ganglion cells in the albino rat: revised morphological classification, *J Comp Neurol* **385**(2):309–23.

Ikeda H and Wright MJ (1972) The outer disinhibitory surround of the retinal ganglion cell receptive field, *J Physiol* **226**(2):511–44.

Ishikane H, Gangi M, Honda S, and Tachibana M (2005) Synchronized retinal oscillations encode essential information for escape behavior in frogs, *Nat Neurosci* **8**(8):1087–95.

Jackman SL, Babai N, Chambers JJ, Thoreson WB, and Kramer RH (2011) A positive feedback synapse from retinal horizontal cells to cone photoreceptors, *PLoS Biol* **9**(5):e1001057.

Javaheri M, Hahn DS, Lakhanpal RR, Weiland JD, and Humayun MS (2006) Retinal prostheses for the blind, *Ann Acad Med Singapore* **35**(3):137–44.

Jeon CJ, Strettoi E, and Masland RH (1998) The major cell populations of the mouse retina, *J Neurosci* **18**(21):8936–46.

Kaminer J, Powers AS, Horn KG, Hui C, and Evinger C (2011) Characterizing the spontaneous blink generator: an animal model, *J Neurosci* **31**(31):11256–67.

Kaplan E, Purpura K, and Shapley RM (1987) Contrast affects the transmission of visual information through the mammalian lateral geniculate nucleus, *J Physiol* **391**:267–88.

Kaupp UB, Niidome T, Tanabe T, Terada S, Bonigk W, Stuhmer W, Cook NJ, Kangawa K, Matsuo H, Hirose T, and et al (1989) Primary structure and functional expression from complementary dna of the rod photoreceptor cyclic gmp-gated channel, *Nature* **342**(6251):762–6.

Kay JN, De la Huerta I, Kim IJ, Zhang Y, Yamagata M, Chu MW, Meister M, and Sanes JR (2011) Retinal ganglion cells with distinct directional preferences differ in molecular identity, structure, and central projections, *J Neurosci* **31**(21):7753–62.

Keller GB, Bonhoeffer T, and Hübener M (2012) Sensorimotor mismatch signals in primary visual cortex of the behaving mouse, *Neuron* **74**(5):809–15.

Kerr JN and Nimmerjahn A (2012) Functional imaging in freely moving animals, *Curr Opin Neurobiol* **22**(1):45–53.

Kim IJ, Zhang Y, Meister M, and Sanes JR (2010) Laminar restriction of retinal ganglion cell dendrites and axons: subtype-specific developmental patterns revealed with transgenic markers, *J Neurosci* **30**(4):1452–62.

Kim IJ, Zhang Y, Yamagata M, Meister M, and Sanes JR (2008) Molecular identification of a retinal cell type that responds to upward motion, *Nature* **452**(7186):478–82.

Kim KJ and Rieke F (2001) Temporal contrast adaptation in the input and output signals of salamander retinal ganglion cells, *J Neurosci* **21**(1):287–99.

King JG, Lettvin JY, and Gruberg ED (1999) Selective, unilateral, reversible loss of behavioral responses to looming stimuli after injection of tetrodotoxin of cadmium chloride into the frog optic nerve, *Brain Res* **841**(1-2):20–6.

Kohl S, Marx T, Giddings I, Jagle H, Jacobson SG, Apfelstedt-Sylla E, Zrenner E, Sharpe LT, and Wissinger B (1998) Total colourblindness is caused by mutations in the gene encoding the alpha-subunit of the cone photoreceptor cgmp-gated cation channel, *Nat Genet* **19**(3):257–9.

Kohl S, Varsanyi B, Antunes GA, Baumann B, Hoyng CB, Jagle H, Rosenberg T, Kellner U, Lorenz B, Salati R, Jurklies B, Farkas A, Andreasson S, Weleber RG, Jacobson SG, Rudolph G, Castellan C, Dollfus H, Legius E, Anastasi M, Bitoun P, Lev D, Sieving PA, Munier FL, Zrenner E, Sharpe LT, Cremers FP, and Wissinger B (2005) Cngb3 mutations account for 50autosomal recessive achromatopsia, *Eur J Hum Genet* **13**(3):302–8.

Kolb H (1994) The architecture of functional neural circuits in the vertebrate retina. the proctor lecture, *Invest Ophthalmol Vis Sci* **35**(5):2385–404.

Kolb H, Linberg KA, and Fisher SK (1992) Neurons of the human retina: a golgi study, *J Comp Neurol* **318**(2):147–87.

Kolb H and Nelson R (1993) Off-alpha and off-beta ganglion cells in cat retina: Ii. neural circuitry as revealed by electron microscopy of hrp stains, *J Comp Neurol* **329**(1):85–110.

Komaromy AM, Alexander JJ, Rowlan JS, Garcia MM, Chiodo VA, Kaya A, Tanaka JC, Acland GM, Hauswirth WW, and Aguirre GD (2010) Gene therapy rescues cone function in congenital achromatopsia, *Hum Mol Genet* **19**(13):2581–93.

Kong JH, Fish DR, Rockhill RL, and Masland RH (2005) Diversity of ganglion cells in the mouse retina: unsupervised morphological classification and its limits, *J Comp Neurol* **489**(3):293–310.

Kording KP, Tenenbaum JB, and Shadmehr R (2007) The dynamics of memory as a consequence of optimal adaptation to a changing body, *Nat Neurosci* **10**(6):779–86.

Krüger J (1980) The shift-effect enhances x- and suppresses y-type response characteristics of cat retinal ganglion cells, *Brain Res* **201**(1):71–84.

Krüger J and Fischer B (1973) Strong periphery effect in cat retinal ganglion cells. excitatory responses in on- and off- center neurones to single grid displacements, *Exp Brain Res* **18**(3):316–8.

Kuffler SW (1953) Discharge patterns and functional organization of mammalian retina, *J Neurophysiol* **16**(1):37–68.

Land MF (1999) Motion and vision: why animals move their eyes, *J Comp Physiol A* **185**(4):341–52.

Land MF and McLeod P (2000) From eye movements to actions: how batsmen hit the ball, *Nat Neurosci* **3**(12):1340–5.

Lee PH, Sooksawate T, Yanagawa Y, Isa K, Isa T, and Hall WC (2007) Identity of a pathway for saccadic suppression, *Proc Natl Acad Sci U S A* **104**(16):6824–7.

Lennie P (1980) Parallel visual pathways: a review, *Vision Res* **20**(7):561–94.

Lettvin JY, Maturana HR, Mcculloch WS, and Pitts WH (1959) What the frogs eye tells the frogs brain, *Proceedings of the Institute of Radio Engineers* **47**(11):1940–1951.

Levick WR (1967) Receptive fields and trigger features of ganglion cells in the visual streak of the rabbits retina, *J Physiol* **188**(3):285–307.

Li CY, Zhou YX, Pei X, Qiu FT, Tang CQ, and Xu XZ (1992) Extensive disinhibitory region beyond the classical receptive field of cat retinal ganglion cells, *Vision Res* **32**(2):219–28.

Loopuijt LD, Silva Filho M, Hirt B, Vonthein R, and Kremers J (2007) Dendritic thickness: a morphometric parameter to classify mouse retinal ganglion cells, *Braz J Med Biol Res* **40**:1367–82.

Ölveczky BP, Baccus SA, and Meister M (2003) Segregation of object and background motion in the retina, *Nature* **423**(6938):401–8.

Maguire AM, Simonelli F, Pierce EA, Pugh EN, Mingozzi F, Bennicelli J, Banfi S, Marshall KA, Testa F, Surace EM, Rossi S, Lyubarsky A, Arruda VR, Konkle B, Stone E, Sun J, Jacobs J, Dell'Osso L, Hertle R, Ma JX, Redmond TM, Zhu X, Hauck B, Zelenaia O, Shindler KS, Maguire MG, Wright JF, Volpe NJ, McDonnell JW, Auricchio A, High KA, and Bennett J (2008) Safety and efficacy of gene transfer for leber's congenital amaurosis, *N Engl J Med* **358**(21):2240–8.

Mancuso K, Hauswirth WW, Li Q, Connor TB, Kuchenbecker JA, Mauck MC, Neitz J, and Neitz M (2009) Gene therapy for red-green colour blindness in adult primates, *Nature* **461**(7265):784–7.

Manu M and Baccus SA (2011) Disinhibitory gating of retinal output by transmission from an amacrine cell, *Proc Natl Acad Sci U S A* **108**(45):18447–52.

Margolis DJ and Detwiler PB (2007) Different mechanisms generate maintained activity in on and off retinal ganglion cells, *J Neurosci* **27**(22):5994–6005.

Marshel JH, Garrett ME, Nauhaus I, and Callaway EM (2011) Functional specialization of seven mouse visual cortical areas, *Neuron* **72**(6):1040–54.

Martinez-Conde S, Macknik SL, and Hubel DH (2004) The role of fixational eye movements in visual perception, *Nat Rev Neurosci* **5**(3):229–40.

Masland RH (2001) The fundamental plan of the retina, *Nat Neurosci* **4**(9):877–86.

Masland RH (2011) Cell populations of the retina: the proctor lecture, *Invest Ophthalmol Vis Sci* **52**(7):4581–91.

McIlwain JT (1964) Receptive fields of optic tract axons and lateral geniculate cells: Peripheral extent and barbiturate sensitivity, *J Neurophysiol* **27**:1154–73.

McIlwain JT (1966) Some evidence concerning the physiological basis of the periphery effect in the cat's retina, *Exp Brain Res* **1**(3):265–71.

Meister M and Berry MJ (1999) The neural code of the retina, *Neuron* **22**(3):435–50.

Meister M, Pine J, and Baylor DA (1994) Multi-neuronal signals from the retina: acquisition and analysis, *J Neurosci Methods* **51**(1):95–106.

Michaelides M, Hunt DM, and Moore AT (2004) The cone dysfunction syndromes, *Br J Ophthalmol* **88**(2):291–7.

Michalakis S, Geiger H, Haverkamp S, Hofmann F, Gerstner A, and Biel M (2005) Impaired opsin targeting and cone photoreceptor migration in the retina of mice lacking the cyclic nucleotide-gated channel cnga3, *Invest Ophthalmol Vis Sci* **46**(4):1516–24.

Michalakis S, Mühlfriedel R, Tanimoto N, Krishnamoorthy V, Koch S, Fischer MD, Becirovic E, Bai L, Huber G, Beck SC, Fahl E, Büning H, Paquet-Durand F, Zong X, Gollisch T, Biel M, and Seeliger MW (2010) Restoration of cone vision in the cnga3-/- mouse model of congenital complete lack of cone photoreceptor function, *Mol Ther* **18**(12):2057–63.

Mitra P and Miller RF (2007) Mechanism underlying rebound excitation in retinal ganglion cells, *Vis Neurosci* **24**(5):709–31.

Münch TA, da Silveira RA, Siegert S, Viney TJ, Awatramani GB, and Roska B (2009) Approach sensitivity in the retina processed by a multifunctional neural circuit, *Nat Neurosci* **12**(10):1308–16.

Naarendorp F, Esdaille TM, Banden SM, Andrews-Labenski J, Gross OP, and Pugh J E N (2010) Dark light, rod saturation, and the absolute and incremental sensitivity of mouse cone vision, *J Neurosci* **30**(37):12495–507.

Nassi JJ and Callaway EM (2009) Parallel processing strategies of the primate visual system, *Nat Rev Neurosci* **10**(5):360–72.

Nelson R and Kolb H (2004) On and off pathways in the vertebrate retina and the visual system, in LM Chalupa and JS Werner (Editors), *The Visual Neurosciences*, pages 260–278, The MIT Press, Cambridge, MA, USA.

Nelson R, Kolb H, and Freed MA (1993) Off-alpha and off-beta ganglion cells in cat retina. i: Intracellular electrophysiology and hrp stains, *J Comp Neurol* **329**(1):68–84.

Niell CM (2011) Exploring the next frontier of mouse vision, *Neuron* **72**(6):889–92.

Noda H (1975) Sustained and transient discharges of retinal ganglion cells during spontaneous eye movements of cat, *Brain Res* **84**(3):515–29.

Noda H and Adey WR (1974a) Excitability changes in cat lateral geniculate cells during saccadic eye movements, *Science* **183**(4124):543–5.

Noda H and Adey WR (1974b) Retinal ganglion cells of the cat transfer information on saccadic eye movement and quick target motion, *Brain Res* **70**(2):340–5.

O'Brien BJ, Isayama T, Richardson R, and Berson DM (2002) Intrinsic physiological properties of cat retinal ganglion cells, *J Physiol* **538**(Pt 3):787–802.

Passaglia CL, Freeman DK, and Troy JB (2009) Effects of remote stimulation on the modulated activity of cat retinal ganglion cells, *J Neurosci* **29**(8):2467–76.

Peng C, Rich ED, and Varnum MD (2004) Subunit configuration of heteromeric cone cyclic nucleotide-gated channels, *Neuron* **42**(3):401–10.

Petrs-Silva H, Dinculescu A, Li Q, Min SH, Chiodo V, Pang JJ, Zhong L, Zolotukhin S, Srivastava A, Lewin AS, and Hauswirth WW (2009) High-efficiency transduction of the mouse retina by tyrosine-mutant aav serotype vectors, *Mol Ther* **17**(3):463–71.

Phongphanphanee P, Mizuno F, Lee PH, Yanagawa Y, Isa T, and Hall WC (2011) A circuit model for saccadic suppression in the superior colliculus, *J Neurosci* **31**(6):1949–54.

Pouzat C, Mazor O, and Laurent G (2002) Using noise signature to optimize spike-sorting and to assess neuronal classification quality, *J Neurosci Methods* **122**(1):43–57.

Powers RK, Dai Y, Bell BM, Percival DB, and Binder MD (2005) Contributions of the input signal and prior activation history to the discharge behaviour of rat motoneurones, *J Physiol* **562**(Pt 3):707–24.

Rapaport DH and Stone J (1988) The periphery effect in cat retinal ganglion cells: variation with functional class and eccentricity, *Exp Brain Res* **70**(1):73–8.

Remtulla S and Hallett PE (1985) A schematic eye for the mouse, and comparisons with the rat, *Vision Res* **25**(1):21–31.

Ridder r W H and Tomlinson A (1997) A comparison of saccadic and blink suppression in normal observers, *Vision Res* **37**(22):3171–9.

Ridder WH and Tomlinson A (1995) Spectral characteristics of blink suppression in normal observers, *Vision Res* **35**(18):2569–78.

Rivlin-Etzion M, Zhou K, Wei W, Elstrott J, Nguyen PL, Barres BA, Huberman AD, and Feller MB (2011) Transgenic mice reveal unexpected diversity of on-off direction-selective retinal ganglion cell subtypes and brain structures involved in motion processing, *J Neurosci* **31**(24):8760–9.

Rizzolatti G and Camarda R (1977) Influence of the presentation of remote visual stimuli on visual responses of cat area 17 and lateral suprasylvian area, *Exp Brain Res* **29**(1):107–22.

Rockhill RL, Daly FJ, MacNeil MA, Brown SP, and Masland RH (2002) The diversity of ganglion cells in a mammalian retina, *J Neurosci* **22**(9):3831–43.

Rodieck RW (1998) *The First Steps in Seeing*, Sinauer Associates, Sunderland, MA, USA.

Roska B and Werblin F (2001) Vertical interactions across ten parallel, stacked representations in the mammalian retina, *Nature* **410**(6828):583–7.

Roska B and Werblin F (2003) Rapid global shifts in natural scenes block spiking in specific ganglion cell types, *Nat Neurosci* **6**(6):600–8.

Ross J, Morrone MC, Goldberg ME, and Burr DC (2001) Changes in visual perception at the time of saccades, *Trends Neurosci* **24**(2):113–21.

Saito HA (1983) Morphology of physiologically identified x-, y-, and w-type retinal ganglion cells of the cat, *J Comp Neurol* **221**(3):279–88.

Schiller PH (2010) Parallel information processing channels created in the retina, *Proc Natl Acad Sci U S A* **107**(40):17087–94.

Schlack A, Krekelberg B, and Albright TD (2007) Recent history of stimulus speeds affects the speed tuning of neurons in area mt, *J Neurosci* **27**(41):11009–18.

Schwartz EA (1973) Organization of on-off cells in the retina of the turtle, *J Physiol* **230**(1):1–14.

Schwartz G, Taylor S, Fisher C, Harris R, and Berry MJ (2007) Synchronized firing among retinal ganglion cells signals motion reversal, *Neuron* **55**(6):958–69.

Schwartz O, Pillow JW, Rust NC, and Simoncelli EP (2006) Spike-triggered neural characterization, *J Vis* **6**(4):484–507.

Segev R, Schneidman E, Goodhouse J, and Berry MJ (2007) Role of eye movements in the retinal code for a size discrimination task, *J Neurophysiol* **98**(3):1380–91.

Shapley RM and Victor JD (1978) The effect of contrast on the transfer properties of cat retinal ganglion cells, *J Physiol* **285**:275–98.

Sharpe LT and Stockman A (1999) Rod pathways: the importance of seeing nothing, *Trends Neurosci* **22**(11):497–504.

Siegert S, Scherf BG, Del Punta K, Didkovsky N, Heintz N, and Roska B (2009) Genetic address book for retinal cell types, *Nat Neurosci* **12**(9):1197–204.

Solomon SG, Lee BB, and Sun H (2006) Suppressive surrounds and contrast gain in magnocellular-pathway retinal ganglion cells of macaque, *J Neurosci* **26**(34):8715–26.

Solomon SG, White AJ, and Martin PR (2002) Extraclassical receptive field properties of parvocellular, magnocellular, and koniocellular cells in the primate lateral geniculate nucleus, *J Neurosci* **22**(1):338–49.

Stein A, Mullikin W, and Stevens J (1983) The spatiotemporal building blocks of x-, y- and w-ganglion cell receptive fields of the cat's retina, *Exp Brain Res* **49**(3):341–52.

Sterling P and Demb JB (2004) Retina, in GM Shepherd (Editor), *The Synaptic Organization of the Brain*, pages 217–269, Oxford University Press, New York, NY, USA.

Sun W, Deng Q, Levick WR, and He S (2006) On direction-selective ganglion cells in the mouse retina, *J Physiol* **576**(Pt 1):197–202.

Sun W, Li N, and He S (2002) Large-scale morphological survey of mouse retinal ganglion cells, *J Comp Neurol* **451**(2):115–26.

Sundaram V, Moore AT, Ali RR, and Bainbridge JW (2012) Retinal dystrophies and gene therapy, *Eur J Pediatr* **171**(5):757–65.

Tatler BW (2001) Characterising the visual buffer: real-world evidence for overwriting early in each fixation, *Perception* **30**(8):993–1006.

Taylor WR (1999) Ttx attenuates surround inhibition in rabbit retinal ganglion cells, *Vis Neurosci* **16**(2):285–90.

Thiadens AA, Slingerland NW, Roosing S, van Schooneveld MJ, van Lith-Verhoeven JJ, van Moll-Ramirez N, van den Born LI, Hoyng CB, Cremers FP, and Klaver CC (2009) Genetic etiology and clinical consequences of complete and incomplete achromatopsia, *Ophthalmology* **116**(10):1984–9 e1.

Thibos LN and Werblin FS (1978) The properties of surround antagonism elicited by spinning windmill patterns in the mudpuppy retina, *J Physiol* **278**:101–16.

tom Dieck S, Specht D, Strenzke N, Hida Y, Krishnamoorthy V, Schmidt KF, Inoue E, Ishizaki H, Tanaka-Okamoto M, Miyoshi J, Hagiwara A, Brandstätter JH, Löwel S, Gollisch T, Ohtsuka T, and Moser T (2012) Deletion of the presynaptic scaffold cast reduces active zone size in rod photoreceptors and impairs visual processing, *J Neurosci* **32**(35):12192–12203.

Valberg A, Lee BB, Tigwell DA, and Creutzfeldt OD (1985) A simultaneous contrast effect of steady remote surrounds on responses of cells in macaque lateral geniculate nucleus, *Exp Brain Res* **58**(3):604–8.

Venkataramani S and Taylor WR (2010) Orientation selectivity in rabbit retinal ganglion cells is mediated by presynaptic inhibition, *J Neurosci* **30**(46):15664–76.

Völgyi B, Abrams J, Paul DL, and Bloomfield SA (2005) Morphology and tracer coupling pattern of alpha ganglion cells in the mouse retina, *J Comp Neurol* **492**(1):66–77.

Völgyi B, Chheda S, and Bloomfield SA (2009) Tracer coupling patterns of the ganglion cell subtypes in the mouse retina, *J Comp Neurol* **512**(5):664–87.

Volkmann FC (1962) Vision during voluntary saccadic eye movements, *J Opt Soc Am* **52**:571–8.

Volkmann FC (1986) Human visual suppression, *Vision Res* **26**(9):1401–16.

Volkmann FC, Riggs LA, Ellicott AG, and Moore RK (1982) Measurements of visual suppression during opening, closing and blinking of the eyes, *Vision Res* **22**(8):991–6.

Wang Q and Burkhalter A (2007) Area map of mouse visual cortex, *J Comp Neurol* **502**(3):339–57.

Wang Q, Gao E, and Burkhalter A (2011) Gateways of ventral and dorsal streams in mouse visual cortex, *J Neurosci* **31**(5):1905–18.

Wark B, Fairhall A, and Rieke F (2009) Timescales of inference in visual adaptation, *Neuron* **61**(5):750–61.

Watanabe J and Tasaki K (1980) Shift-effect in the rabbit retinal ganglion cells, *Brain Res* **181**(1):198–201.

Watkins PV and Barbour DL (2008) Specialized neuronal adaptation for preserving input sensitivity, *Nat Neurosci* **11**(11):1259–61.

Wei W, Elstrott J, and Feller MB (2010) Two-photon targeted recording of gfp-expressing neurons for light responses and live-cell imaging in the mouse retina, *Nat Protoc* **5**(7):1347–52.

Weng S, Sun W, and He S (2005) Identification of on-off direction-selective ganglion cells in the mouse retina, *J Physiol* **562**(Pt 3):915–23.

Werblin FS (1972) Lateral interactions at inner plexiform layer of vertebrate retina: antagonistic responses to change, *Science* **175**(4025):1008–10.

Werblin FS and Copenhagen DR (1974) Control of retinal sensitivity. 3. lateral interactions at the inner plexiform layer, *J Gen Physiol* **63**(1):88–110.

Wässle H (2004) Parallel processing in the mammalian retina, *Nat Rev Neurosci* **5**(10):747–57.

Wässle H, Puller C, Müller F, and Haverkamp S (2009) Cone contacts, mosaics, and territories of bipolar cells in the mouse retina, *J Neurosci* **29**(1):106–17.

Wurtz RH (2008) Neuronal mechanisms of visual stability, *Vision Res* **48**(20):2070–89.

Yarbus AL (1967) *Eye Movements and Vision*, Plenum Press, New York, NY, USA.

Yonehara K, Balint K, Noda M, Nagel G, Bamberg E, and Roska B (2011) Spatially asymmetric reorganization of inhibition establishes a motion-sensitive circuit, *Nature* **469**(7330):407–10.

Yonehara K, Ishikane H, Sakuta H, Shintani T, Nakamura-Yonehara K, Kamiji NL, Usui S, and Noda M (2009) Identification of retinal ganglion cells and their projections involved in central transmission of information about upward and downward image motion, *PLoS One* **4**(1):e4320.

Yonehara K, Shintani T, Suzuki R, Sakuta H, Takeuchi Y, Nakamura-Yonehara K, and Noda M (2008) Expression of spig1 reveals development of a retinal ganglion cell subtype projecting to the medial terminal nucleus in the mouse, *PLoS One* **3**(2):e1533.

Zaghloul KA, Boahen K, and Demb JB (2005) Contrast adaptation in subthreshold and spiking responses of mammalian y-type retinal ganglion cells, *J Neurosci* **25**(4):860–8.

Zaghloul KA, Manookin MB, Borghuis BG, Boahen K, and Demb JB (2007) Functional circuitry for peripheral suppression in mammalian y-type retinal ganglion cells, *J Neurophysiol* **97**(6):4327–40.

Zagotta WN and Siegelbaum SA (1996) Structure and function of cyclic nucleotide-gated channels, *Annu Rev Neurosci* **19**:235–63.

Zhang Y, Kim IJ, Sanes JR, and Meister M (2012) The most numerous ganglion cell type of the mouse retina is a selective feature detector, *Proc Natl Acad Sci U S A* **109**(36):E2391–E2398.

Figure Acknowledgments

Figure 1.1 reprinted by permission from Macmillan Publishers Ltd: Nature Reviews. Neuroscience, Martinez-Conde et al. (2004), copyright 2004.

Figure 1.2 reprinted by permission from Macmillan Publishers Ltd: Nature Reviews. Neuroscience, Wässle (2004), copyright 2004.

Figure 1.3 reprinted by permission from Elsevier: Trends in Neuroscience, Sharpe and Stockman (1999), copyright 1999.

Figure 1.4 reprinted by permission from Macmillan Publishers Ltd: Nature Reviews. Neuroscience, Martinez-Conde et al. (2004), copyright 2004.

Figure 5.1 reprinted from Molecular Therapy, Michalakis et al. (2010), no permission required.

Curriculum Vitae

Personal Details	Vidhyasankar Krishnamoorthy Born 10th of October 1978 in Cuddalore, India
Education	
Since July 2008	PhD student in the group of Prof. Dr. Tim Gollisch, Max Planck Institute of Neurobiology, Martinsried and University of Göttingen, Göttingen
2001 - 2003	M.Sc. (Biotechnology), Bharathidasan University, India Dissertation: Rhizosecretion studies in *Mucuna pruriens* L.
1995 - 1998	B.Sc. (Biochemistry), University of Madras, India
Research Positions	
2005 - 2008	Project Assistant in the group of Dr. Narender Dhingra, National Brain Research Centre, India
2004 - 2005	Junior Research Fellow, University of Mysore, India
2003 - 2004	Research Assistant Trainee, Neobiotics India (P) Ltd., Mysore, India. (*Under "Biotech Industrial Training Programme-2003-04", a training programme of the Dept. of Biotechnology, Government of India*)
1998 - 1999	Research Assistant Trainee, Bush Boake Allen (India) Ltd, Chennai, India. (now "International Flavours & Fragrances India Ltd.")

Publications

Krishnamoorthy V, Jain V, Cherukuri P, Baloni S, Dhingra NK (2008)
Intravitreal injection of fluorochrome-conjugated peanut agglutinin results in specific and reversible labeling of mammalian cones in vivo.
Invest. Ophtalmol. Vis. Sci., **49**(6):2643-2650

Nagar S*, **Krishnamoorthy V***, Cherukuri P*, Jain V, Dhingra NK (2009)
Early remodeling in an inducible animal model of retinal degeneration.
Neuroscience, **160**(2):517-529, **equal contribution*

Michalakis S*, Mühlfriedel R*, Tanimoto N, **Krishnamoorthy V**, Koch S, Fischer MD, Becirovic E, Bai L, Huber G, Beck SC, Fahl E, Büning H, Paquet-Durand F, Zong X, Gollisch T, Biel M, Seeliger MW (2010)
Restoration of cone vision in the CNGA3$^{-/-}$ mouse model of congenital complete lack of cone photoreceptor function.
Mol. Ther., **18**(12):2057-2063, **equal contribution*

Michalakis S, Mühlfriedel R, Tanimoto N, **Krishnamoorthy V**, Koch S, Fischer MD, Becirovic E, Bai L, Huber G, Beck SC, Fahl E, Büning H, Schmidt J, Zong X, Gollisch T, Biel M, Seeliger MW (2012)
Gene therapy restores missing cone-mediated vision in the CNGA3$^{-/-}$ mouse model of achromatopsia.
Adv. Exp. Med. Biol., **723**:183-189

tom Dieck S*, Specht D*, Strenzke N, Hida Y, **Krishnamoorthy V**, Schmidt K-F, Inoue E, Ishizaki H, Tanaka-Okamoto M, Miyoshi J, Hagiwara A, Brandstätter JH, Löwel S, Gollisch T, Ohtsuka T, Moser T (2012)
Deletion of the presynaptic scaffold CAST reduces active zone size in rod photoreceptors and impairs visual processing.
J. Neurosci., **32**(35):12192-12203, **equal contribution*

Patent Application

Narender K. Dhingra and Vidhyasankar Krishnamoorthy (2007)
In vivo labeling of mammalian cone photoreceptors by intravitreal injection of fluorescently tagged peanut agglutinin.
PCT Application No. PCT/IN08/000321; priority of 2136/Del/07 (pending).

Abstracts and Conference Proceedings

Vidhyasankar Krishnamoorthy and Tim Gollisch (2012)
Contextual Encoding of Saccadic Scene Changes in the Retina.
Bernstein Conference 2012, Munich, Germany, (12-14 September, 2012)

Tim Gollisch, Vidhyasankar Krishnamoorthy and Christian B. Mendl (2012)
Neural Encoding of Saccadic Stimuli in the Retina.
10th International Neural Coding Workshop, Prague, Czech Republic, (2-7 September, 2012)

Vidhyasankar Krishnamoorthy* and Tim Gollisch (2011)
Encoding of Saccadic Scene Changes in the Mouse Retina.
European Retina Meeting 2011, Amsterdam, The Netherlands, (22-24 September, 2011) **oral presentation*

Daisuke Takeshita, Vidhyasankar Krishnamoorthy and Tim Gollisch (2011)
Correlations in first-spike latency of retinal ganglion cells during saccade-like stimuli.
European Retina Meeting 2011, Amsterdam, The Netherlands, (22-24 September, 2011)

Vidhyasankar Krishnamoorthy and Tim Gollisch (2010)
Encoding of Saccadic Scene Changes in the Mouse Retina.
XIII Annual Vision Research Conference, Retinal Ganglion Cells: Development, Function and Disease, Fort Lauderdale, USA, (30 April - 1 May, 2010)

Vidhyasankar Krishnamoorthy and Tim Gollisch (2009)
Modulation of Response properties in Retinal Ganglion Cells by Remote Stimulation.
European Retina Meeting 2009, Oldenburg, Germany, (8-10 October, 2009)

Vidhyasankar Krishnamoorthy, Pitchaiah Cherukuri, Sonia Baloni and Narender K. Dhingra (2007)
In Vivo Labeling of Mammalian Cone Photoreceptors by Intravitreal Injection of Fluorescently Tagged Peanut Agglutinin - A Potential Tool for Assessing Photoreceptor Degeneration in Humans [Abstract].
Journal of Vision, 7(15):75, 75a, OSA Fall Vision Meeting-2007, Berkeley, USA, (16-19 September, 2007)

Narender K. Dhingra, Pitchaiah Cherukuri, Vidhyasankar Krishnamoorthy, Sonia Baloni, and Stanley K. Jose (2007)
Morphological and Behavioral Characterization of N-methyl N-Nitrosourea-Induced Mouse Model of Retinal Degeneration.
Soc. Neurosci. Abstr. 699.19; Neuroscience-2007, SFN, San Diego, USA, (3-7 November 2007)